



KAUNAS UNIVERSITY OF TECHNOLOGY
FACULTY OF CIVIL ENGINEERING AND ARCHITECTURE

Siddeshwaran Parthiban

INVESTIGATION OF SHEAR STRENGTH OF SANDS
UNDER CYCLIC LOADING

Master's Degree Final Project

Supervisor

Prof. Dr. Viktoras Doroševas
Department of Building Structures
Faculty of Civil Engineering
KTU, Lithuania.

KAUNAS, 2017

KAUNAS UNIVERSITY OF TECHNOLOGY
FACULTY OF CIVIL ENGINEERING

“Investigation of shear strength of sands under cyclic loading”

Master’s Degree Final Project
CIVIL ENGINEERING (621H20001)

Supervisor

(signature) Prof. Dr. Viktoras Doroševas
(date)

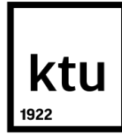
Reviewer

(signature) Assoc Prof. Dr. Donatas Rekus
(date)

Project made by

(signature) Siddeshwaran Parthiban
(date)

KAUNAS, 2017



KAUNAS UNIVERSITY OF TECHNOLOGY

Civil Engineering

(Faculty)

Siddeshwaran Parthiban

(Student's name, surname)

Civil Engineering, 621H20001

(Title of study programme, code)

“Investigation of shear strength of sands under cyclic loading”

Final project

DECLARATION OF ACADEMIC INTEGRITY

_____ 20 17
_____ Kaunas

I confirm that the final project of mine, **Siddeshwaran Parthiban**, on the subject, **“Investigation of shear strength of sands under cyclic loading”** is written completely by myself; all the provided data and research results are correct and have been obtained honestly. None of the parts of this thesis have been plagiarized from any printed, Internet-based or otherwise recorded sources; all direct and indirect quotations from external resources are indicated in the list of references. No monetary funds (unless required by law) have been paid to anyone for any contribution to this thesis.

I fully and completely understand that any discovery of any facts of dishonesty inevitably results in me incurring a penalty under procedure effective at Kaunas University of Technology.

(name and surname filled in by hand)

(signature)

KAUNAS UNIVERSITY OF TECHNOLOGY
FACULTY OF CIVIL ENGINEERING AND ARCHITECTURE
DEPARTMENT OF.....BUILDING STRUCTURES.....

Master final work

**TITLE : INVESTIGATION OF SHEAR STRENGTH OF SANDS UNDER CYCLIC
LOADING**

Vardas Pavardė SIDDESHWARAN PARTHIBAN

ABSTRACT

This present research work is based on study of shear strength of sands under statical and dynamical loading condition in a laboratory setting and performed index properties tests on classification and grading of sands as per guidelines of Eurocode 7 and study the influence of applied frequency of a range between 10 to 50 Hz using a vibrating table.

The study is mainly experimental is to understand the cyclic loading effect on sands in a simple shear box apparatus helping to estimate shear strength at failure for statical and dynamic loads. It is proposed to use an alternate approach to study cyclic loading as the present advancements in this research area is still evolving and no definite research framework has been standardised to assess the influence of cyclic loading on sands as a reference for researchers and geotechnical engineers. It is proposed to also perform settlement analysis using a model footing calibrated to study scaling effect to understand applicability of laboratory results to practical field application like insitu testing and correlation of onsite data. It is also proposed to study liquefaction potential of sands to understand the mechanism of liquefaction using empirical relationships.

Keywords (up to 8 words): cyclic loading, liquefaction, settlement, shear strength, sand.

Siddeshwaran Parthiban. "Investigation of shear strength of sands under cyclic loading". Master's thesis Final Project / supervisor Prof. Dr. Viktoras Doroševas; Faculty of Civil Engineering, Kaunas University of Technology.

Study field and area: Building Structures, Civil Engineering

Keywords: cyclic loading, liquefaction, settlement, shear strength, sand.

Kaunas, 2017. 84 p.

SUMMARY

This present research work is based on study of shear strength of sands under statical and dynamical loading condition in a laboratory setting and performed index properties tests on classification and grading of sands as per guidelines of Eurocode 7 and study the influence of applied frequency of a range between 10 to 50 Hz using a vibrating table.

The study is mainly experimental so as to understand the cyclic loading effect on sands in a simple shear box apparatus helping to estimate shear strength at failure for statical and dynamic loads. It is proposed to use an alternate approach to study cyclic loading as the present advancements in this research area is still evolving and no definite research framework has been standardised to assess the influence of cyclic loading on sands as a reference for researchers and geotechnical engineers. The purpose is to describe how the sandy soil behaves when subjected to cyclic loading. As mentioned cyclic loading can be caused by environmental loads from wind, transport systems, earthquakes and even human induced loads like explosions. This form of loading will have an effect on soil properties such as soil stiffness, shear strength, and void ratio. It is proposed to also perform settlement analysis using a model footing calibrated to study scaling effect to understand applicability of laboratory results to practical field application like insitu testing and correlation of onsite data. It is also proposed to study liquefaction potential of sands to understand the mechanism of liquefaction using empirical relationships.

Siddeshwaran Parthiban “Smėlio veikiamo ciklinės apkrovos kerpamojo stiprio tyrimas”.
Magistro baigiamasis projektas / vadovas prof. dr. Viktoras Doroševas; Kauno technologijos
universitetas, Statybos ir architektūros fakultetas.

Mokslo kryptis ir sritis: statybos inžinerija

Reikšminiai žodžiai: ciklinė apkrova, suskystėjimas, nuosėdis, kerpamasis stipris, smėlis
Kaunas, 2017. 84 p.

SANTRAUKA

Darbe nagrinėjamas smėlio veikiamo statinių ir dinaminių apkrovų kerpamasis stipris. Tam laboratorijoje atliekami grunto granulimetrinių savybių tyrimai ir smėlio pavyzdžių klasifikavimas bei jų naudojimas tyrimams, kurie neįeina į Eurokodo 7 turinį, tokių kaip 10 iki 50 Hz dažnio vibracijų įtaką smėlio grunto stiprumui. Tyrimų tikslas yra eksperimentiškai, naudojant nešiojamą smėlio kirpimo aparatą, nustatyti ciklinės ir statinės apkrovos įtaką smėlio stiprumui.

Tiriamam smėlio ciklinio apkrovimo poveikio įtaką jo stiprumui siūloma naudoti alternatyvu požiūrį, nes ši mokslinių tyrimų sritis vis dar vystosi ir nėra standartizuotų geotechninių reikalavimų. Tikslas yra apibūdinti smėlio grunto elgseną esant cikliniam apkrovimui, kuris gali būti sukeltas vėjo sąveikos su statiniu, transporto sistemų, žemės drebėjimo ar net žmogaus sukeltų sprogių. Šių apkrovų poveikis turi įtakos grunto stiprumą įtakojantiems parametrams: grunto standumas, šlyties įtempiai ir poringumo koeficientas. Darbe pateikiami nuosėdžio po tolygiai išskirstyta apkrova smėlio grunte eksperimentinio modeliavimo ir tyrimo rezultatai, siekiant iširti sąveikos parametrų koreliacijas, atitikimą teoriniams skaičiavimams, mastelinį efektą ir laboratorinių duomenų naudojimo tinkamumą nuosėdžiū apskaičiavimui *insitu* praktikoje. Darbe nagrinėtas smėlio suskystėjimo procesas ir jo sąveika per empirinius ryšius.

ACKNOWLEDGEMENT

I would like to thank my supervisor and mentor Prof. Dr. Viktoras Doroševas, Kaunas University of Technology, Lithuania, who gave me wonderful guidance, and support right from the start of research projects I, II and III and till the end of master thesis project. His continuous guidance and depth of knowledge helped me to complete my thesis successfully.

I would like to thank all the faculty members and support staff of Department of Civil Engineering, Kaunas University of Technology, Lithuania, for all the support and help given to me during my master degree program in the Department.

Special thanks to my colleagues Arun Kishore, Harrish Mydeen for all the good memories in the department and would like to thank Vadimas Kitovas for helping with sample preparation and testing at the department laboratory and very thankfully for kind permission of Technological Systems Diagnostics Institute at Kaunas University of Technology for use of their vibration table for testing.

Last but not least, I would like to thank my close friends Dr. Ramesh Kannan Kandasami, Research Associate at University of Cambridge UK and Dr. Shashidhar S, Geotechnical Consultant with Mott MacDonald, India for believing in my ability to pursue higher studies abroad and I am eternally indebted to my family for all their love and sacrifices for my sake to pursue my studies abroad.

Table of Contents

1. Introduction	16
1.1. Aim of present thesis	18
1.2. Tasks to be performed.....	18
1.3. Nature of problem	18
1.4. Journal papers written based on present thesis	19
1.5. Organization of thesis	19
2. Literature review:	21
2.1. Different types of cyclic loading.....	26
2.1.1. Cyclic stresses during earthquakes.....	26
2.1.2. Traffic loading.....	27
2.1.3. Wave-induced loading.....	28
2.2. Laboratory tests for cyclic loading	30
2.2.1. Simple Shear Test:	30
2.2.2. Triaxial Test	32
2.2.3. Cyclic Triaxial Test.....	33
2.2.4. Cyclic simple shear test.....	35
2.2.5. Torsional shear test apparatus	36
2.2.6. Resonant column test	39
2.3. Factors influencing cyclic loading	41
2.3.1. Effect of particle size and relative density	41
2.3.2. Effect of void ratio and presence of fines	44
3. Experimentation.....	49
3.1. Theoretical background	49
3.2. Tests on sands	50

3.2.1.	Particle size distribution	50
3.2.2.	Simple shear tests under static and cyclic loading	51
3.2.3.	Friction angle tests on sands.....	53
3.2.4.	Settlement Studies	56
3.3.	Results.....	62
3.3.1.	Shear test results.....	62
3.3.2.	Friction angle test results.....	64
3.3.3.	Settlement test results.....	66
4.	Conclusions and Discussions.....	75
4.1.	Effect of statical loads on sands.....	75
4.2.	Effect of cyclic loads on sands.....	75
4.3.	Settlement analysis of model footing.....	75
4.4.	Discussions and scope of further work	76
5.	References	77

Table of figures

FIGURE 1 CLASSIFICATION OF DYNAMIC PROBLEMS(AFTER KENJI ISHIHARA 1996).....	17
FIGURE 2 SCHEMATIC BEHAVIOUR OF LOOSE SAND PARTICLES UNDER RAPID SHAKING (BRENNAN ET AL. 2007).....	22
FIGURE 3 EXAMPLES OF PRINCIPAL STRESS DIRECTION VARIATION ALONG POTENTIAL FAILURE SURFACES.(VAID ET AL 1997).....	23
FIGURE 4 SKETCH OF A GROUP OF SOIL PARTICLES ILLUSTRATING THE CHANGE IN PACKING DURING CYCLIC LOADING (YOU D 1977).....	23
FIGURE 5 TYPICAL STRENGTH DEGRADATION CURVES FOR SOILS AGAINST LIQUEFACTION(LIN 1983)	24
FIGURE 6 SAND BOIL AFTER LIQUEFACTION-INDUCED BOILING FROM THE 1989 LOMA PRIETA, CALIFORNIA EARTHQUAKE HAS CEASED(EERI ARCHIVES)	24
FIGURE 7 DEPOSITION OF LIQUEFIED SAND THROUGH GROUND CRACKS BHUJ EARTHQUAKE 2001 INDIA(EERI ARCHIVES)	24
FIGURE 8 PLAUSIBLE SETTLEMENT MECHANISM OF FAILURE SHOWING THE TILTING THE TOWER, ASSUMING THERE IS NO STRUCTURAL FAILURE OF PILES(BHATTACHARYA ET AL 2008)	25
FIGURE 9 FACTOR OF SAFETY AGAINST CYCLIC MOBILITY AND LIQUEFACTION AND PERCENTAGE DEGRADATION IN STRENGTH OF SOIL DURING EARTHQUAKE FOR THE CONSIDERED SOIL PROFILE (BHATTACHARYA ET AL 2008)	25
FIGURE 10 STRESSES INDUCED BY BODY WAVE PROPAGATION(ISHIHARA 1983)	26
FIGURE 11 STATE OF STRESSES INDUCED BY PROPAGATION OF COMPRESSIONAL WAVE(ISHIHARA 1983)	26
FIGURE 12 UNIFORM LOADS ON AN ELASTIC HALF-SPACE(ISHIHARA 1983).....	28
FIGURE 13 CHARACTERISTIC CHANGES IN TWO SHEAR STRESS COMPONENTS IN THREE TYPICAL DYNAMIC LOADING(ISHIHARA 1983)	28
FIGURE 14 WAVE-INDUCED STRESSES IN A SEABED DEPOSIT(ISHIHARA 1983).....	29
FIGURE 15 SIMPLE SHEAR TEST APPARATUS (VENKATARAMAIAH 2006).....	31
FIGURE 16 STRESS CONTROLLED SHEAR TEST (VENKATARAMAIAH 2006)	31
FIGURE 17 STRAIN CONTROLLED SHEAR TEST (VENKATARAMAIAH 2006).....	31
FIGURE 18 DIRECT SHEAR TEST RESULTS IN LOOSE, MEDIUM AND DENSE SANDS (VENKATARAMAIAH 2006)	32

FIGURE 19 TRIAXIAL TEST APPARATUS(ISHIHARA 1996)	33
FIGURE 20 CYCLIC TRIAXIAL SETUP (ISHIHARA 1996).....	34
FIGURE 21 CYCLIC SHEAR MOULD(ISHIHARA 1996)	35
FIGURE 22 SIMPLE SHEAR TEST APPARATUS WITH TWO-DIRECTIONAL LOADING DEVICE(ISHIHARA 1996)	36
FIGURE 23 HOLLOW-CYLINDRICAL TORSIONAL TEST APPARATUS(ISHIHARA 1996)	37
FIGURE 24 HOLLOW CYLINDER STRESS STATES (KANDASAMI 2015)	38
FIGURE 25 AN IMAGE OF HCT APPARATUS WITH SPECIMEN INSIDE HCT CELL (SINGH, KANDASAMI AND MURTHY 2017).....	38
FIGURE 26 A)BASE - EXCITED TOP - FREE TYPE B) TOP - EXCITED TYPE RESONANT COLUMN(ISHIHARA 1996).....	39
FIGURE 27 BOTTOM EXCITING TYPE RESONANT COLUMN TEST DEVICE (SHANNON ET AL. 1959)	40
FIGURE 28 RESONANT COLUMN TEST APPARATUS (DRNEVICH, 1972)	40
FIGURE 29 INDUCED STRAIN IN SAND DEPOSITS.(TOKIMATSU, K. AND H.B. SEED. 1987).....	41
FIGURE 30 GRAIN SIZE DISTRIBUTION OF SOIL LIQUEFACTION PROPOSED BY (IWASAKI, 1986).42	
FIGURE 31 RELATIONSHIP BETWEEN NORMALIZED PORE PRESSURE RATIO AND CYCLE RATIO (GOVINDARAJU ET AL 2007)	43
FIGURE 32 EFFECT OF VOID RATIO ON CYCLIC LOADING(SEED 1982)	44
FIGURE 33 EFFECTS OF PLASTICITY INDEX ON THE CYCLIC STRENGTH(ISHIHARA 1993).....	44
FIGURE 34 EFFECTS OF CONFINING STRESS ON SHEAR MODULUS (KOKUSHO, 1980).	45
FIGURE 35 EFFECT OF STRAIN AMPLITUDE ON CONFINING STRESS (KOKUSHO, 1987).....	46
FIGURE 36 RELATIONSHIP BETWEEN SHEAR STRAIN AND NUMBER OF CYCLES FOR INITIAL LIQUEFACTION AT VARYING FREQUENCIES(GOVINDARAJU ET AL 2007)	46
FIGURE 37 VOID RATIO VERSUS CYCLIC SHEAR DISPLACEMENT, SHOWING DENSIFICATION OF A SAND SPECIMEN WITH SUCCESSIVE CYCLES OF DRAINED SIMPLE SHEAR LOADING (YOUNG 1972)	47
FIGURE 38 EFFECT OF CYCLIC LOADING ON DAMPING RATIOS OF SAND(GOVINDARAJU ET AL 2007)	48
FIGURE 39 EFFECT OF POST-LIQUEFACTION VOLUMETRIC STRAIN PLOTTED AGAINST MAXIMUM SHEAR STRAIN (ISHIHARA 1993)	48
FIGURE 40 PARTICLE SIZE DISTRIBUTION OF SAND SAMPLES	50
FIGURE 41 EXPERIMENTAL SETUP WITH SHAKING TABLE.....	51
FIGURE 42 VIBRATION TABLE WITH VARYING CYCLIC LOADING.....	52

FIGURE 43 UVT-2(1) AND UO (2) TESTS FOR SAND A	53
FIGURE 44 UVT-2 TEST FOR SAND B	54
FIGURE 45 UO TESTS FOR SAND B	54
FIGURE 46 VIBRATION TABLE WITH UO	55
FIGURE 47 VIBRATION TABLE WITH UO	55
FIGURE 48 MODEL FOOTING PROTOTYPE	57
FIGURE 49 PROTOTYPE MODEL FOOTING TYPE 1	57
FIGURE 50 PROTOTYPE MODEL FOOTING TYPE 2	58
FIGURE 51 ACTUAL MODEL FOOTING TYPE 1 AND 2.....	58
FIGURE 52 SHEAR TEST RESULTS FOR STATICAL LOADS	62
FIGURE 53 SHEAR TEST RESULT FOR SAND A TESTED AT FACULTY.....	62
FIGURE 54 SHEAR TEST RESULT FOR SAND B TESTED AT FACULTY	63
FIGURE 55 SHEAR TEST RESULT FOR SAND A TESTED AT TECHNOLOGICAL SYSTEMS DIAGNOSTICS INSTITUTE.....	63
FIGURE 56 SHEAR TEST RESULT FOR SAND B TESTED AT TECHNOLOGICAL SYSTEMS DIAGNOSTICS INSTITUTE.....	64
FIGURE 57 FRICTION ANGLE RESULTS FOR SAND A AT TECHNOLOGICAL SYSTEMS DIAGNOSTICS INSTITUTE FACULTY	64
FIGURE 58 FRICTION ANGLE RESULTS FOR SAND B AT TECHNOLOGICAL SYSTEMS DIAGNOSTICS INSTITUTE FACULTY	65
FIGURE 59 COMBINED FRICTION ANGLES RESULTS FOR SAND A AND B AT TECHNOLOGICAL SYSTEMS DIAGNOSTICS INSTITUTE FACULTY	65
FIGURE 60 SETTLEMENT RESULT FOR SAND A LINEAR VARIATION.....	66
FIGURE 61 SETTLEMENT CURVE FOR SAND A LINEAR VARIATION TRIAL NO 1.....	66
FIGURE 62 SETTLEMENT CURVE FOR SAND A LINEAR VARIATION TRIAL NO 2.....	67
FIGURE 63 SECOND ORDER(QUADRATIC) AVERAGE SETTLEMENT CURVE FOR SAND A	67
FIGURE 64 SECOND ORDER(QUADRATIC) SETTLEMENT CURVE FOR SAND A TRIAL NO1	68
FIGURE 65 SECOND ORDER(QUADRATIC) SETTLEMENT CURVE FOR SAND A TRIAL NO 2.....	68
FIGURE 66 SETTLEMENT RESULT FOR SAND B LINEAR VARIATION	69
FIGURE 67 SETTLEMENT RESULT FOR SAND B LINEAR VARIATION TRIAL 1	69
FIGURE 68 SETTLEMENT RESULT FOR SAND B LINEAR VARIATION TRIAL 2.....	70
FIGURE 69 SECOND ORDER(QUADRATIC) SETTLEMENT CURVE FOR SAND B.....	70
FIGURE 70 SECOND ORDER(QUADRATIC) SETTLEMENT CURVE FOR SAND B TRIAL 1.....	71
FIGURE 71 SECOND ORDER(QUADRATIC) SETTLEMENT CURVE FOR SAND B TRIAL 2.....	71

FIGURE 72 CALCULATED SETTLEMENT RESULT FOR SAND A	72
FIGURE 73 CALCULATED SETTLEMENT RESULT FOR SAND B	72
FIGURE 74 SCALING EFFECT ON SAND A	73
FIGURE 75 SCALING EFFECT ON SAND B	74

List of tables

TABLE 1 REFERENCE VALUES FOR CALCULATING MAXIMUM SHEAR MODULUS G PROPOSED BY SEED ET AL. 1972)	42
TABLE 2 CONSTANTS IN PROPOSED EMPIRICAL EQUATIONS ON SHEAR STRAIN MODULUS: G_0 “(KOKUSHO, 1987)	45
TABLE 3 INDEX PROPERTIES OF SANDS	50
TABLE 4 SHEAR STRESS VALUES FOR SAND A	52
TABLE 5 SHEAR STRENGTH VALUES OF SAND B	53
TABLE 6 FRICTION ANGLES FOR VARIOUS CYCLIC LOADS FOR SAND A.....	56
TABLE 7 FRICTION ANGLES FOR VARIOUS CYCLIC LOADS FOR SAND B	56
TABLE 8 SETTLEMENT TEST DATA FOR SAND A.....	60
TABLE 9 SETTLEMENT DATA FOR SAND B	61

List of Equations

EQUATION 1 TRAFFIC LOAD STRESSES CALCULATIONS (ISHIHARA 1983).....	27
EQUATION 2 TWO-DIMENSIONAL PLANE STRAIN PROBLEM FOR WAVE LOADING (ISHIHARA 1983)	29
EQUATION 3 WAVE LOADING STRESS EQUATIONS (ISHIHARA 1983).....	30
EQUATION 4 STRESS PARAMETERS FOR HOLLOW CYLINDER TESTS (KANDASAMI 2015)	38
EQUATION 5 EFFECTIVE DENSITY	41
EQUATION 6 MAXIMUM SHEAR MODULUS BY FIELD DATA.....	41
EQUATION 7 EMPIRICAL RELATIONSHIP FOR VOID RATIO (RICHART 1963)	44
EQUATION 8 SKEMPTON EMPIRICAL RELATIONSHIP FOR N AND D_r	49
EQUATION 9 SETTLEMENT EQUATIONS FOR SANDS.....	59

SYMBOLS AND ACRONYMS

BPT	Becker penetration test
C_{2D}	adjustment factor for the effects of two-directional cyclic loading
CPT	cone penetration test
CRR	cyclic resistance ratio
CRRM	cyclic resistance ratio at a given earthquake magnitude
CSL	critical-state line
CSR	cyclic stress ratio
D_R	relative density
$D_{R, cs}$	relative density at critical state
DSS	direct simple shear
ER_m	measured value of SPT energy ratio
F	CPT friction ratio
FC	finer content
FS	factor of safety
FS_{liq}	factor of safety against triggering of liquefaction
i	hydraulic gradient
K_α	correction factor for the effects of an initial static shear stress ratio
K_o	coefficient of lateral earth pressure at rest
ϵ_a	axial strain
ϵ_v	volumetric strain
ϕ'	effective friction angle
ϕ_{Cv}	critical-state effective friction angle
γ	total unit weight, or shear strain
γ_{lim}	limiting value of shear strain
γ_{max}	maximum shear strain
ξ_R	relative state parameter, or relative state parameter index
σ_1	major principal total stress
σ_3	minor principal total stress
σ_v	vertical total stress
τ_{cyc}	cyclic shear stress
τ_{max}	maximum shear stress
τ_s	static shear stress

1. Introduction

Sand is a granular material freely available in nature and are the by-products of natural weathering of rocks. The load which is applied by external loading gets transmitted in sand via grain to grain contact. Understanding the cyclic stress–strain behaviour of sandy soil under dynamic loading is very important design problem to engineers working in the fields of mining, underground excavation, infrastructure construction. Laboratory testing makes it possible to study soil behaviour in detail under control and well known boundary conditions. However, it is not possible to use laboratory test results for practical purposes without a high degree of correlation between the test condition in the laboratory and the condition in situ. The mechanical behaviour of sand is mainly controlled by its density and confining stress. Relative density is commonly used to describe the state of sand in reconstituted samples. However, it is well known that relative density cannot fully describe the mechanical behaviour of sand. Therefore, a parameter which can incorporate the density and stress state of soil, is needed to characterize the engineering behaviour of sand.

The soil mass has a complex structure consists of different phases and particle mixtures, hence it is very difficult to precisely describe its constitutive relation, especially when it is subjected to different water content values and is under dynamic load conditions caused due to natural calamities like earthquakes, volcanic eruptions, landslides, avalanches and also due to human induced action like underground tunneling, mining, vibration of industrial machines. It is imperative to approach this dynamic problem using empirical formulas as well as experimental data based approach to augment an idealization of dynamic behaviour of sands and design cost effective solutions to geotechnical structures.

Ishihara (1996) states “In what is called the dynamic phenomenon, the load is repetitively applied many times with some frequency. Thus repetitiveness in loading is another prime attribute used to classify dynamic problems. The events frequently encountered in engineering practice are classified in this context and as shown in figure 1. The length of time at which a certain level of stress or strain is attained in soils may be defined as the time of loading. The rapidity of load application is certainly a feature characterizing the dynamic phenomenon. The problems associated with rapid application of one single impulse are represented by the shock such as that generated by dropping of bombs or blasting of explosives. The duration of loading is as short as $10^{-3} - 10^{-2}$ seconds and the load is commonly called an impulse or shock load. Main shaking during earthquakes involves 10-20 times repetition of loads with differing amplitudes. While the seismic loading is irregular in time history, the

period of each impulse, is within the range between 0.1 and 3.0 seconds, giving the corresponding time of loading on the order of 0.02 to 1.0 seconds as accordingly indicated in Fig. 1. In the case of pile driving, vibro-compaction, and operation of vibrating rollers, the loads are applied to soils 100 to 1000 times with a frequency 10 to 60 Hz. The foundations on which electric generators or compressors are mounted are also subjected to motions with similar frequencies, but the number of load applications is much larger.”

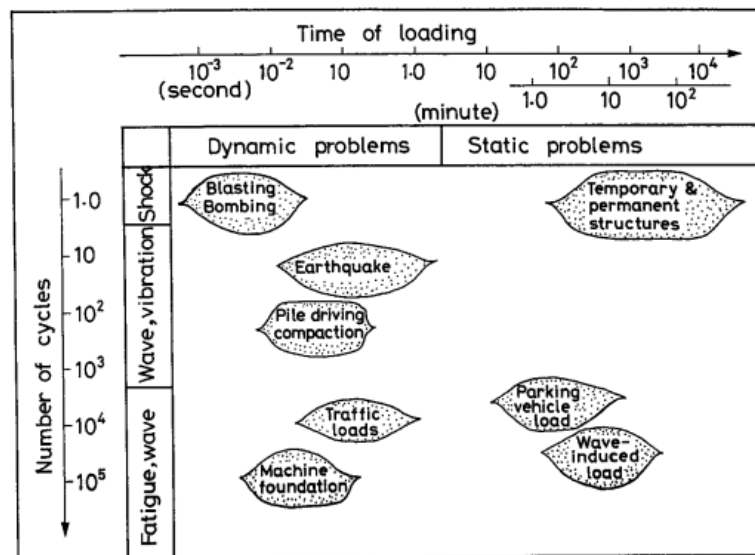


Figure 1 Classification of dynamic problems(after Kenji Ishihara 1996)

Ishihara 1983 explains how “the above events are mainly related to what is termed as vibration or wave propagation. Another kind of problem in soil behaviour while undergoing the repetitive loads induced by traffic or propagation of water waves. The soils in the subgrade underneath railways or road pavements are subjected to a large number of loads during the life span of their service. Though variable to a large degree, the time of loading may be deemed on the order of 0.1 second to a few seconds. This type of loading is characterized by the number of repetitions being formidably large and, therefore, even though the intensity is trivial, its accumulated effects could be of engineering significance. In the case as above where the number of repetitions is unmeasurably large, the problem may need to be understood as a phenomenon of fatigue. The behaviour of soils as manifested by the load repetitions as above will be referred to as the effect of repetition.”

The phenomenon of liquefaction is generally associated with cohesionless soils like sands and gravels. It is a result of seismic shaking that is of a sufficient intensity and duration. It denotes a condition where a soil will undergo continued deformation at a constant rate of residual stress or with no residual resistance, due to the build-up and maintenance of high pore

water pressure which reduces the effective confining pressure to a very low value. Two necessary conditions for liquefaction to occur are the presence of soils of sufficiently low density that can tend to undergo volume reduction upon shaking action, and a state of full or near full saturation. Under these conditions, cohesionless soils will tend to densify when subjected to cyclic shear stresses from ground vibrations but will be temporarily prevented from doing so at depth due to restricted drainage. The bearing capacity of soils for foundation loads is directly related to their strength, liquefaction poses a serious hazard to constructed structures and must be assessed in seismic areas where susceptible deposits exist. Liquefaction has been observed in earthquakes for many years. In fact, written records dating back hundreds of years describe earthquake effects that are now known to be associated with liquefaction (example: 1891 Mino-Owari, 1906 San Francisco, 1940 Fukai).

1.1. Aim of present thesis

To study the influence of cyclic loading on shear strength of medium sands using simple shear apparatus with different frequency range from 10-50 Hz. Two different sands are used for the present study.

1.2. Tasks to be performed

- To perform index properties tests on sands and classify them as per Eurocode 7 guidelines
- To study shear strength at different confining pressures for static and cyclic loads in dry and saturated conditions
- To study influence of friction angle on shear strength of sands under static and dynamic loads
- To study settlement of model footing developed at the faculty of civil engineering for static loads only to understand scaling effect.
- To cross verify experimental values to analytical solutions for settlement analysis

1.3. Nature of problem

Cyclic loading is a complex phenomenon to study and model in a laboratory as the conditions assumed in the analysis like isotropic and elastic behaviour are untrue in real on field conditions tend to be anisotropic and visco plastic behaviour. Cyclic loading of sands was first studied in detail by Dr. Seed (1972) and found few important conditions which influences it

- Effect of particle size

- Effect of void ratio
- Effect of relative density
- Effect of water content

It is an important phenomenon and key area of current research to understand Earthquake Geotechnics from insitu tests and lab tests on reconstituted soil samples. Many researchers have contributed various theories and hypothesis for cyclic loading yet there is no universal standard framework for cyclic loading analysis as it is yet to be standardized in design codes.

This thesis is an attempt to understand cyclic loading as a tool to study shear strength of medium sands which are known to liquefy during earthquakes or heavy operations like pile driving with a simple shear apparatus with external vibration source. Generally, the available research is for smaller cyclic loads of 0.1 to 5 Hz for seismic site analysis as reported by various researchers, very few have tried higher cyclic loads for 10 -80 Hz as experiments are difficult to model and conduct in a lab setting and generally opt for onsite experimentation using penetration tests like standard penetration test (SPT) and cone penetration test (CPT) which give a fair assessment of ground conditions. Yet it is important to understand the micromechanics and validation of soil models in a lab setting so as to quantify the behaviour of sands in terms of safe and economical design of structures in seismically active regions and prevent catastrophic failures of foundation systems.

1.4. Journal papers written based on present thesis

- Siddeshwaran Parthiban, Gediminas Stelmokaitis, Viktoras Doroševas “Investigation of Behaviour of Sands Under Cyclic Loading” (accepted manuscript) Journal of Sustainable Architecture and Civil Engineering, Kaunas university of technology.
- Siddeshwaran Parthiban, Ramesh Kannan Kandasami (2016), “Latest advancements in Geotechnical testing methodologies - Laboratory and In-situ” Advanced construction 2016: proceedings of the 5th international conference, 6 October, 2016, Kaunas, Lithuania, p. 77-85, ISSN 2029-1213
- Siddeshwaran Parthiban, Vadimas Kitovas (2016), “A study of mobilization of residual shear in different clays during an earthquake event” Student conference 2016, Kaunas university of technology.

1.5. Organization of thesis

The present thesis is organized into four main parts, introduction, literature review, testing and results, conclusion and discussions.

It is proposed to include all the current advancements of research in the field of cyclic loading in the literature review as it is a very important concept in the field of earthquake engineering and plays a key role in furthering our understanding of this complex phenomenon. Followed by experimentation and result analysis of two sand samples namely Sand A and Sand B which are chosen as medium sands since it is very important to study its liquefaction capability as it is widely reported by various researchers that medium sands have a higher probability of failures under dynamic loads and detailed conclusions and discussion of the results and suggestions for further future research possibilities on the same topic

2. Literature review:

Engineering the soils requires extensive understanding of the physical, chemical and mechanical behaviour at multiple length scales. Any engineering design (foundation, retaining walls, slope stability etc.) requires a complete understanding of the material behaviour. This understanding of the material response will be useful in development of advanced constitutive models or refine the existing ones. Elemental testing under laboratory conditions has many advantages such as well controlled boundary conditions, high degree of accuracy, radial interpretation, strictly controlled drainage conditions, predefined stress paths, imposing uniform strain fields across the specimen etc. over in situ testing. However, have some limitations such as obtaining undisturbed samples, smaller specimens cannot represent the features and inhomogeneity of the soil deposits, more expensive and time consuming etc. Similarly, the elemental tests under in situ conditions have many advantages like larger volume is tested, tests are quick and inexpensive, can obtain undisturbed soil parameters etc. over laboratory testing and has limitations such as poorly defined boundary conditions, drainage conditions cannot be controlled, stress and strain field are non-uniform, degree of disturbance to the surrounding soil is higher and generally unknown (Jamiolkowski et al. 1985). The fundamental assumption based on which all these elemental tests are carried out both in laboratory as well as in the field is that the elemental volume used for these behavioural understanding satisfies continuum. (Parthiban et al. 2016)

Laboratory testing of geomaterials started in the early 20th century where Professor Lambe published a book in 1951 on 13 different types of soil tests. Even though these classical tests are very simple and confined to certain boundary conditions, the results are accurate and a reliable assessment of the strength characteristics can be made. Later several experimental geo mechanists and researchers like Bowles (1986), Head (1984, 1992), Day (2001), Das (2008), Germaine and Germaine (2009) etc. have given the experimental protocols, assumptions, nitty-gritty details of each test which will be useful in performing and troubleshooting many experiments. With advancements in geotechnical engineering and increased awareness in geo environmental engineering, new materials and new equipments have been developed to perform tests under complex boundary conditions. (Parthiban et al. 2016)

Rapid loading due to an earthquake or a static event may induce large pore pressures in loose, saturated sandy deposits. The associated decrease in effective stresses could cause the

sand to liquefy. The term liquefaction encompasses all phenomena involving excessive deformation of saturated cohesionless soils (National Research Council 1985). Under static loading, liquefaction is associated with the sand responding in a strain-softening manner. The field consequences of this type of sand behaviour is a flow slide as explained by (Brennen et al. 2007) in figure 2. Liquefaction under cyclic loading can occur either because of strain softening, in a manner similar to that under static loading, or because of cyclic mobility or a combination of the two (Vaid and Chern 1985). The term cyclic mobility, in triaxial tests, refers to excursions of the stresses in sand through transient states of zero effective stress, but with limited development of shear strains (Castro 1969; Seed 1979; Vaid and Chern 1985). Its consequences may be unacceptable deformations in the sand structure.

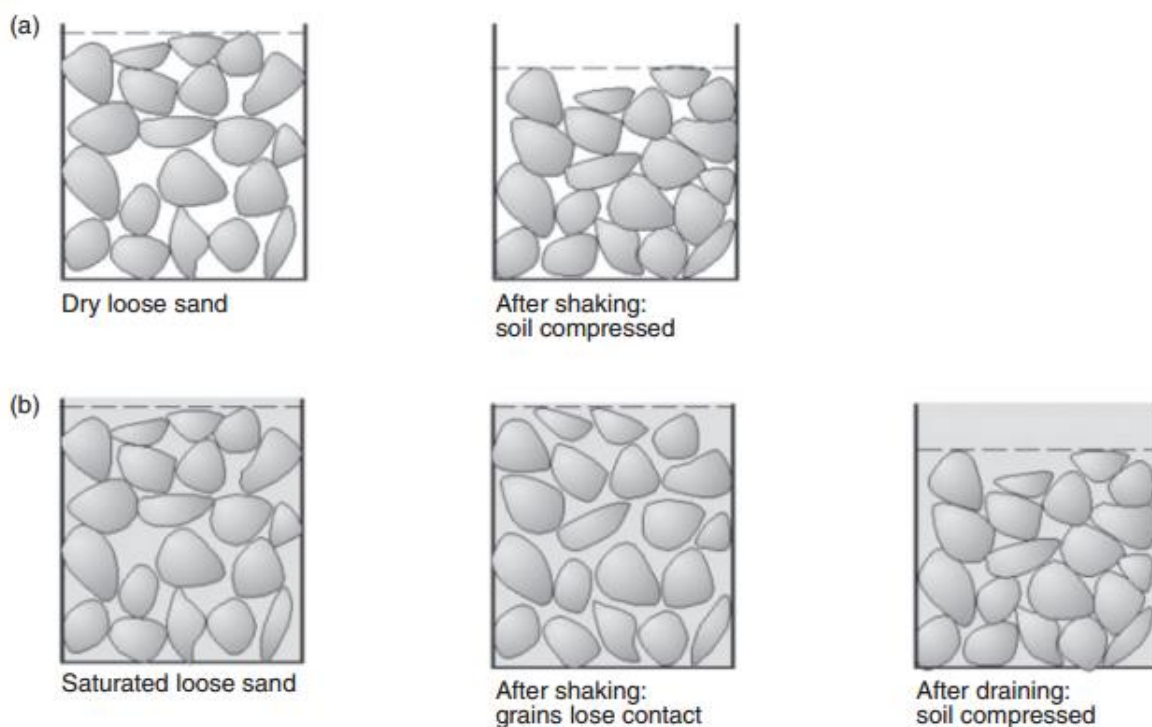


Figure 2 Schematic behaviour of loose sand particles under rapid shaking (Brennan et al. 2007)

Vaid (1997) states that “The nature of stresses acting on soil elements involves principal stress rotation, during both construction and performance. In addition, principal stress directions may vary from element to element in the soil mass. Embankment loading and cutting of slopes are two examples where gradual rotation of principal stresses occurs. Figure 2 shows two cases where the direction of major principal stress σ_1 varies from element to element along the potential failure surface. Repetitive loading due to an earthquake causes a continuous cyclic rotation of principal stresses. Cyclic rotation of principal stresses also occurs in soil elements under the ocean floor due to wave loading, and under pavements due to traffic loading.”

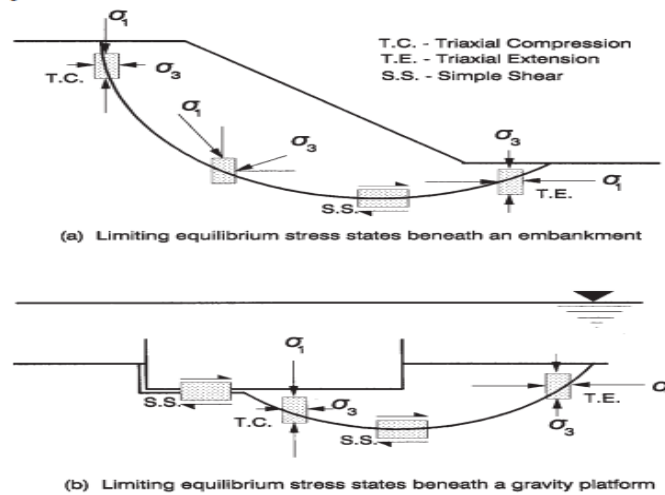


Figure 3 Examples of principal stress direction variation along potential failure surfaces. (Vaid et al 1997)

Saada (1988) states that “Most natural sands have anisotropic strength and deformation characteristics. This anisotropy is of two types. The first, inherent anisotropy, which is attributed to a preferred particle arrangement during gravitational sedimentation through either air or water. From such sand deposits if identical specimens are sheared under identical principal stress increments, but with directions inclined at different angles to the vertical, their response will be different. The second type is the stress-induced anisotropy. This is caused by straining leading to a continuous evolution of particle arrangement during shear loading.” Despite the large number of studies on the undrained response of saturated sands in triaxial or simple shear devices, only a few have dealt specifically with undrained anisotropy in these materials. These few studies have nevertheless established that the response is stress path dependent.

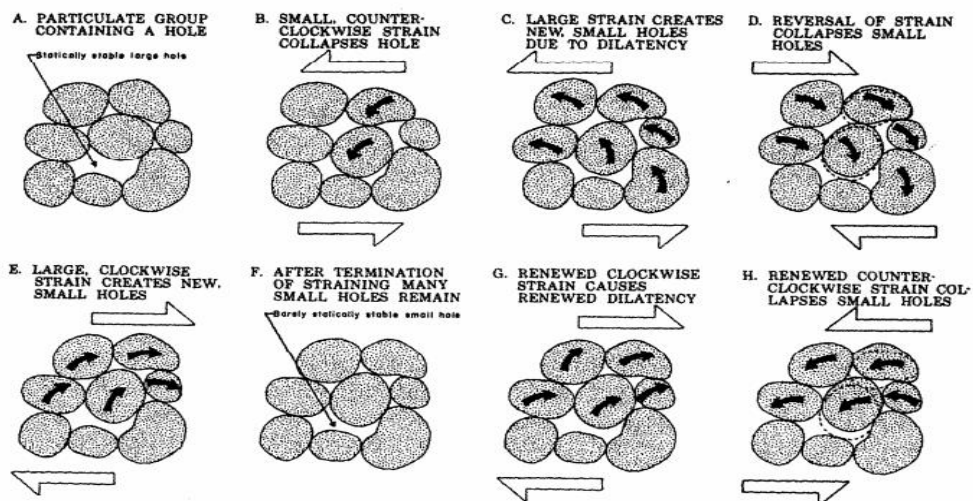


Figure 4 Sketch of a group of soil particles illustrating the change in packing during cyclic loading (Youd 1977)

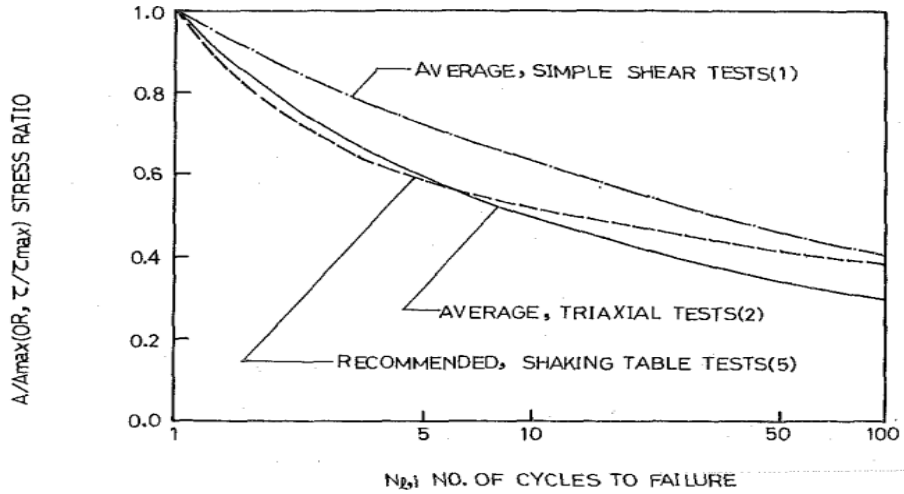


Figure 5 Typical Strength Degradation Curves for Soils against Liquefaction(Lin 1983)

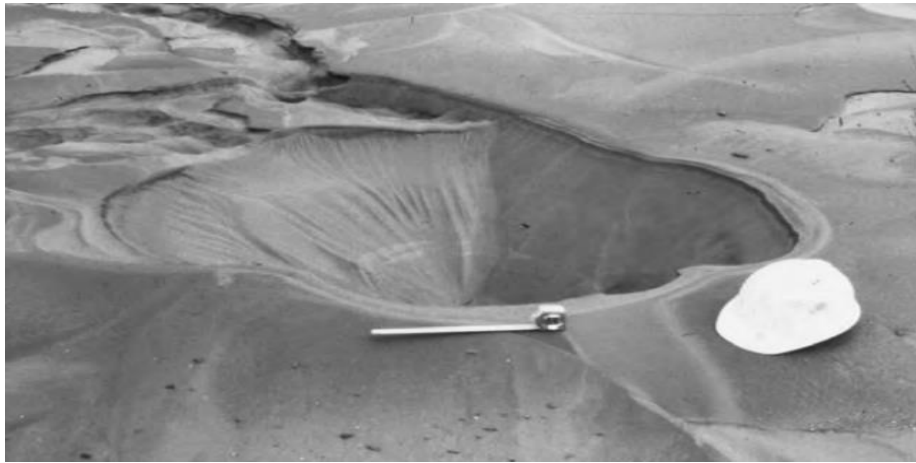


Figure 6 Sand boil after liquefaction-induced boiling from the 1989 Loma Prieta, California earthquake has ceased(EERI archives)



Figure 7 Deposition of liquefied sand through ground cracks Bhuj earthquake 2001 India(EERI archives)

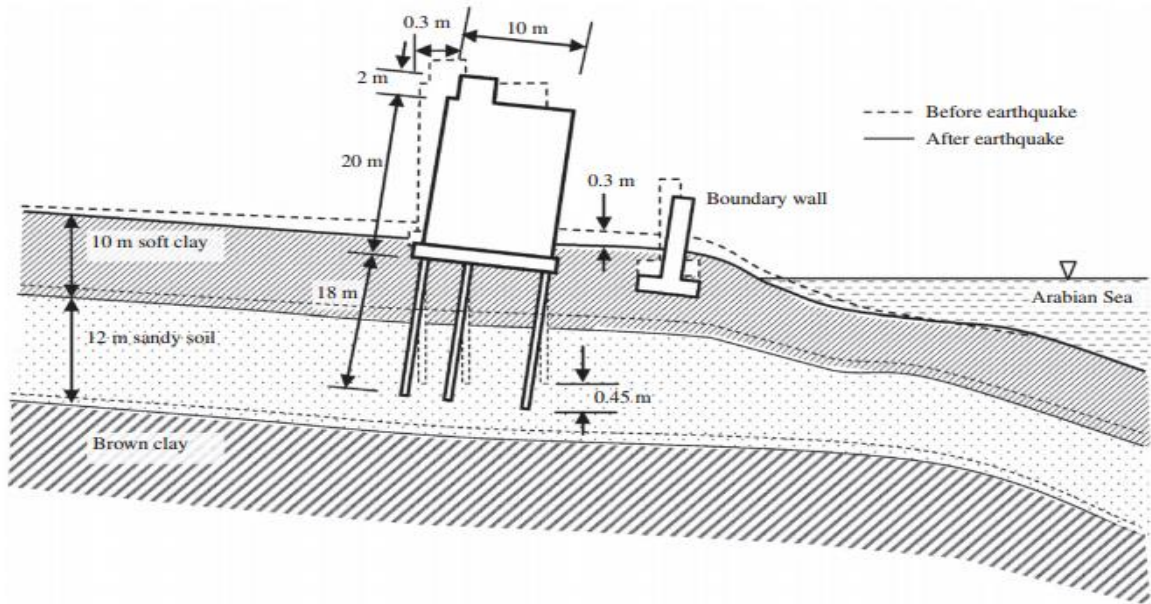


Figure 8 Plausible settlement mechanism of failure showing the tilting the Tower, assuming there is no structural failure of piles (Bhattacharya et al 2008)

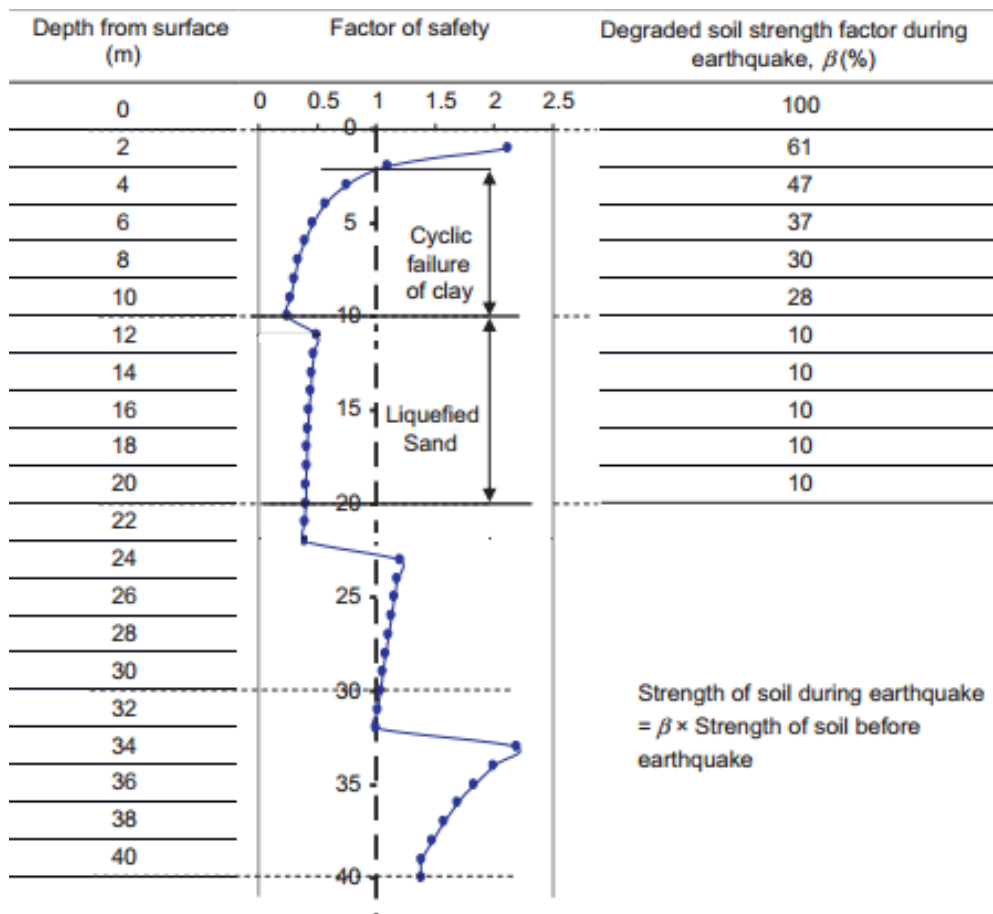


Figure 9 Factor of safety against cyclic mobility and liquefaction and percentage degradation in strength of soil during earthquake for the considered soil profile (Bhattacharya et al 2008)

2.1. Different types of cyclic loading

2.1.1. Cyclic stresses during earthquakes

Ishihara 1983 explained the behaviour of cyclic stresses in soil that “It has been generally accepted that the major part of the ground shaking during an earthquake is due to the upward propagation of body waves from an underlying rock formation. Although surface waves are also involved, their effects are generally considered of secondary importance. The body waves consist of shear waves and compressional (or longitudinal) waves. In the case of level ground, each of the waves produces, respectively, shear stress and compressional stress as illustrated in Fig. 10. During the propagation of compressional waves, normal stress is induced in the vertical as well as horizontal direction, thereby producing the triaxial mode of deformation in an element of soil under level ground.”

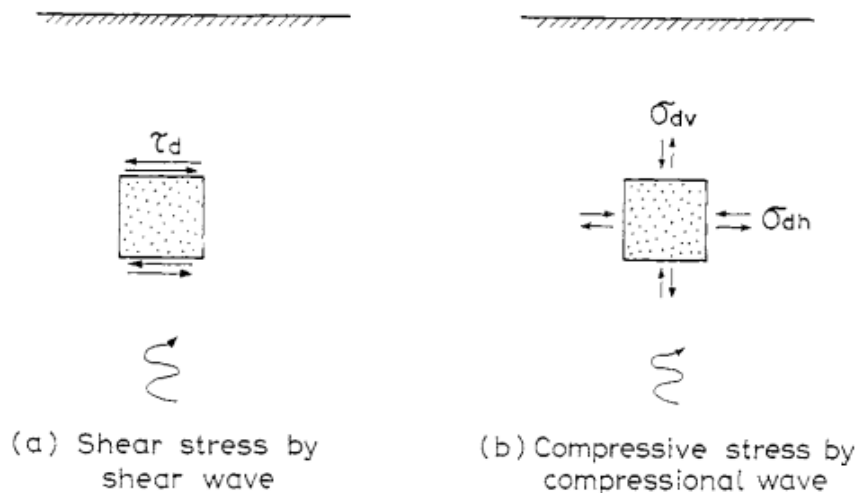


Figure 10 Stresses induced by body wave propagation(Ishihara 1983)

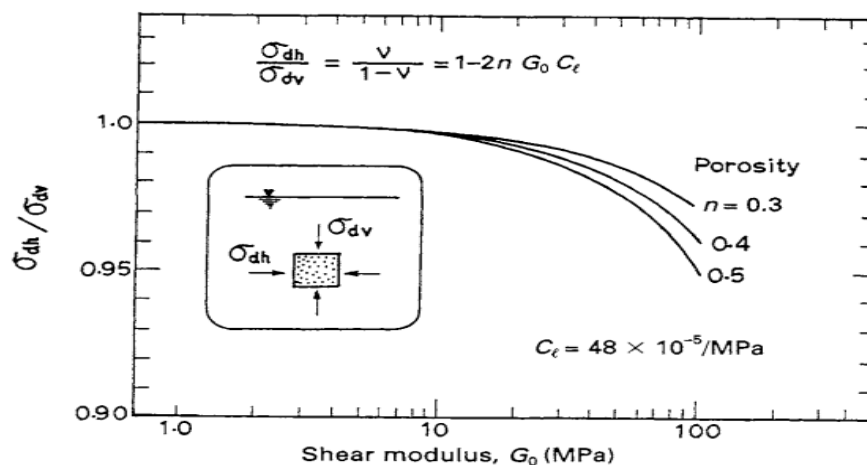


Figure 11 State of stresses induced by propagation of compressional wave(Ishihara 1983)

This implies the fact that the propagation of compressional wave through saturated soft soils induces almost purely compressional stress and the component of deviator stress σ_d , - σ_{dh} is practically equal to zero as shown in figure 11. Since the compressional stress is transmitted through water in the pores, there is no change in the effective stress induced by the compressional wave. For this reason, effects of the compressional wave are disregarded in evaluating the stability of the ground such as liquefaction and consequent settlements in sandy ground. Thus horizontal shear stress due to the propagation of shear waves is the main component of stress that is to be considered in one-dimensional stability analysis of level ground during earthquakes.

2.1.2. Traffic loading

Ishihara (1983) explained how traffic loading is cyclic. Since the traffic loading as encountered in pavements of roads or airfields may be represented for simplicity by an elastic half-space subjected to a uniform load of P_0 over the surface with a width of $2a$. According to the Boussinesq solution for the case of the two-dimensional plane strain condition, the stress components are given by

$$\begin{aligned}\sigma_{dv} &= \frac{P_0}{\pi} [\sigma_0 + \sin \theta_0 \cos(\theta_1 + \theta_2)] \\ \sigma_{dh} &= \frac{P_0}{\pi} [\sigma_0 - \sin \theta_0 \cos(\theta_1 + \theta_2)] \\ \tau_d &= \frac{P_0}{\pi} \sin \theta_0 \sin(\theta_1 + \theta_2) \\ \theta_0 &= \theta_2 - \theta_1\end{aligned}$$

Equation 1 traffic load stresses calculations(Ishihara 1983)

where θ_1 and θ_2 indicate the angles between the vertical and the lines connecting the edge of the loaded area to the point in question. as illustrated in Figure. 12

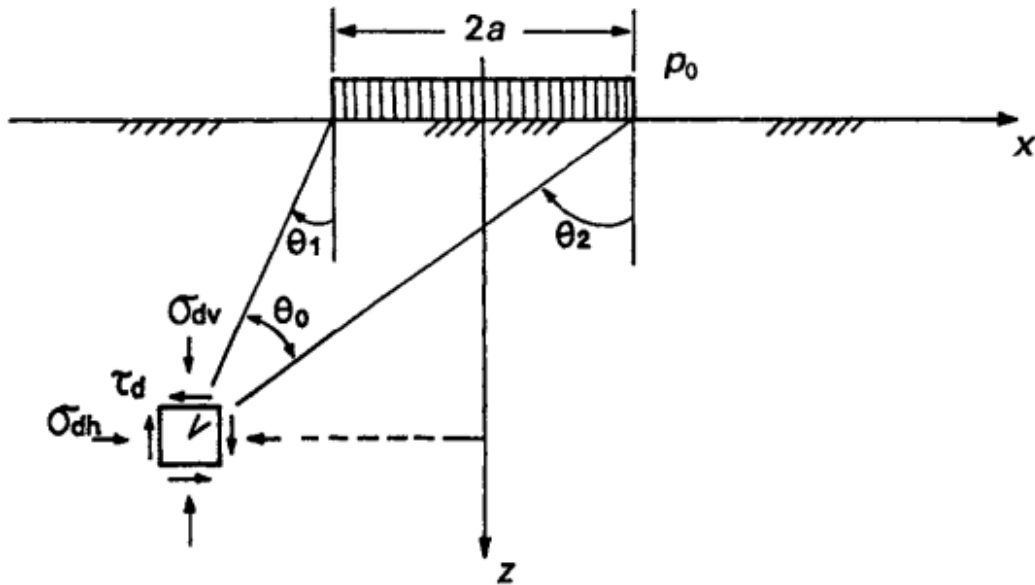


Figure 12 Uniform loads on an elastic half-space(Ishihara 1983)

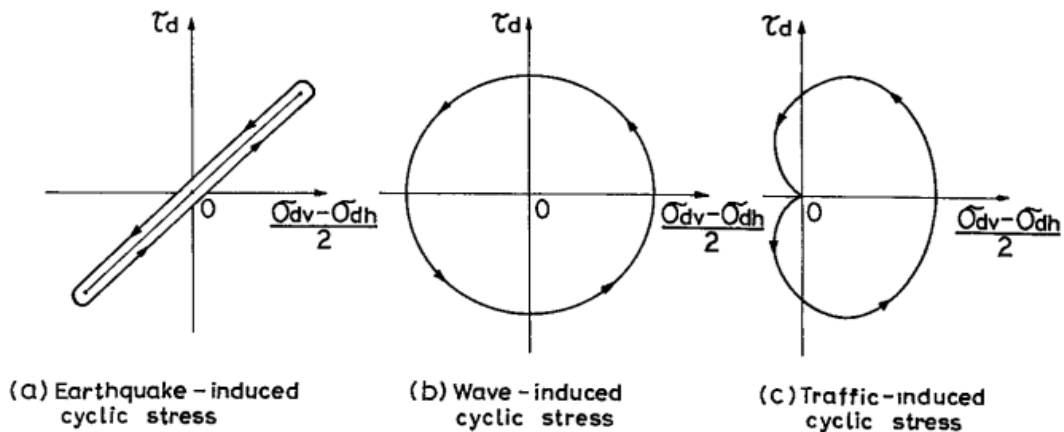


Figure 13 Characteristic changes in two shear stress components in three typical dynamic loading(Ishihara 1983)

2.1.3. Wave-induced loading

Ishihara 1983 explained the effect of waves induced loading on seabed as water waves propagating on the ocean may be considered to consist of an infinite number of wave trains having a constant amplitude and wave length. Passage of such an array of waves on the sea creates harmonic pressure changes on the sea floor, increasing the pressure under the crest and reducing it under the trough. The stresses induced in the seabed are, therefore, analyzed by applying a sinusoidally changing load on the horizontal surface from minus to plus infinity, as illustrated in Fig. 14. If the seabed deposit is assumed to consist of a homogeneous elastic half

space, the stresses can be readily determined by using the classical solution of Boussinesq for the two-dimensional plane strain problem. Assume that a harmonic load

$$p(x) = p_0 \cos\left(\frac{2\pi}{L}x - \frac{2\pi}{T}t\right)$$

Equation 2 two-dimensional plane strain problem for wave loading (Ishihara 1983) is distributed on the surface of an elastic half space, where P_0 is the amplitude of the load, L is the wave length and T is the period of waves. The vertical normal stress σ_{dv} , horizontal normal stress σ_{dh} and shear stress τ_d induced in the half-space by this load are determined (Yamamoto, 1978; Madsen, 1978) as

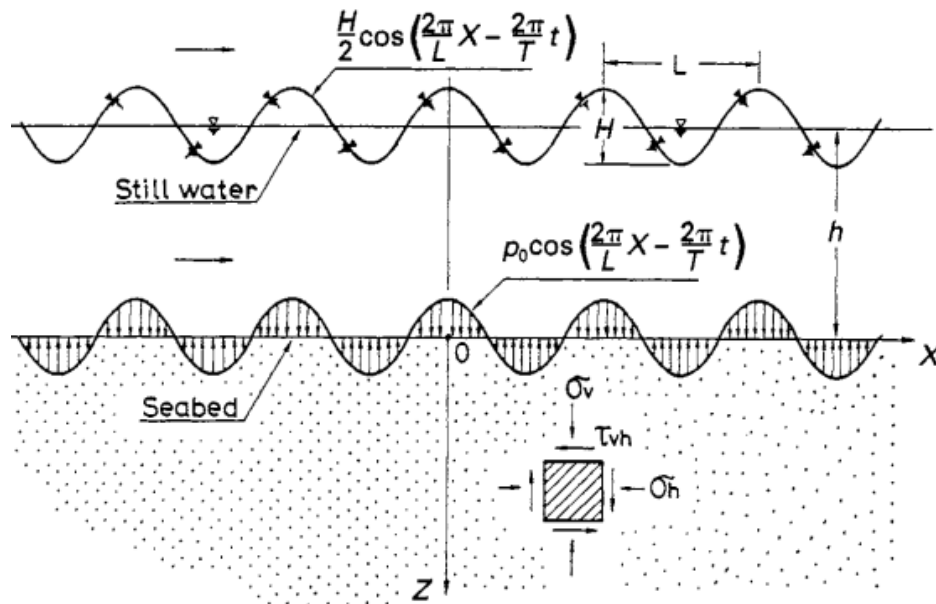


Figure 14 Wave-induced stresses in a seabed deposit(Ishihara 1983)

$$\sigma_{dv} = p_0 \left(1 + \frac{2\pi z}{L} \right) e^{-\frac{2\pi z}{L}} \cdot \cos\left(\frac{2\pi x}{L} - \frac{2\pi t}{T}\right)$$

$$\sigma_{dh} = p_0 \left(1 - \frac{2\pi z}{L} \right) e^{-\frac{2\pi z}{L}} \cdot \cos\left(\frac{2\pi x}{L} - \frac{2\pi t}{T}\right)$$

$$\tau_d = p_0 \frac{2\pi z}{L} e^{-\frac{2\pi z}{L}} \cdot \sin\left(\frac{2\pi x}{L} - \frac{2\pi t}{T}\right)$$

Equation 3 wave loading stress equations(Ishihara 1983)

It can be stated in summary that the cyclic change of shear stress induced in an elastic half space by a harmonic load moving on its surface is characterized by a continuous rotation of the principal stress direction with the deviator stress being always maintained constant. This is the characteristic feature of the cyclic change in stress induced in the seabed deposit by travelling waves on the sea (Ishihara and Yamazaki, 1984). The earthquake-induced loading is characterized by the jump rotation of the principal stress axes and its continuous rotation is an attribute to the cyclic loads induced by travelling sea waves and traffic as shown in fig 13.

2.2.Laboratory tests for cyclic loading

2.2.1. Simple Shear Test:

A schematic diagram of the direct shear test equipment is shown in Figure 15. Basically, the test equipment consists of a metal shear box into which the soil specimen is placed. The specimen can be square or circular in plan, about 3 to 4 (19.35 to 25.80 cm²) in area, and about 1 in (25.4 mm) in height. The box is split horizontally into two halves. Normal force on the specimen is applied from the top of the shear box by dead weights. The normal stress on the specimens obtained by the application of dead weights can be as high as 1035 kN/m². Shear force is applied to the side of the top half of the box to cause failure in the soil specimen. (The two porous stones shown in Figure 15 are not required for tests on dry soil). During the test, the shear displacement of the top half of the box and the change in specimen thickness are recorded by the use of horizontal and vertical dial gauges.

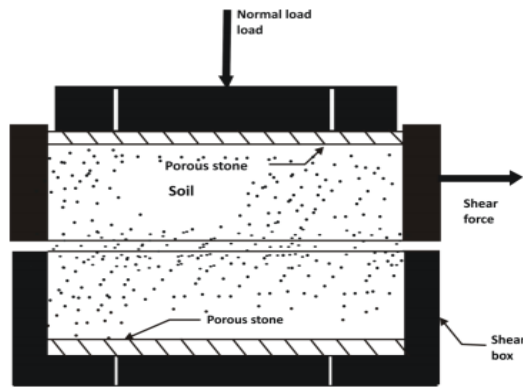


Figure 15 simple shear test apparatus (Venkataramaiah 2006)

Two variations of simple shear apparatus are available namely stress controlled simple shear test and strain controlled simple shear test as shown in figure 16 and 17

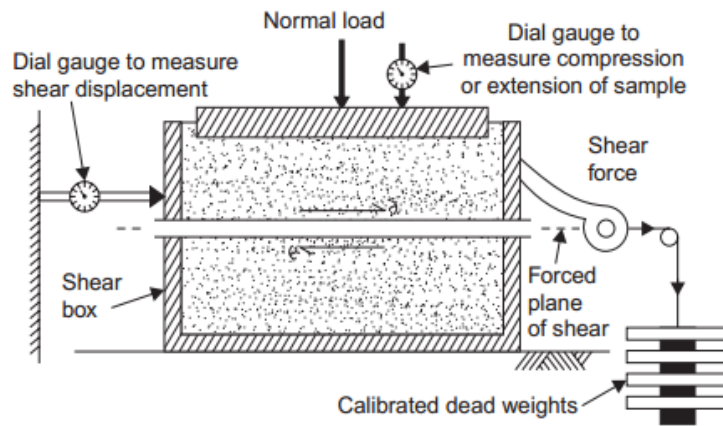


Figure 16 stress controlled shear test (Venkataramaiah 2006)

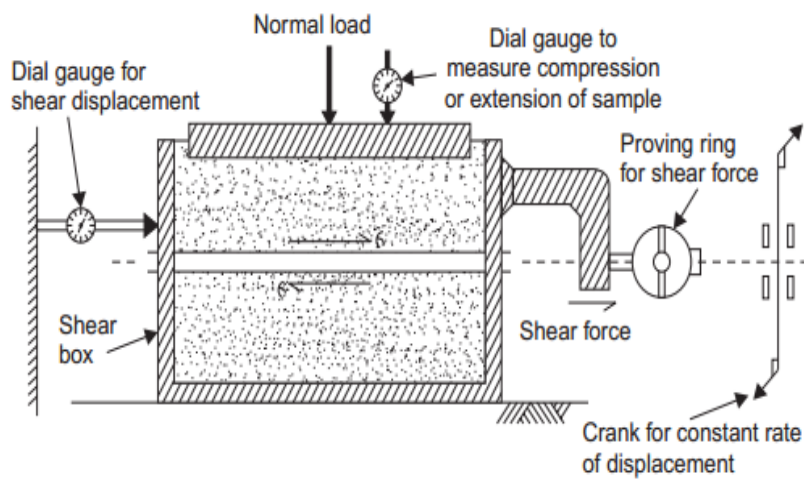


Figure 17 strain controlled shear test (Venkataramaiah 2006)

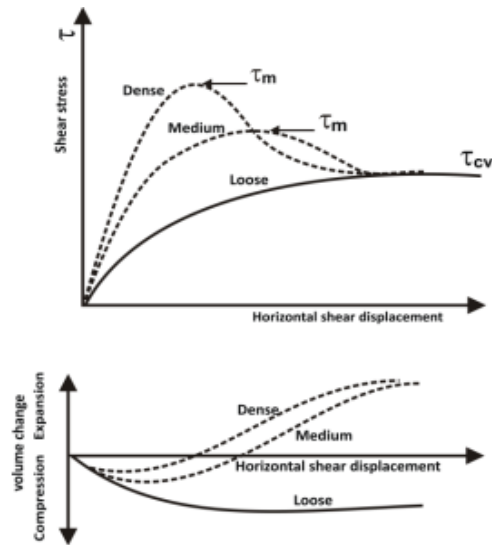


Figure 18 Direct shear test results in loose, medium and dense sands (Venkataramaiah 2006)

2.2.2. Triaxial Test

A schematic diagram of a triaxial test equipment is shown in Figure 19. In this type of test, a soil specimen about 1.5 in (38.1 mm) in diameter and 3 in (76.2 mm) in length is generally used. The specimen is enclosed inside a thin rubber membrane and placed inside a cylindrical plastic chamber. For conducting the test, the chamber is usually filled with water or glycerine. The specimen is subjected to a confining pressure σ_3 by application of pressure to the fluid in the chamber. (Air can sometimes be used as a medium for applying the confining pressure). Connections to measure drainage into or out of the specimen or pressure in the pore water are provided. To cause shear failure in the soil, an axial stress $\Delta\sigma$ is applied through a vertical loading ram. This is also referred to as deviator stress. For determination of ϕ dry or fully saturated soil can be used. If saturated soil is used, the drainage connection is kept open during the application of the confining pressure and the deviator stress. Thus, during the test the excess pore water pressure in the specimen is equal to zero. The volume of the water drained from the specimen during the test provides a measure of the volume change of the specimen.

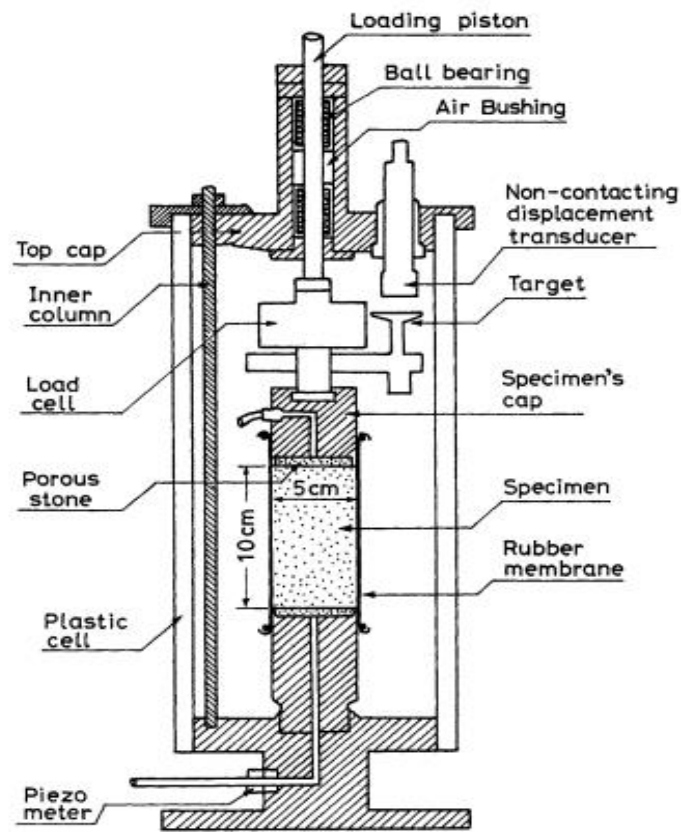


Figure 19 Triaxial test apparatus(Ishihara 1996)

2.2.3. Cyclic Triaxial Test

One of the most important features required of the cyclic triaxial test is that it should be capable of applying extensional loads to the specimen's cap so that a state of triaxial extension can be produced cyclically in the specimen without changing the chamber pressure. This is necessary to achieve the so-called two-way loading in which cyclic stresses reverse its direction between the triaxial compression and extension. For this purpose, the vertical piston should be firmly connected to the specimen's cap. An example of the assemblage for the cyclic biaxial test is shown in Fig. 20. In this system, air pressure is generated by a compressor and transmitted to two different static loading paths. The first is the chamber pressure system. The air pressure controlled by B is transmitted to a tank B after being reduced to a desired pressure by a pressure regulator. This air pressure is transmitted to water leading to the triaxial chamber. Since the vertical stress induced by the chamber pressure is smaller than the horizontal stress due to the existence of the vertical rod within the cell, it is generally necessary to have another

system to apply an additional vertical stress which can be achieved by the regulator A indicated in Fig. 20.

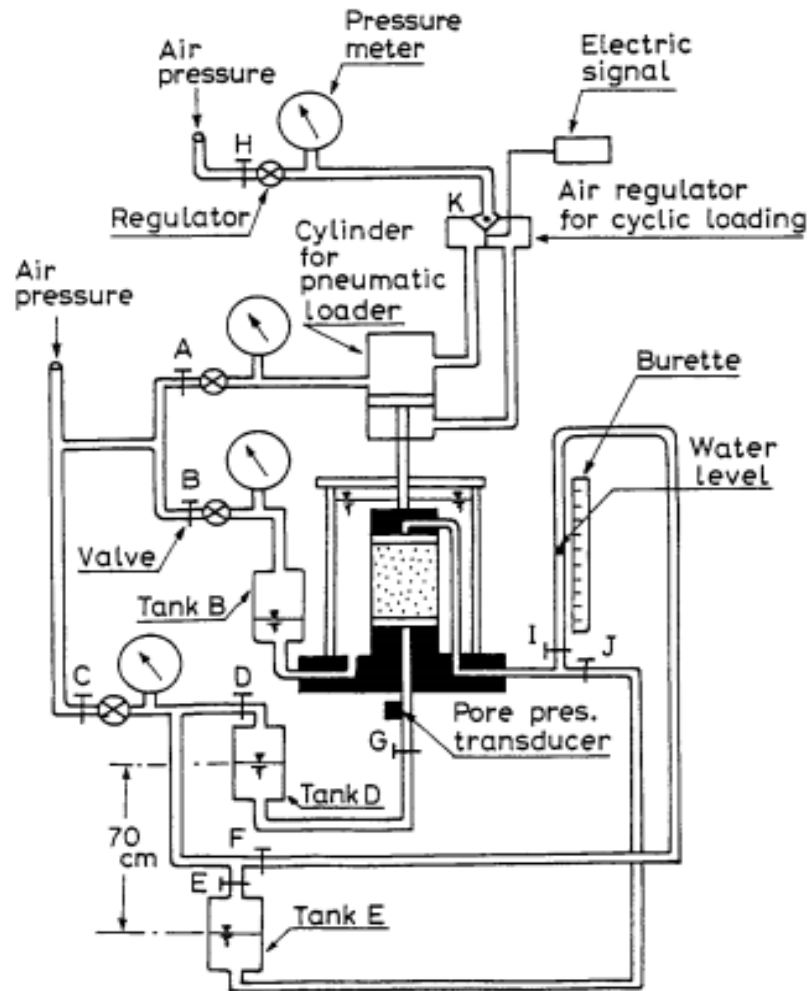


Figure 20 cyclic triaxial setup (Ishihara 1996)

The cyclic axial stress is produced either by means of a pneumatic loader mechanism or an electro-hydraulic system. In the pneumatic system, an air regulator is used to control the movement of the loading piston with a desired amplitude and frequency. A function generator is used to feed signals to the regulator. Signals of irregular time sequence retrieved from a magnetic tape can also be fed to the air regulator. The loading ram is driven by the compressed air which is controlled by the air regulator K in Fig. 20. The cyclic loader connected to the piston of the triaxial apparatus is thus capable of producing any irregular wave form to be transmitted to the soil specimen within the cell. Any time sequence of irregular wave forms stored on a magnetic tape or computer diskette can be retrieved as an analog command and transmitted to the loader which is driven by air pressure.

2.2.4. Cyclic simple shear test

If connected to the cyclic loader, any type of simple shear test apparatus can be used for testing soil specimens under cyclic or dynamic loading conditions. One of the models as it sits with the forming mould is shown in Fig. 21. The specimen enclosed by the rubber membrane is flanked by a stack of ring-shaped Teflon rings so that the simple shear mode of deformation can be produced by inhibiting the displacement in the lateral direction. When the vertical stress is applied at the stage of consolidation the lateral stress is induced in accordance with the K_0 condition. When the cyclic stress is applied undrained, the pore pressure builds upon within the saturated specimen and reaches a value in excess of the initial lateral stress induced under the K_0 condition. In this situation, the rubber membrane tends to expand and even to extrude from a thin space at the upper periphery of the specimen.

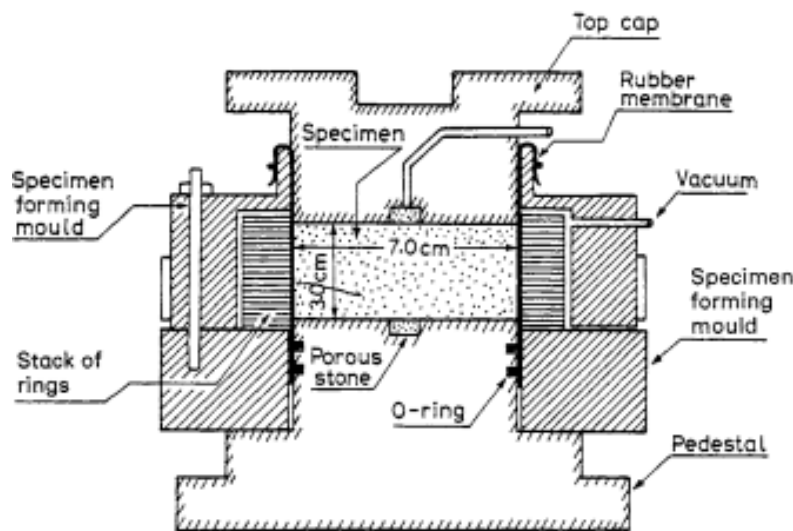


Figure 21 cyclic shear mould(Ishihara 1996)

To avoid this undesirable situation, the simple shear device as shown in Fig. 21 needs to be put inside the chamber. If a cell pressure equal to the vertical stress is applied to produce initially an isotropic state of consolidation the simple shear test can be performed without difficulty. The conduct of such tests is described by Ishihara and Yamazaki (1980). It is generally difficult to perform simple shear tests in ideal conditions because of several other disadvantages such as non-uniformity of strain distribution. If the cyclic loaders are connected to the specimen's top cap in two horizontal mutually perpendicular directions, multidirectional simple shear tests can be conducted. This type of arrangement is shown in Fig. 22

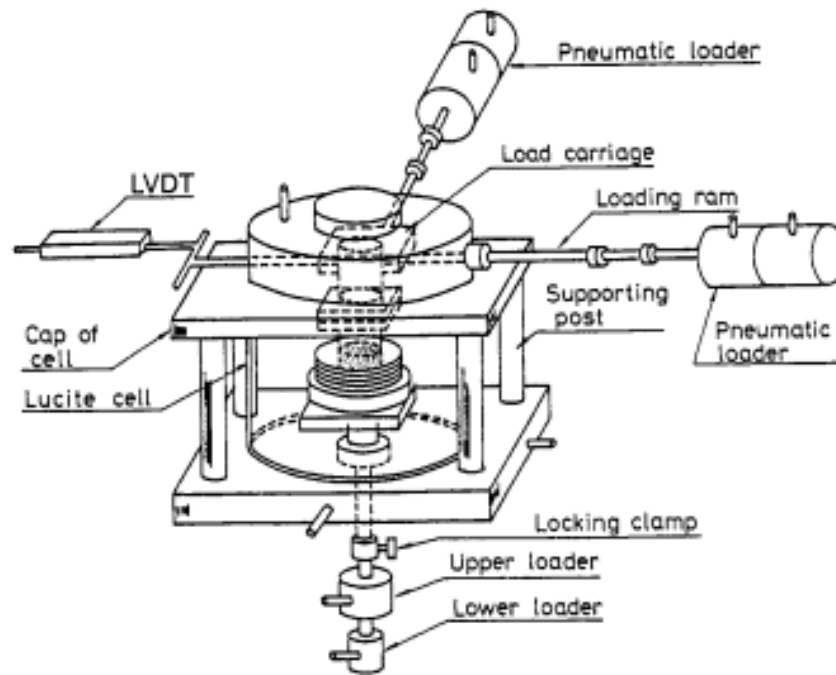


Figure 22 Simple shear test apparatus with two-directional loading device(Ishihara 1996)

2.2.5. Torsional shear test apparatus

A solid cylindrical or hollow cylindrical specimen can be tested in the torsional test apparatus. The tests on solid cylindrical specimens have a shortcoming in that the strain distribution is not uniform in the radial direction in the horizontal plane of the sample. To minimize this effect, the use of the hollow cylindrical samples has been preferred in recent years.

There are several design models in use, and one of the pieces developed in Japan is displayed in Fig. 23 In this type of apparatus, four components of stress, namely vertical, torsional, and two lateral stresses (inner and outer cell pressures) can be applied to the specimen under controlled conditions. By connecting the inner and outer cells, the tests are commonly performed under the condition of equal lateral stress. By means of what is called the torsional test apparatus, the triaxial loading tests can also be performed. It is further possible to have a specimen subjected to any combined application of torsional and triaxial shear stresses. Thus complex stress change involving rotation of principal stress axes can be produced in the test specimen (Ishihara and Towhata, 1983; Towhata and Ishihara, 1985). The torsional apparatus is versatile and useful for investigating basic aspects of deformation characteristics of soils, but for practical purposes it may not be suitable

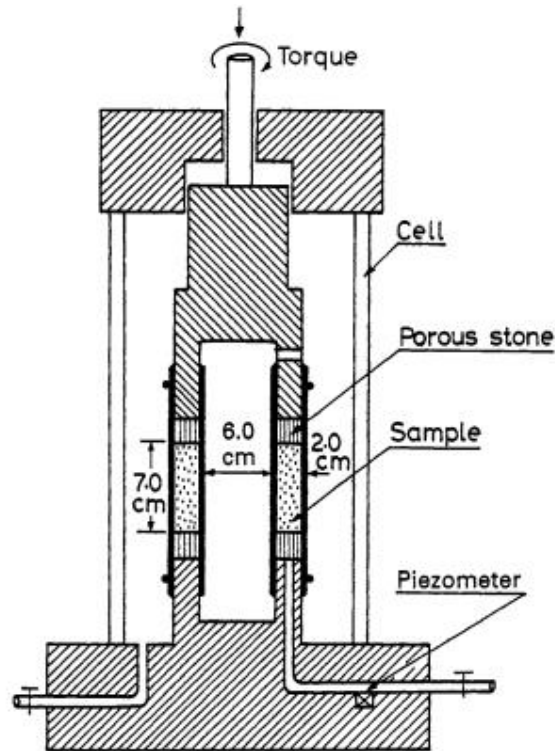


Figure 23 Hollow-cylindrical torsional test apparatus(Ishihara 1996)

Hollow cylinder torsion (HCT) apparatus is an advanced triaxial testing apparatus which is capable of applying complex boundary conditions to study the effect of intermediate principal stress and anisotropy on the mechanical behaviour of granular and c- ϕ materials. This apparatus like any other fully automated triaxial set up is capable of performing tests on any geo material under different drainage conditions. GDS Instruments Limited, UK, are the pioneers of developing advanced geotechnical instruments. The automated hollow cylinder torsion testing system used in this study is developed by GDS Instruments. This HCT apparatus provided an independent control of the axial load (W – measured with a load cell of capacity = 10 kN), torque (M_T – measured with a torque cell of capacity 100 Nm), internal and external pressures (P_i & P_o respectively – measured with pressure volume controllers of capacity 2 MPa). By controlling the load, torque, internal and external pressure one can independently control four out of the six independent components of the stress tensor (Eqn.4). This is the only apparatus that has the ability to control the maximum stress components of a stress tensor. The ability to control the four stress components independently allows control of the direction and the magnitude of the principal stresses. The average axial, radial, tangential and shear stresses on an element is obtained by solving the balance equations (Hight et al., 1983). The average axial displacements, and rotation angles were measured using high precision digital encoders,

while the change in the volume of the specimen was recorded using the digital pressure volume controllers (DPVC). (Parthiban et al., 2016)

$$[\sigma] = \begin{pmatrix} \sigma_r & 0 & 0 \\ 0 & \sigma_\theta & \tau_{\theta z} \\ 0 & \tau_{z\theta} & \sigma_z \end{pmatrix}$$

Equation 4 stress parameters for hollow cylinder tests(Kandasami 2015)

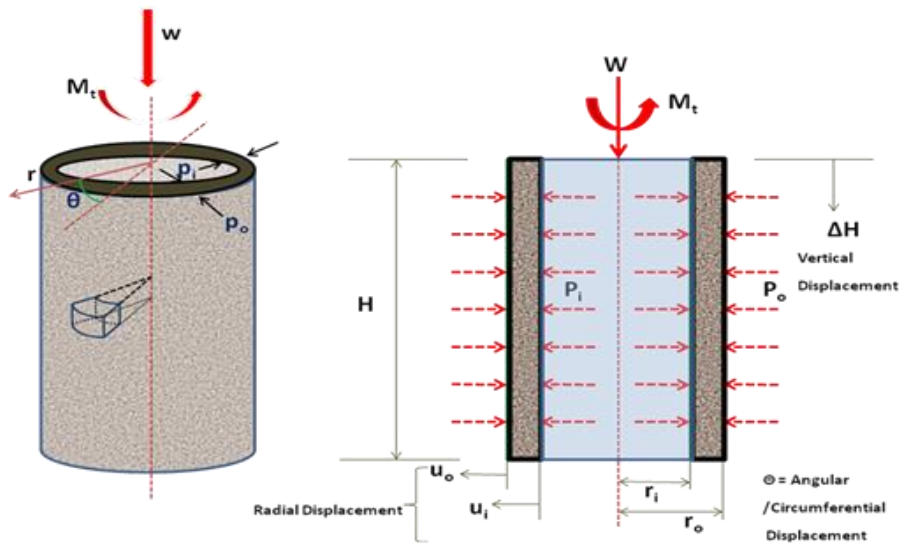


Figure 24 Hollow cylinder stress states (Kandasami 2015)



Figure 25 An image of HCT apparatus with specimen inside HCT cell (Singh, Kandasami and Murthy 2017)

2.2.6. Resonant column test

In this test, a solid or hollow cylindrical column of soil specimen is fixed in place in a triaxial cell and set into motion in either the torsional or longitudinal mode of vibration. The frequency of the electro-magnetic drive system is changed until the first mode resonant condition is encountered in the soil specimen. With known value of the resonant frequency, together with the sample geometry and conditions of end restraint, it is possible to back-calculate the velocity of wave propagation through the soil specimen. After finishing the measurement at the resonant condition, the drive system is cut off and the specimen is brought to a state of free vibration. By observing the decaying pattern of the free vibration, the damping property of the soil specimen is determined. The above procedure is repeated several times with stepwise increased power of the driving force. As the driving force is increased, the specimen is tuned to resonate with a lower frequency because of the reduction in stiffness caused by increased level of induced shear strain. In the phase of the free vibration test that follows, an increased damping ratio would be obtained because of higher level of nonlinearity of the specimen due to the increased shear strain. As a result of several sequences of the tests, a set of data will be obtained for the velocity and damping ratio as functions of shear strains. There are several versions in the resonant column test apparatus employing different conditions to constrain the specimen's deformation at the top and bottom ends. The most commonly used conditions at the ends are displayed in Fig. 25 for the case of the tests employing the torsional mode of vibration. In the model shown in Fig. 25(a), the specimen is excited at the bottom and the response is picked up at the top end in terms of either velocity or acceleration.

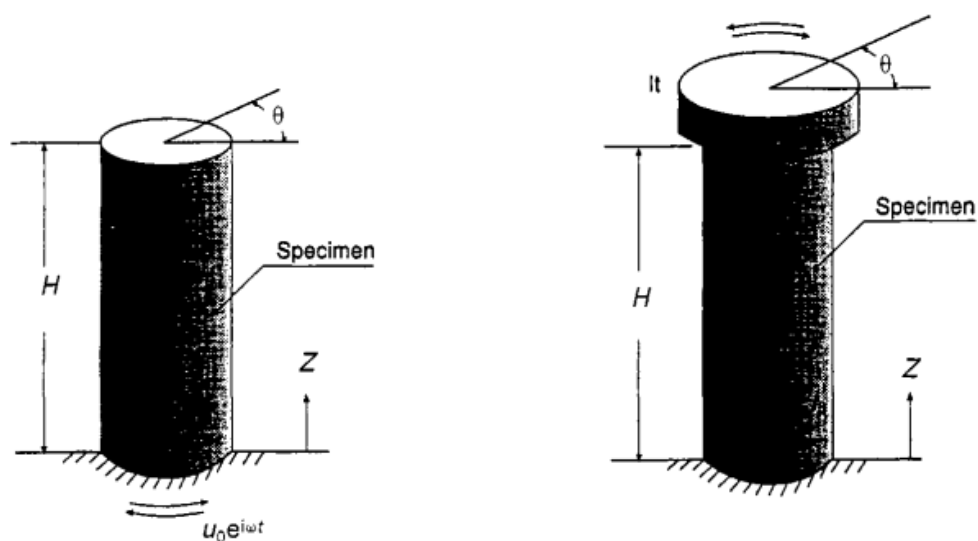


Figure 26 a) Base - excited top - free type b) Top - excited type resonant column (Ishihara 1996)

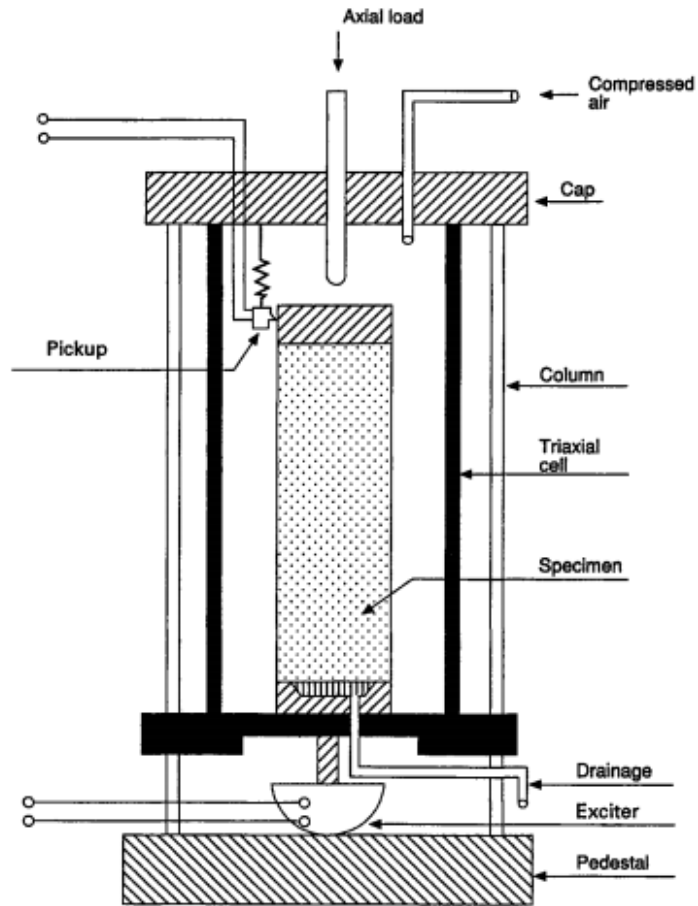


Figure 27 Bottom exciting type resonant column test device (Shannon et al. 1959)

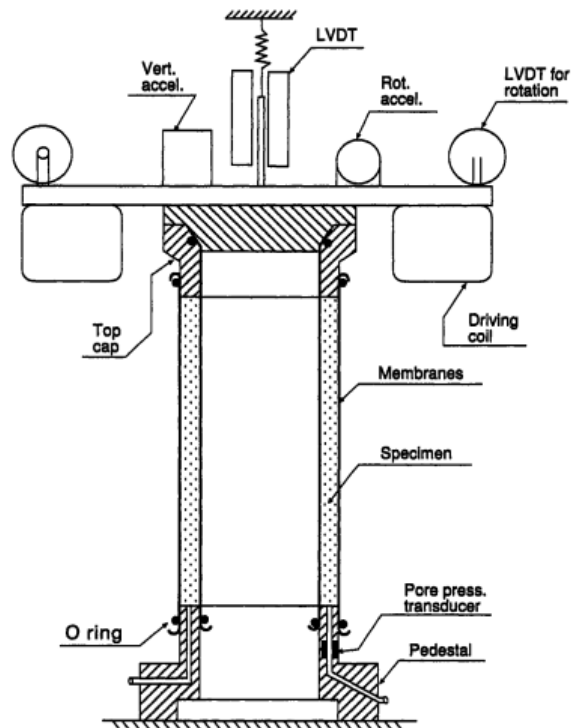


Figure 28 Resonant column test apparatus (Drnevich, 1972)

2.3. Factors influencing cyclic loading

2.3.1. Effect of particle size and relative density

Loose sand deposits that are prone to liquefaction during an earthquake are also susceptible to settlement, which has proven to be very damaging to structures, pavements, and lifelines. However, estimating settlement resulting from seismic shaking is a difficult proposition and errors of 50% or more can be expected when making predictions (Kramer, 1996). Although detailed ground response analysis can be conducted to estimate settlements, and this may be necessary for dams or other instances where the ground surface is non level, a simplified procedure may be sufficient in many cases (Tokimatsu and Seed, 1987). Liquefaction settlement in dry sands is a function of the density of the soil, the number of strain cycles and the magnitude of the cyclic shear strain induced by seismic shaking (Silver and Seed, 1971).

An effective shear strain, γ_{eff} , can be calculated from the average cyclic shear stress, τ_{av} , as follows:

$$\gamma_{eff} = \frac{\tau_{av}}{G_{max} \left(\frac{G_{eff}}{G_{max}} \right)}$$

Equation 5 effective density

where G_{max} is the small-strain shear modulus and G_{eff} the effective shear modulus

$$G_{max} = 1,000 \times (K_2)_{max} \times (\sigma'_m)^{1/3}$$

Equation 6 maximum shear modulus by field data

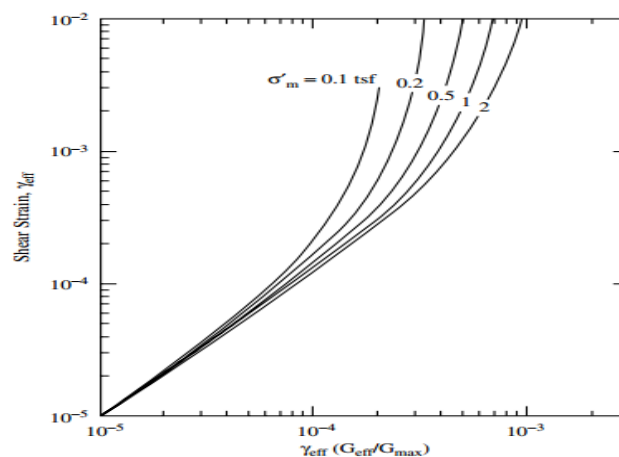


Figure 29 Induced strain in sand deposits.(Tokimatsu, K. and H.B. Seed. 1987)

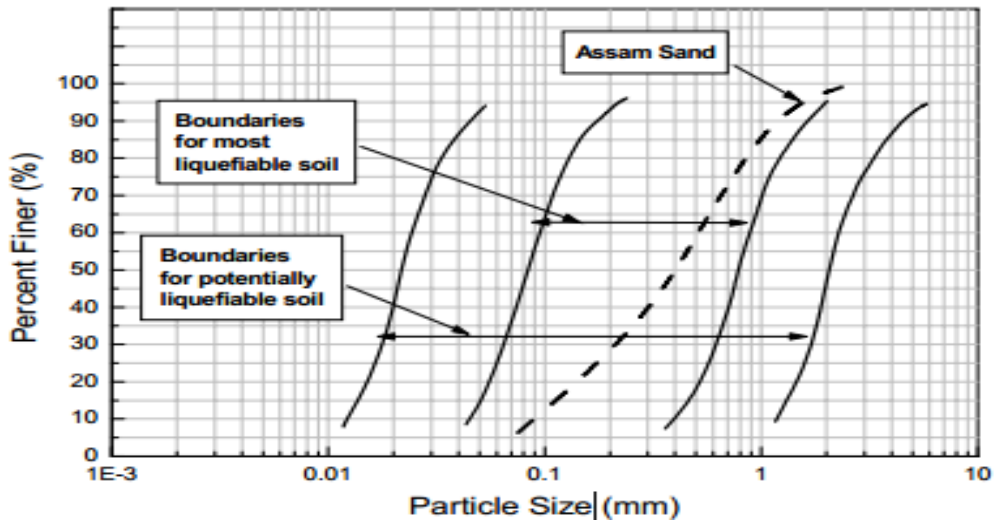


Figure 30 Grain size distribution of soil liquefaction proposed by (Iwasaki, 1986)

Table 1 Reference values for calculating maximum shear modulus G proposed by Seed et al. (1972)

Relative density D_r	$(K_2)_{max}$	Void ratio, e	$(K_2)_{max}$
30	34	0.4	70
40	40	0.5	60
45	43	0.6	51
60	52	0.7	44
75	59	0.8	39
90	70	0.9	34

Cyclic stress-controlled tests indicate that the factors such as fabric and its associated anisotropy, stress-strain history, applied stress path and aging, etc., affect the cyclic strength as well as shear modulus of sands (Drnevich and Richart, 1970; Seed and Idriss, 1971; Hardin and Drnevich, 1972; Pyke et al., 1974; Anderson and Stokoe, 1977; Dobry and Ladd, 1980). As demonstrated by Dobry et al., (1982), if both cyclic shear strength (τ) and shear modulus (G) are influenced by the above factors, then the ratio $\gamma = (\tau/G)$ may be affected less by the same factors (in which γ shear strain). Further, the pore pressure buildup in soils using strain-controlled tests will be less sensitive to the above factors than in stress-controlled tests.

The effect of frequency on liquefaction of soils were also studied by Wong et al. (1975) and Wang and Kavazanjian (1989) using stress-controlled technique. However, the effect of frequency on pore water pressure build up and liquefaction potential of soils using strain controlled technique remains unexplored. Also, studies were carried out by Lin and

Huang (1996) employing cyclic torsional shear tests on dry Ottawa sands under constant volume conditions to study the effect of frequency on shear moduli and damping ratios in the range of shear strains 0.004 % to 0.01%.

Talaganov (1996) conducted cyclic triaxial strain-controlled tests on dry and saturated sands reconstituted at relative densities ranging from 44% to 85% under constant volume conditions. Tests were conducted on these samples at confining pressures of 100, 200 and 300 kPa. In case of dry sands, as a result of cyclic shearing in constant volume conditions a decrease in initial effective confining pressure of the sample takes place. The effect of pore pressure increase in saturated samples was simulated through the decrease in initial pressure. Based on the analysis of the results,

Talaganov (1996) indicated that the relationship between normalized pore water pressures and normalized cycles is different from the standard relationships obtained by the application of the stress-controlled tests. Instead of having a tendency of separating the different relationships between the amplitude of shear strain and the number of cycles for pore water pressure build up based on separate relative density and confining pressure, there exists a single relationship range between normalized pore pressures and normalized cycles for prediction of pore water pressure build up for all relative densities and confining pressures. The relationship is shown in figure 28. But, these studies by Talaganov (1996) do not account for the effect of frequencies on pore pressure build up. Govindaraju (2007) took into account the effect of frequency on pore water pressure build up is explored by plotting the data for Assam sand along with the bounds reported by Talaganov (1996) (Fig.29). As observed from this figure, it is clear that the data obtained at ten cycles fall within the band suggested by Talaganov (1996) which indicates that the pore water pressure builds up in sands is independent of frequency of cyclic loading.

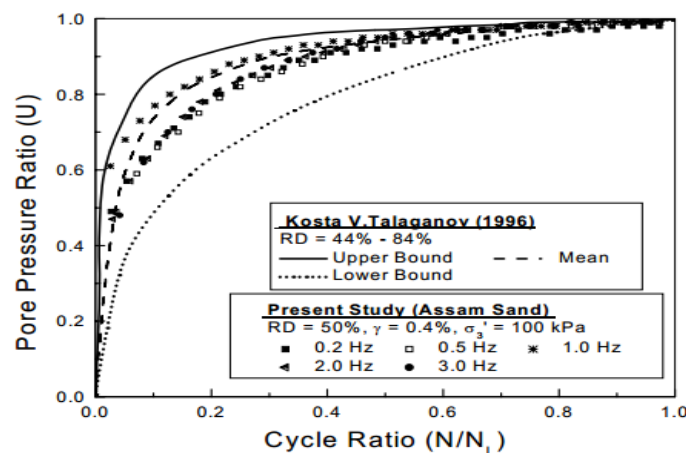


Figure 31 Relationship between normalized pore pressure ratio and cycle ratio (Govindaraju et al 2007)

2.3.2. Effect of void ratio and presence of fines

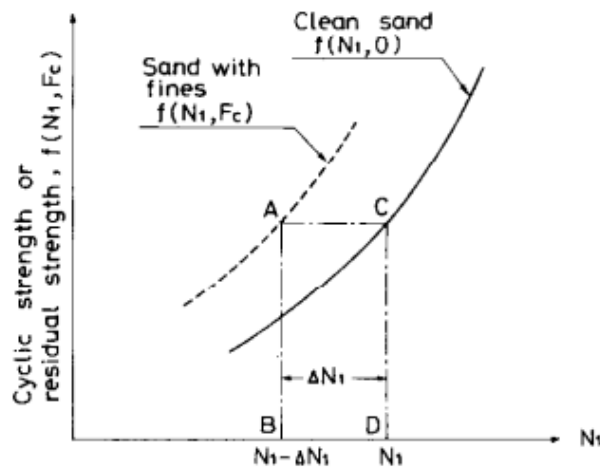


Figure 32 Effect of void ratio on cyclic loading(Seed 1982)

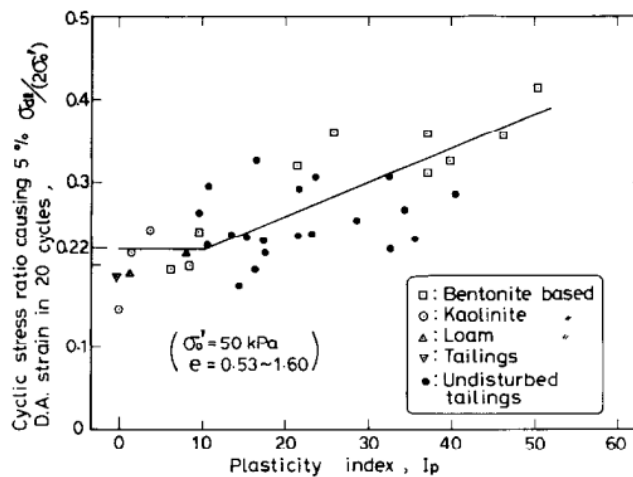


Figure 33 Effects of plasticity index on the cyclic strength(Ishihara 1993)

In any type of laboratory test, the shear modulus at small strains of cohesionless soils is measured under different effective confining stresses σ_b for various states of packing represented by different void ratios e . In the early works by Hardin and Richart (1963), the effects of void ratio were found to be expressed in terms of a function $F(e)$ as

$$F(e) = \frac{(2.17 - e)^2}{1 + e} \text{ or } F(e) = \frac{(2.97 - e)^2}{1 + e}.$$

Equation 7 Empirical relationship for void ratio(Richart 1963)

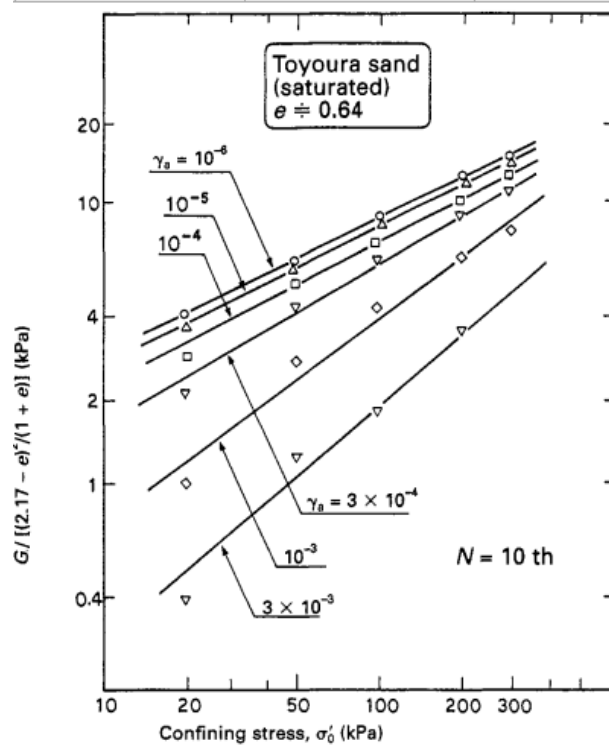


Figure 34 Effects of confining stress on shear modulus (Kokusho, 1980).

Table 2 Constants in proposed empirical equations on shear strain modulus: G_0 (Kokusho, 1987)

	References	A	$F(e)$	n	Soil material	Test method
Sand	Hardin-Richart (1963)	7000	$(2.17 - e)^2 / (1 + e)$	0.5	Round grained Ottawa sand	Resonant column
		3300	$(2.97 - e)^2 / (1 + e)$	0.5	Angular grained crushed quartz	Resonant column
	Shibata-Soelarno (1975)	42000	$0.67 - e / (1 + e)$	0.5	Three kinds of clean sand	Ultrasonic pulse
	Iwasaki <i>et al.</i> (1978)	9000	$(2.17 - e)^2 / (1 + e)$	0.38	Eleven kinds of clean sand	Resonant column
	Kokusho (1980)	8400	$(2.17 - e)^2 / (1 + e)$	0.5	Toyoura sand	Cyclic triaxial
	Yu-Richart (1984)	7000	$(2.17 - e)^2 / (1 + e)$	0.5	Three kinds of clean sand	Resonant column
Clay	Hardin-Black (1968)	3300	$(2.97 - e)^2 / (1 + e)$	0.5	Kaolinite, etc.	Resonant column
	Marcuson-Wahls (1972)	4500	$(2.97 - e)^2 / (1 + e)$	0.5	Kaolinite, $I_p^{**} = 35$	Resonant column
		450	$(4.4 - e)^2 / (1 + e)$	0.5	Bentonite, $I_p = 60$	Resonant column
	Zen-Umehara (1978)	2000 ~ 4000	$(2.97 - e)^2 / (1 + e)$	0.5	Remolded clay, $I_p = 0 \sim 50$	Resonant column
	Kokusho <i>et al.</i> (1982)	141	$(7.32 - e)^2 / (1 + e)$	0.6	Undisturbed clays, $I_p = 40 \sim 85$	Cyclic triaxial

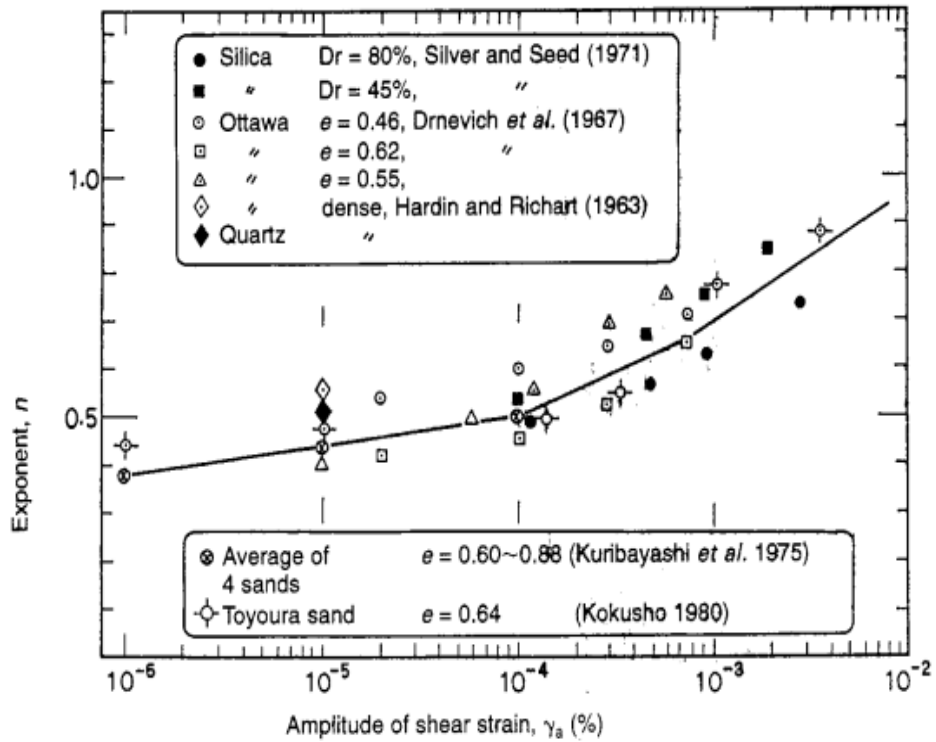


Figure 35 Effect of strain amplitude on confining stress (Kokusho, 1987)

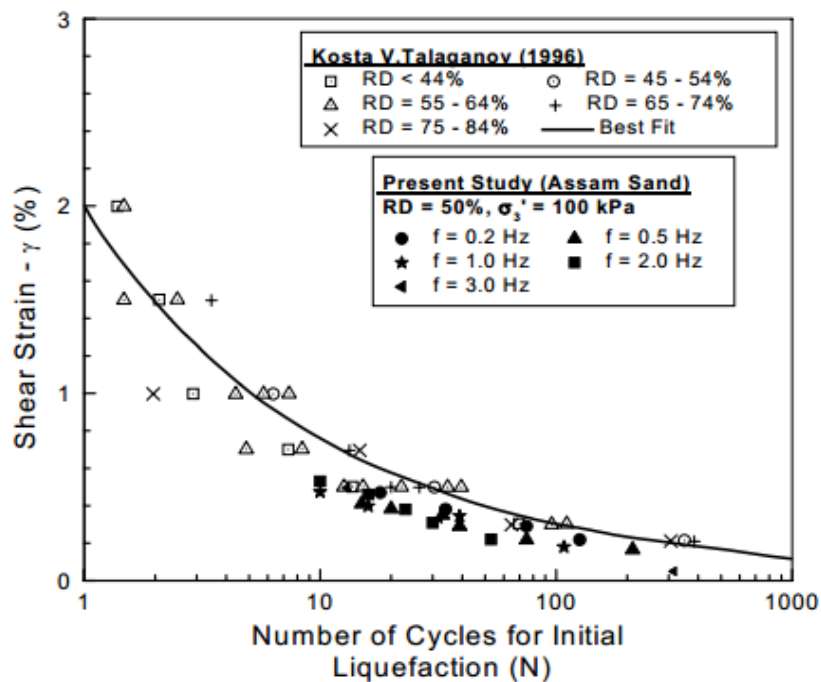


Figure 36 Relationship between shear strain and number of cycles for initial liquefaction at varying frequencies (Govindaraju et al 2007)

Youd 1972 experimented on cyclic loading of sands and found that “Drained cyclic loading with shear stress reversals can cause a net contraction (densification) of sand over a wide range of relative densities. This is why vibration is effective in compacting dry sand to a high relative

density. The progressive densification of a sand specimen subjected to strain-controlled, drained, cyclic loading is shown in Figure 36. The specimen went through alternating cycles of incremental contraction (a decrease in void ratio) and incremental dilation (an increase in void ratio), with the net effect being an accumulation of contractive strains. As shown in the figure, the initial shear loading caused the specimen to contract from point A to point B, after which further shear loading caused incremental dilation from point B to point C. At point C, the specimen was looser than it was at the start of the test (that is, at point A). Upon reversal of the shear loading, the specimen then incrementally contracted from point C to point D (where it was now denser than at the start of the test) before it transitioned to incremental dilation from point D to E. This process repeated within each cycle of shear loading, resulting in a steady accumulation of net contractive strains. The specimen became progressively denser as cyclic loading continued, with the change in void ratio per loading cycle becoming progressively smaller.”

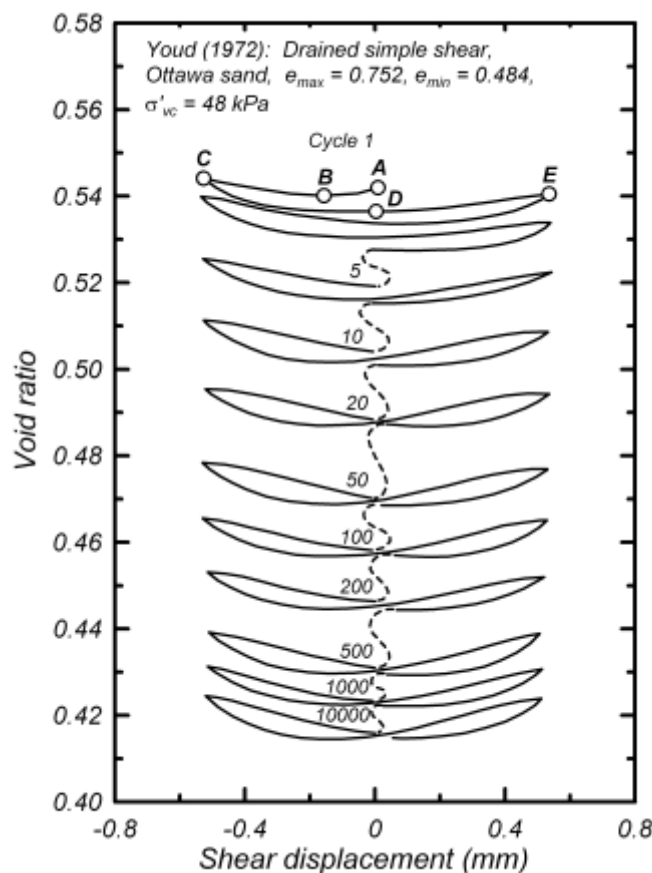


Figure 37 Void ratio versus cyclic shear displacement, showing densification of a sand specimen with successive cycles of drained simple shear loading (Youd 1972)

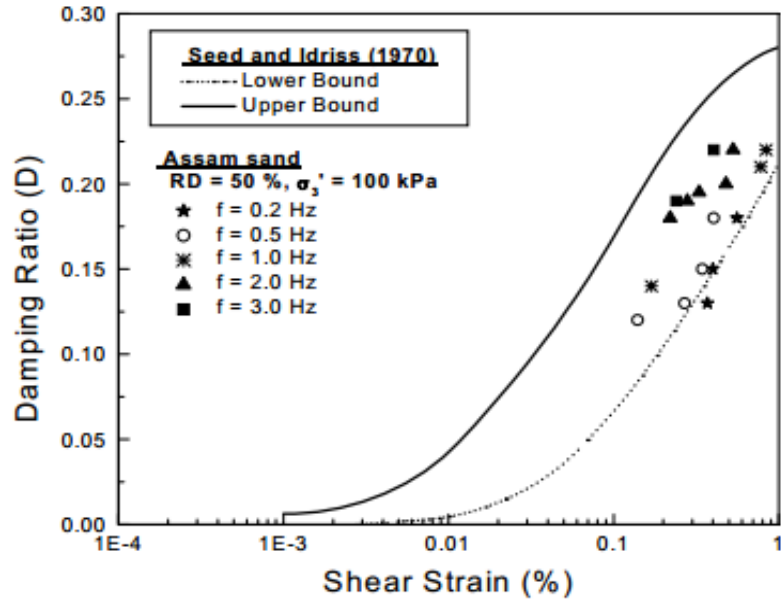


Figure 38 Effect of cyclic loading on damping ratios of sand(Govindaraju et al 2007)

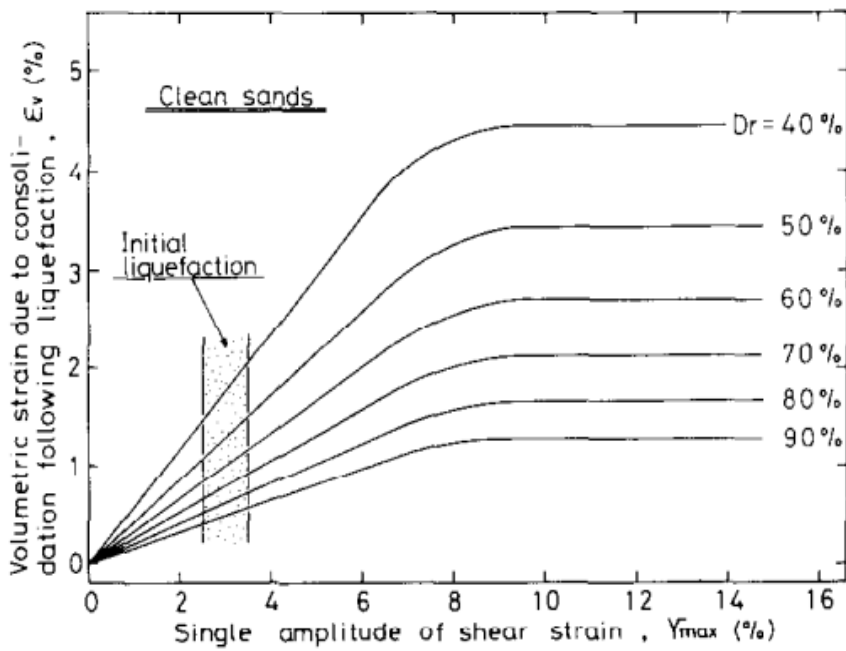


Figure 39 Effect of Post-liquefaction volumetric strain plotted against maximum shear strain (Ishihara 1993)

3. Experimentation

3.1. Theoretical background

Mohr–Coulomb Failure Criteria

In 1900, Mohr presented a theory for rupture in materials. According to this theory, failure along a plane in a material occurs by a critical combination of normal and shear stresses, and not by normal or shear stress alone. The functional relation between normal and shear stress on the failure plane can be given by

$$S = F(\sigma) \dots\dots\dots (1)$$

Where S is the shear stress at failure and σ is the normal stress on the failure plan. The shear strength of a soil can be defined as

$$S = C + \sigma' \tan \phi \dots\dots\dots (2)$$

For granular soils with $C = 0$,

$$\tau = \sigma' \tan \phi' \dots\dots\dots (3)$$

Ishihara 1983 researched on settlement of toyoura sands and he found that the settlements of the ground surface resulting from liquefaction of sand deposits during earthquakes can be estimated if the factor of safety and relative density of sand at each depth of the deposit are known. The relative density of in situ sand deposits can be assessed from a knowledge of the penetration resistance in the SPT or the CPT. Several attempts have been made to establish an empirical correlation between the relative density D_r and N value in the SPT. From an extensive survey of many sets of existing in situ data on the N value of the SPT, this correlation was expressed by Skempton (1986) in a general form as

$$N = (a + b\sigma_v')(D_r/100)^2$$

Equation 8 Skempton empirical relationship for n and D_r

where σ_v is the effective overburden pressure in kgf/cm^2 and a and b are constants that depend mainly on the grain size.

3.2. Tests on sands

3.2.1. Particle size distribution

The sands were characterised according to Eurocode 7 and subjected to all index properties and particle size distribution. The sand samples were free of any organic matter and had very less fine content less than 2% by mass. The sands grading results are showed in Fig. 10 and characteristics of sand is given in Table 3.

Table 3 Index Properties Of Sands

Sand A	Sand B
1. Specific Gravity – 2.62	Specific Gravity – 2.58
2. Coefficient of uniformity C_u - 6	Coefficient of uniformity C_u - 6
3. Coefficient of Curvature C_c - 2.4	Coefficient of Curvature C_c - 2.1

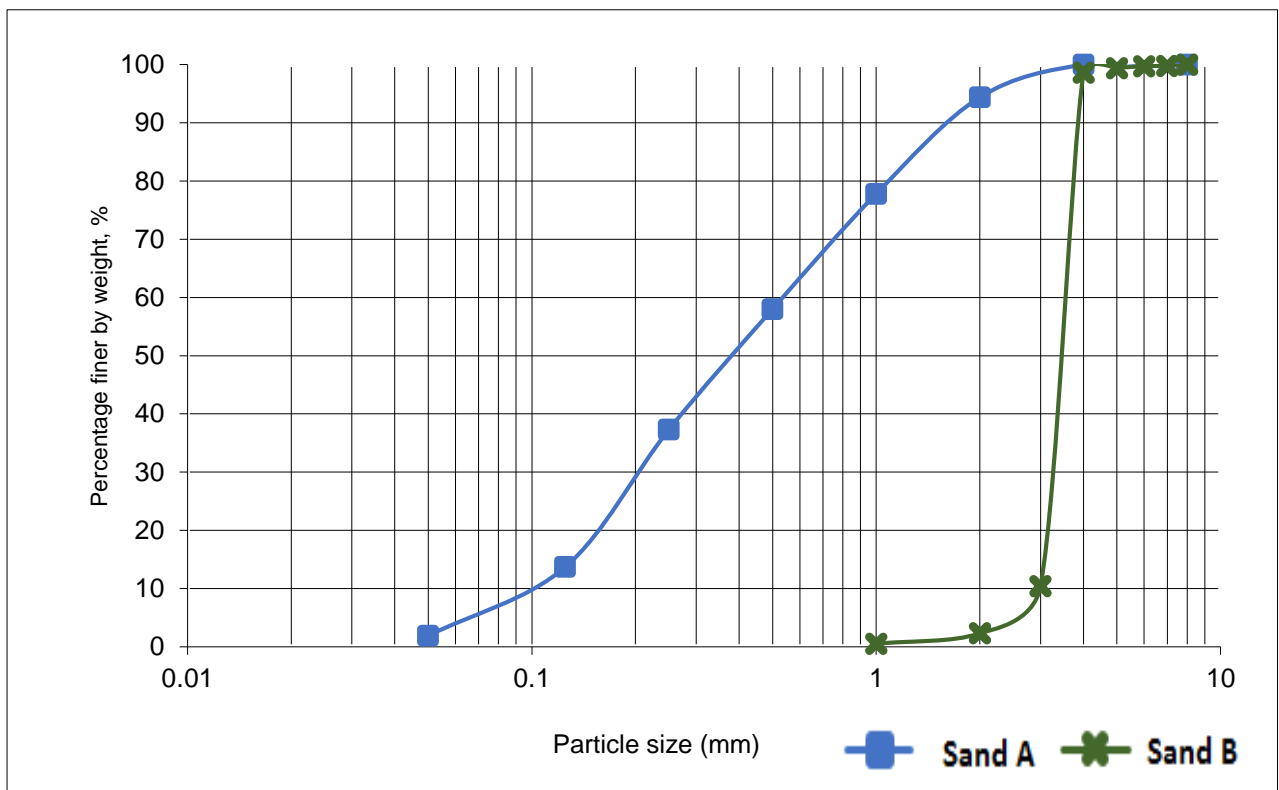


Figure 40 particle size distribution of sand samples

The sands are classified as well graded sand-GW as per soil classification criteria and is used for further experiments. Classification of sand shows a well graded sand with less or no fines and is non plastic type. Hence cementation behaviour is ruled out as no clay like particles were found after sieve analysis as per Eurocode 7 guidelines.

3.2.2. Simple shear tests under static and cyclic loading

The tests first have been performed under static conditions and by applying cyclic loading on sand sample to determine the change of mechanical properties of sand affected by cyclic loading. All tests to find out the failure shear stress of sand with and without cyclic loading have been performed using Field laboratory apparatus PLL-9.



Figure 41 Experimental setup with shaking table

The samples of sand used for testing were cylindrical shape of 56.5 mm diameter and 20 mm height. Shear tests on sand have been performed with three different normal stresses: 100 kPa, 200 kPa and 300 kPa and done under static loading and placing the apparatus on laboratory shaking table that induces vibrations of 50 Hz frequency (Fig 41.). Horizontal load was increased with a step of 4.8 kPa shear stress on sand specimen until it reached limit state and failure shear stress. As known the shear strength of soil can be expressed by Coulomb equation:

$$\tau_f = c + \sigma \tan \varphi \quad (4)$$

where: τ_f – failure shear stress; c – cohesion; σ – normal stress; φ – angle of friction

Shear tests on sand have been carried out under static conditions and with vibrations of 50 Hz frequency. Tests with 50 Hz vibrations were performed on laboratory shaking table (Fig. 41) and the sands were tested in dry state until failure. And also tested for varying cyclic loads at Technological Systems Diagnostics Institute at KTU.



Figure 42 vibration table with varying cyclic loading

Table 4 shear stress values for sand A

	shear stress kPa		
normal stress kPa	100	200	300
no vibration	40.69	64.765	88.84
10 HZ	31.06	64.765	98.47
30 HZ	45.505	62.3575	79.21
50 HZ	35.875	59.95	84.025

Table 5 shear strength values of Sand B

shear stress kPa			
normal stress kPa	100	200	300
no vibration	35.875	50.32	64.765
10 HZ	31.06	50.32	69.58
30 HZ	31.06	40.69	50.32
50 HZ	26.245	40.69	55.135

3.2.3. Friction angle tests on sands

Friction angle tests on sand have been carried out with UVT-2 and UO (Fig. 42) under vibrations with 10 Hz, 20Hz, 40 Hz and 50 Hz frequency. The vibrations were performed using frequency changing vibration table in Technological Systems Diagnostics Institute of Kaunas University of Technology (Fig. 43). The amplitude of vibrations in all tests was set to be 0.3 mm.

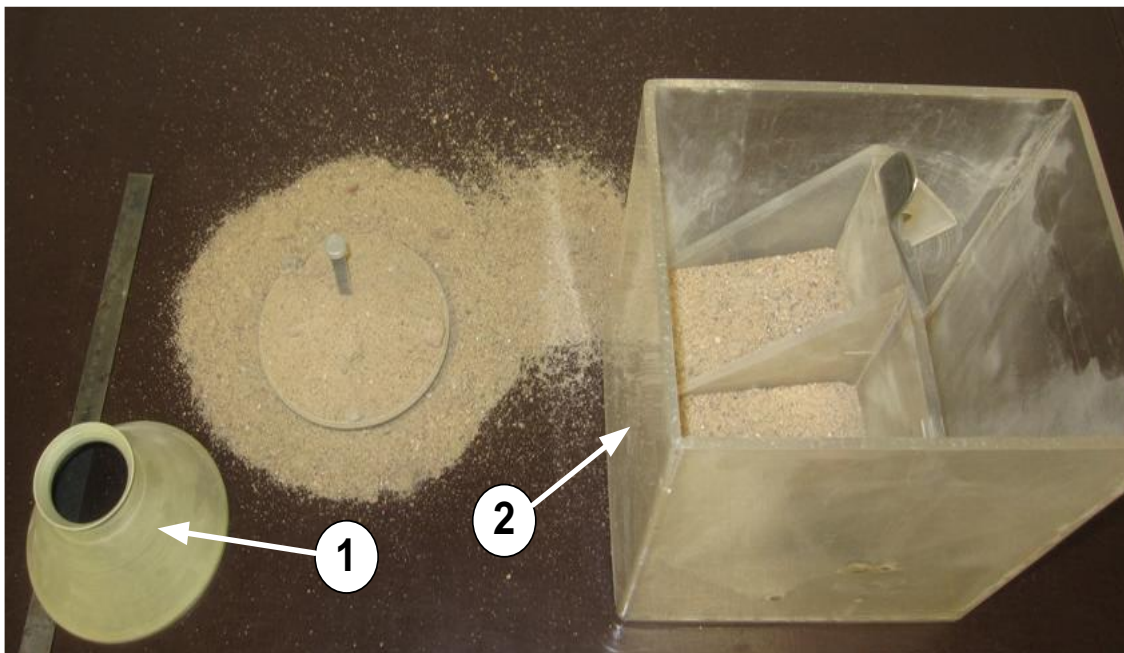


Figure 43 UVT-2(1) and UO (2) tests for sand A



Figure 44 UVT-2 test for sand B



Figure 45 UO tests for sand B



Figure 46 vibration table with UO



Figure 47 vibration table with UO

Table 6 friction angles for various cyclic loads for sand A

frequency in Hz	friction angle
10	35
20	33
30	26
40	21
50	18

Table 7 friction angles for various cyclic loads for sand B

frequency in Hz	friction angle
10	35
20	31
30	23
40	20
50	16

3.2.4. Settlement Studies

Model footing was first prototyped and designed in faculty to study the settlement in fine sands as they are highly susceptible to liquefaction during an earthquake event in order to understand statical settlement to dynamic settlement based on available research and empirical formulas. Dynamic testing could not be conducted due to high pore pressure build up when saturated with water and had immediate failures it was decided to only conducted statical settlement test to understand scaling and mode of failures for footing.

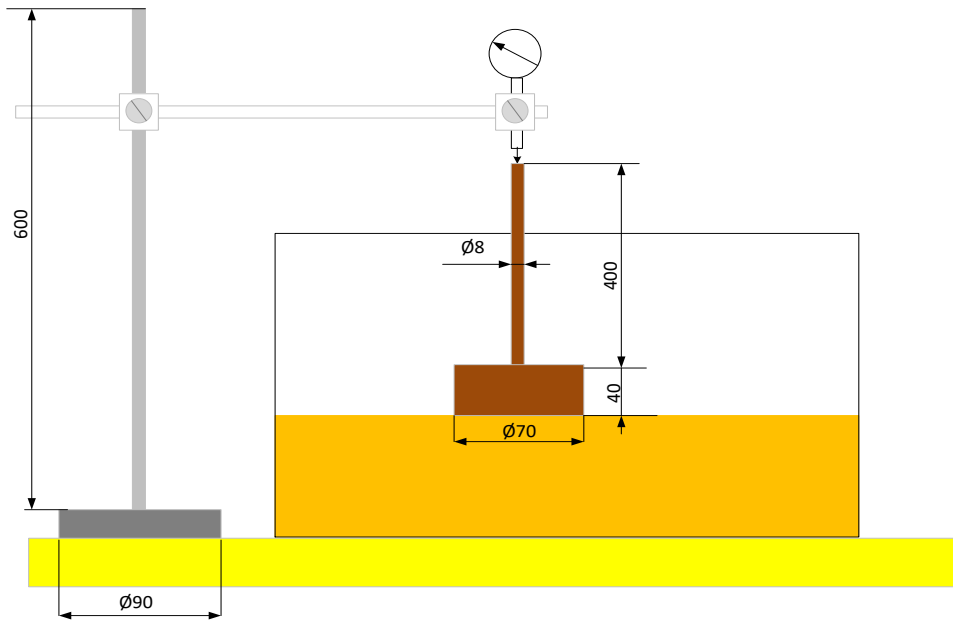


Figure 48 model footing prototype

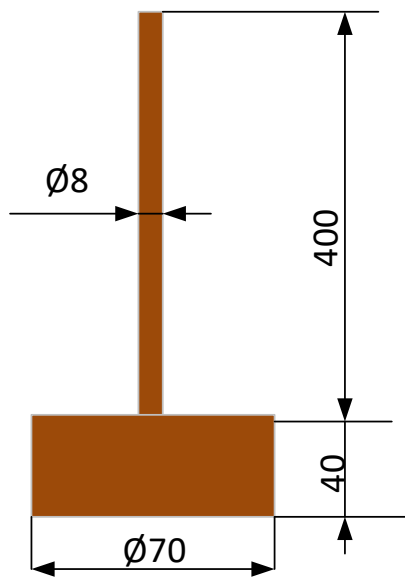


Figure 49 prototype model footing type 1

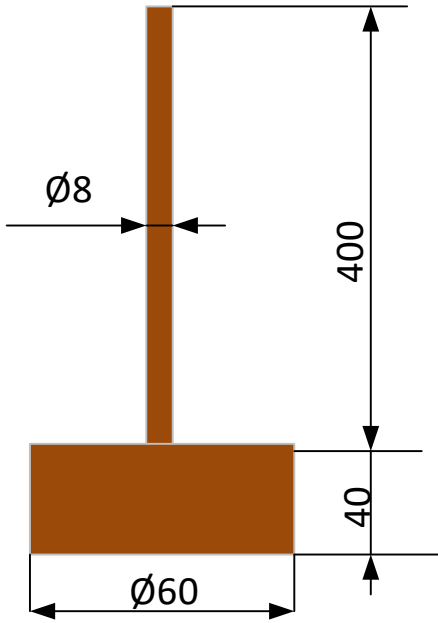


Figure 50 prototype model footing type 2



Figure 51 actual model footing type 1 and 2

Based on the theory of elasticity (Timoshenko & Goodier, 1982), the elastic settlement S_i of a flexible footing, either rectangular of dimensions $L \times B$ ($L > B$) or circular of diameter B , is given by

$$s = 0.94I_s \frac{qB(1-\mu^2)}{E}$$

Equation 9 settlement equations for sands

where: I_s – influence factor depending on the shape and L / B ratio ; (for case A and B $I_s = 0.85$); q – uniform loading; E – modulus of elasticity; μ – Poisson's ratio .

For average settlement

$$s_i = 0.94s$$

Settlement in sandy soils are influenced by following factors

- Must be validated on field test like SPT and CPT
- Check for groundwater levels
- Studying local geology would be essential for deep exploration
- Dependent on relative density and stress history

The sands were tested using a model footing to study settlement studies in static conditions and loaded until general shear failure is obtained.

These studies were done to validate scaling effect and check experimental results to analytical solution.

Table 8 settlement test data for sand A

	Mass (kg)	Uniform load (N/m ²)	trial 1 (mm)	trial 2 (mm)	average	Settlement (mm)
1	0	0	6.27	6.9	6.585	0
2	1	5.15	6.25	6.86	6.555	0.03
3	3	15.4	6.16	6.72	6.44	0.145
4	5	25.64	6.02	6.56	6.29	0.295
5	7	35.9	5.59	6.4	5.995	0.59
6	9	46.15	5.35	6.07	5.71	0.875
7	11	56.41	5.28	5.96	5.62	0.965
8	13	66.67	4.72	5.5	5.11	1.475
9	15	76.92	4.38	4.69	4.535	2.05
10	17	87.18	3.85	4.55	4.2	2.385
11	19	97.43	3.78	4.16	3.97	2.615
12	21	107.7	3.69	3.89	3.79	2.795
13	23	117.95	2.58	2.77	2.675	3.91
14	25	128.21	1.7	1.65	1.675	4.91
15	27	130.47	0.19	0.91	0.55	6.035
16	31	158.97	0.09	0.014	0.052	6.533
17	35	179.49	0	0	0	6.585

Table 9 settlement data for sand B

	Mass (kg)	Uniform load (N/m ²)	trial 1 (mm)	trial 2 (mm)	average	Settlement (mm)
1	0	0	8.78	8.6	8.69	0
2	1	5.15	8.6	8.37	8.485	0.205
3	3	15.4	8.34	8.09	8.215	0.475
4	5	25.64	7.85	7.87	7.86	0.83
5	7	35.9	7.56	7.39	7.475	1.215
6	9	46.15	7.24	6.94	7.09	1.6
7	11	56.41	7.01	6.57	6.79	1.9
8	13	66.67	6.86	6.36	6.61	2.08
9	15	76.92	6.61	6.24	6.425	2.265
10	17	87.18	6.42	5.77	6.095	2.595
11	19	97.43	6.1	5.54	5.82	2.87
12	21	107.7	5.72	5.21	5.465	3.225
13	23	117.95	5.51	4.6	5.055	3.635
14	25	128.21	4.68	3.89	4.285	4.405
15	27	130.47	3.75	2.15	2.95	5.74
16	31	158.97	1.98	1.14	1.56	7.13
17	35	179.49	0.021	0.009	0.015	8.675

3.3.Results

3.3.1. Shear test results

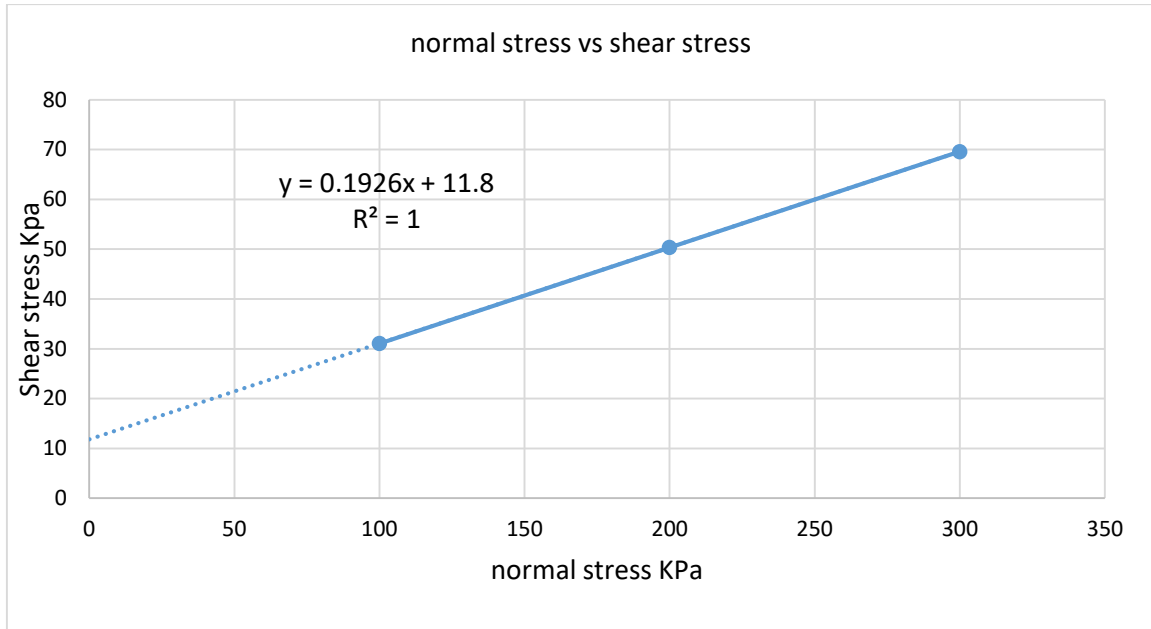


Figure 52 shear test results for statical loads

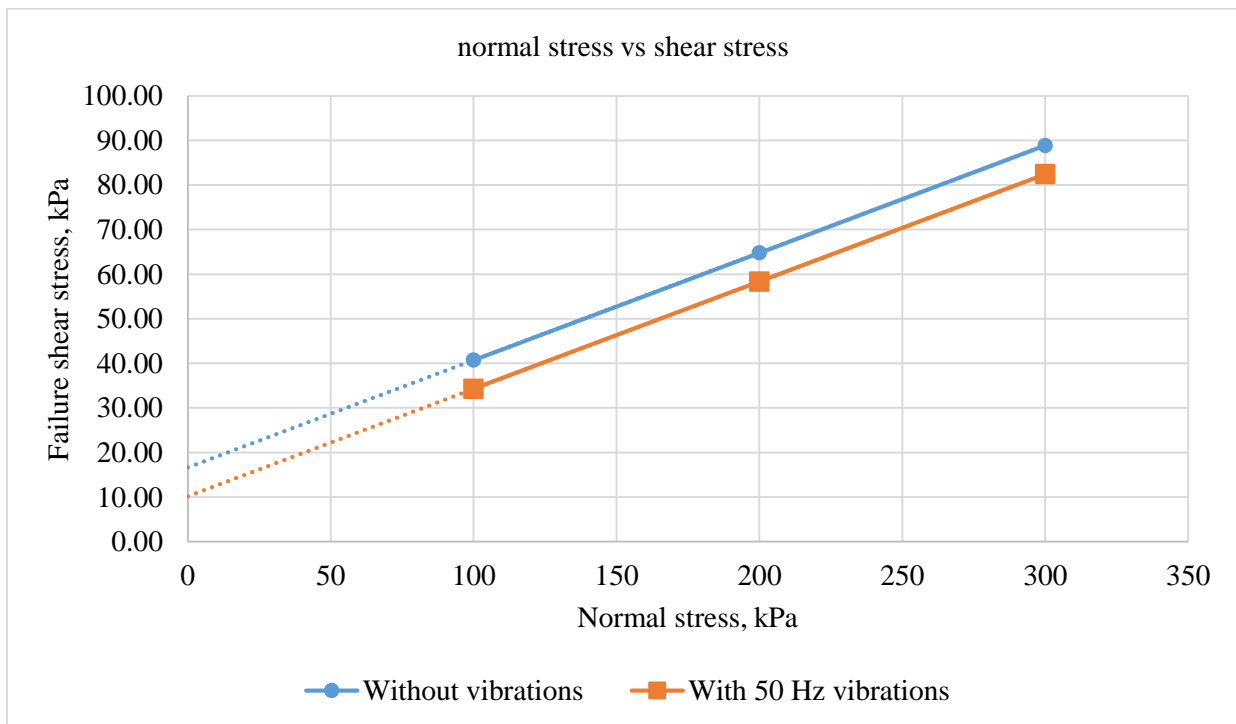


Figure 53 shear test result for sand A tested at faculty

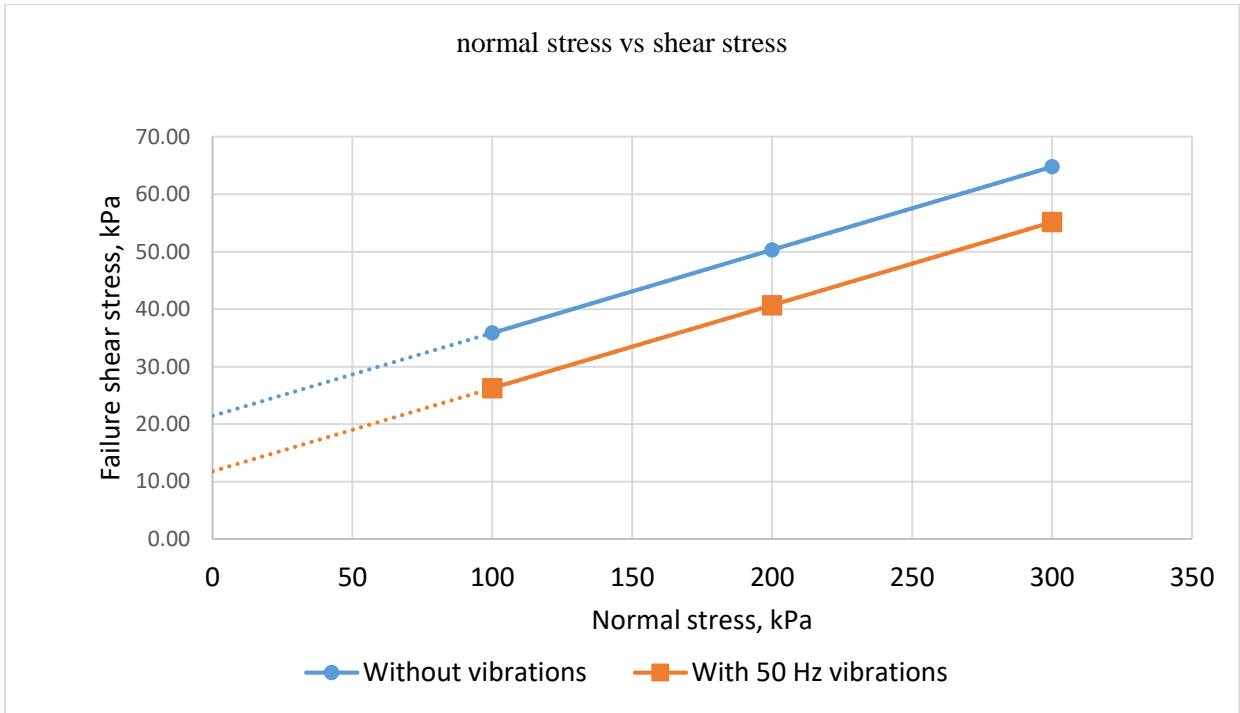


Figure 54 shear test result for sand B tested at faculty

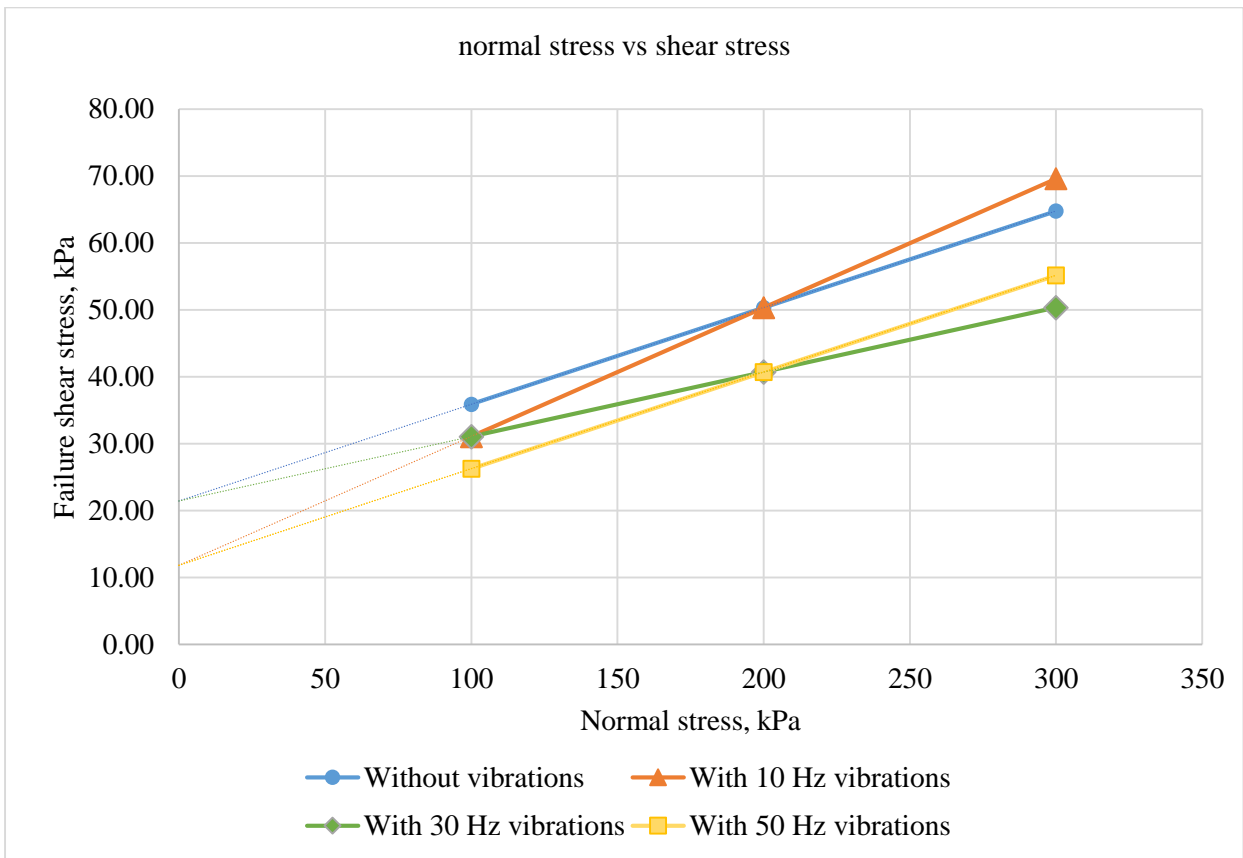


Figure 55 Shear test result for sand A tested at Technological Systems Diagnostics Institute faculty

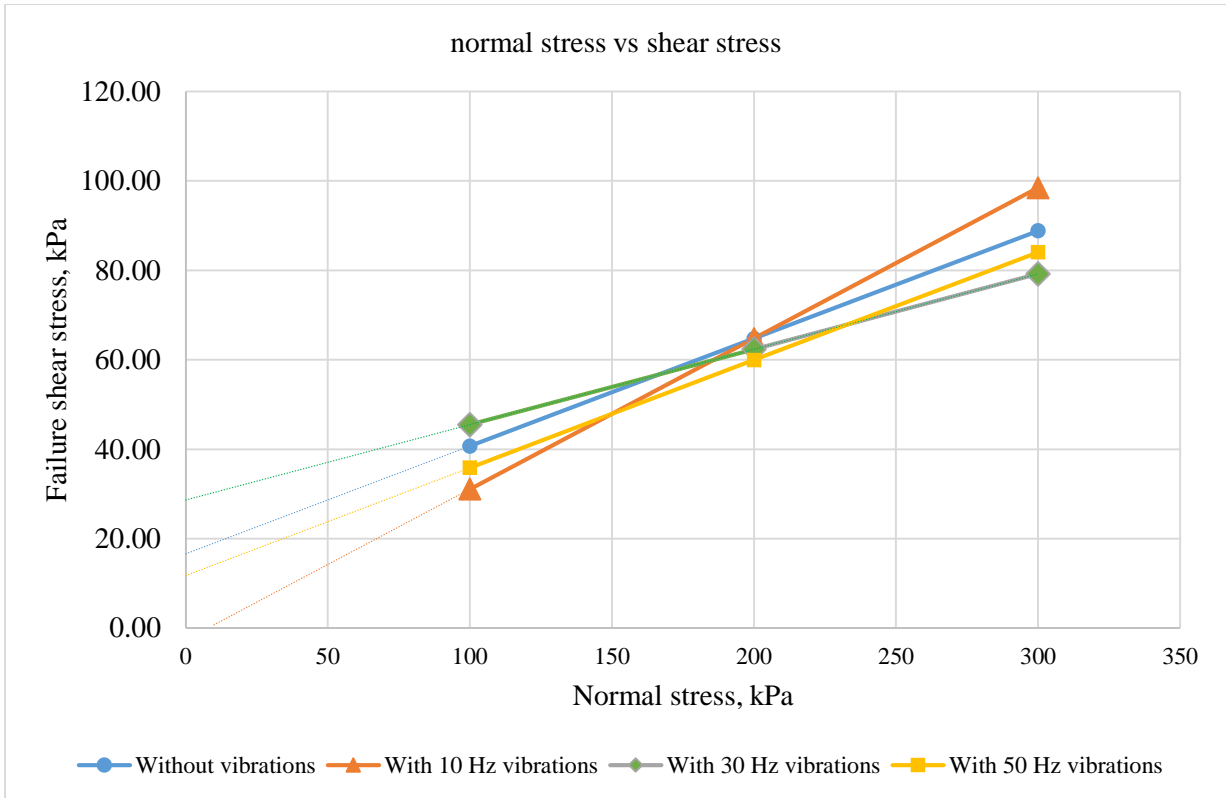


Figure 56 Shear test result for sand B tested at Technological Systems Diagnostics Institute faculty

3.3.2. Friction angle test results

Friction test for sand A

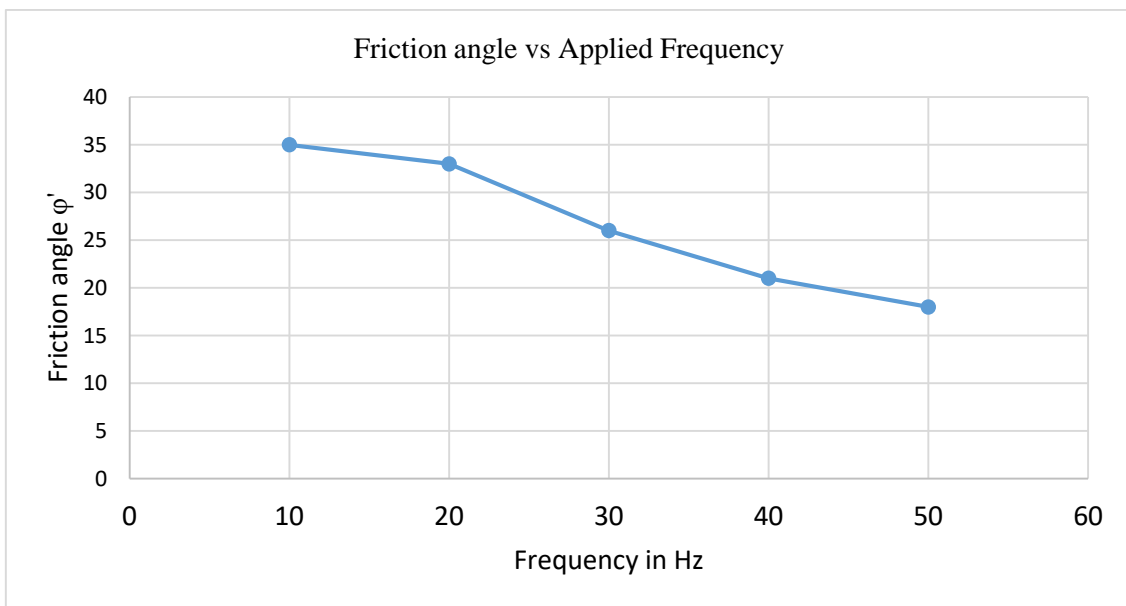


Figure 57 Friction angle results for sand A at Technological Systems Diagnostics Institute faculty

Friction test for sand B

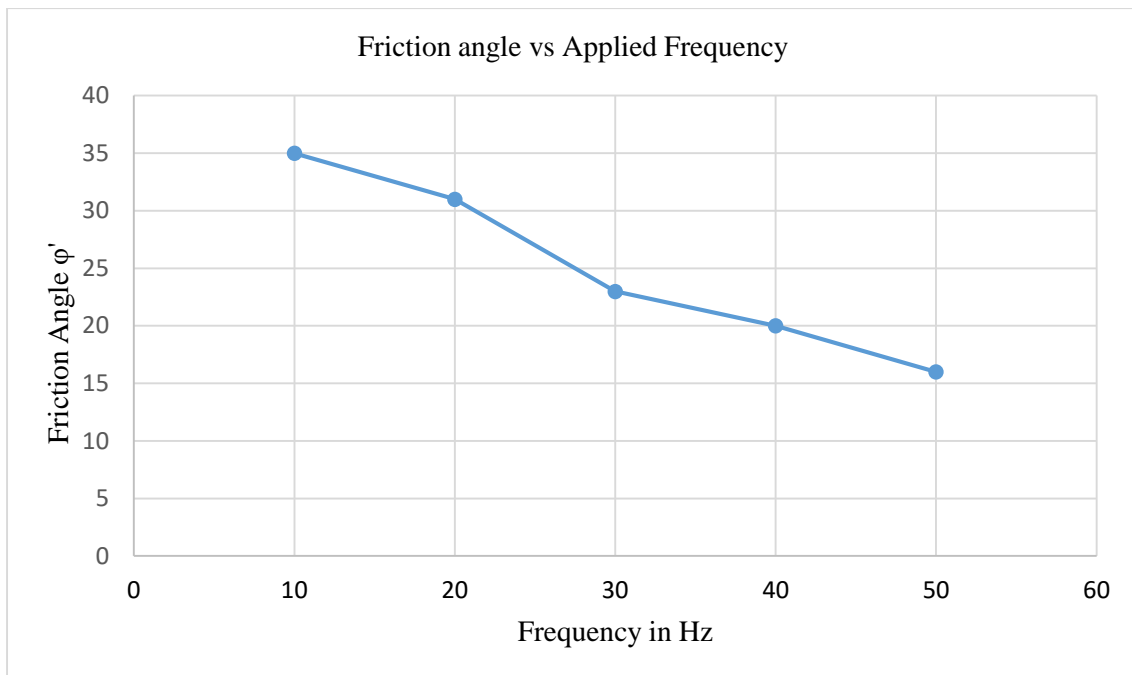


Figure 58 Friction angle results for sand B at Technological Systems Diagnostics Institute faculty

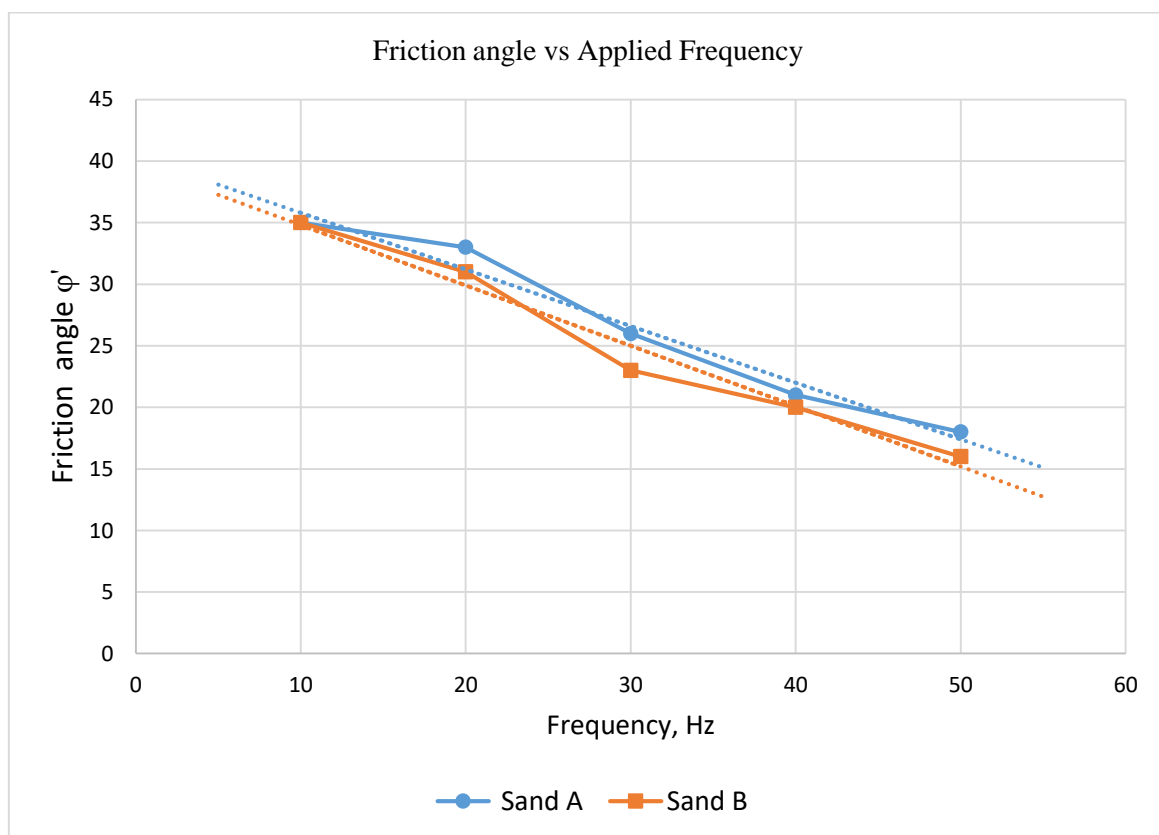


Figure 59 Combined friction angles results for sand A and B at Technological Systems Diagnostics Institute faculty

3.3.3. Settlement test results

Linear settlement curve for sand A

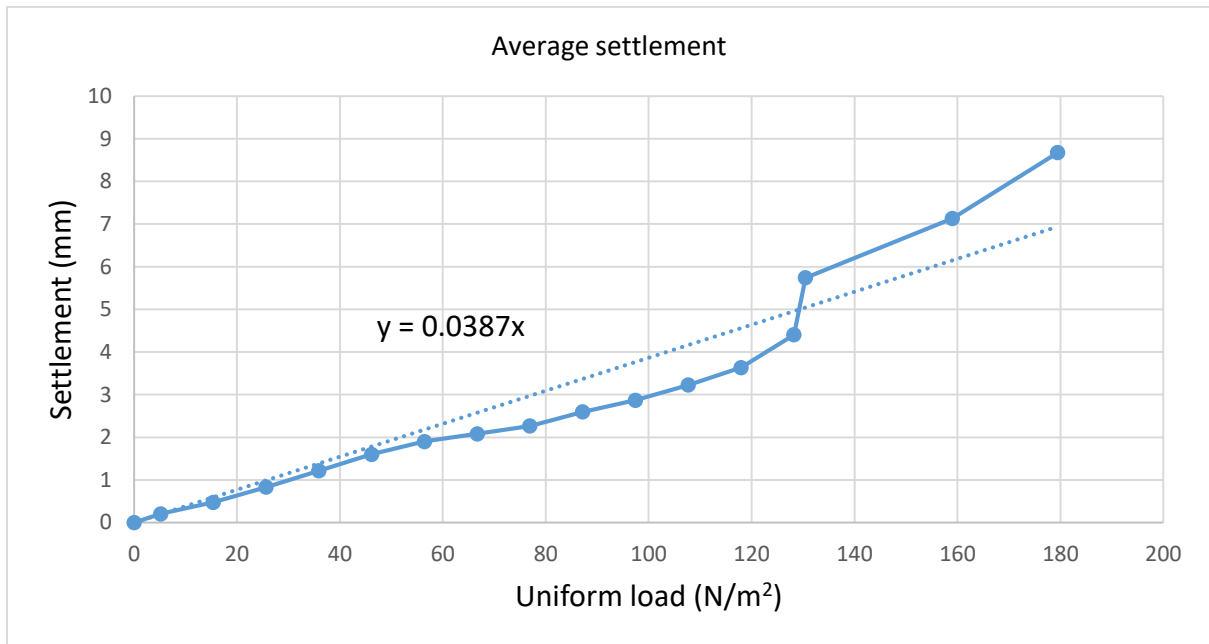


Figure 60 Settlement result for sand A linear variation

Trial no 1 for linear settlement curve for sand A

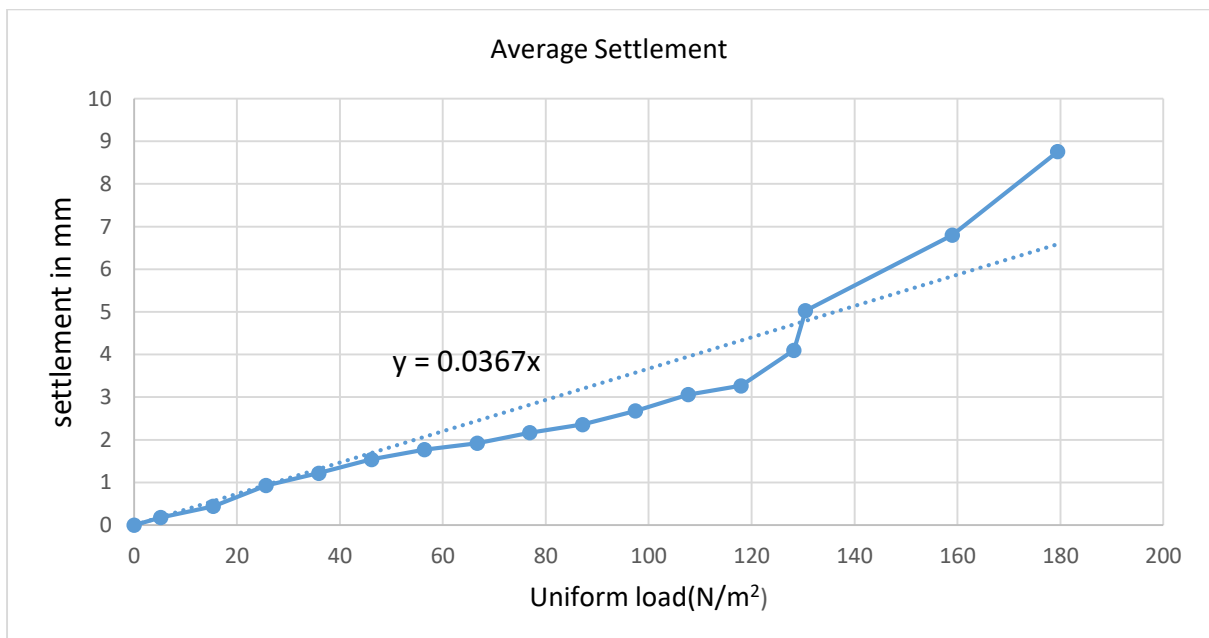


Figure 61 Settlement curve for sand A linear variation trial no 1

Trail no 2 for linear settlement curve for sand A

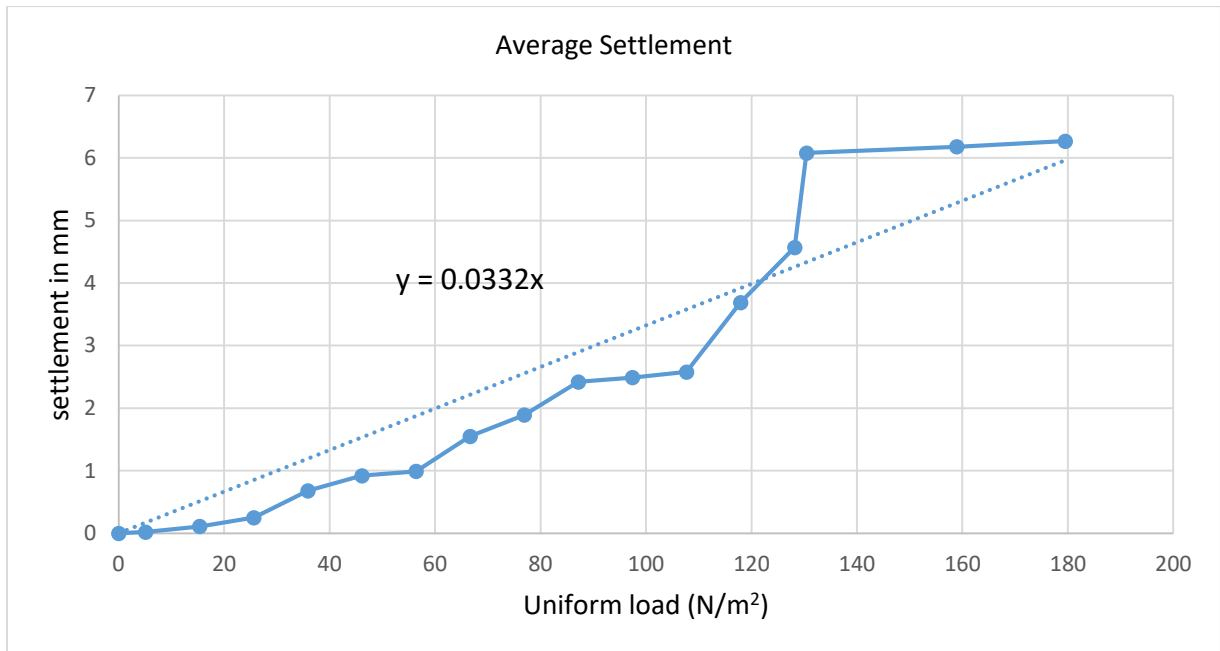


Figure 62 Settlement curve for sand A linear variation trial no 2

Second order(quadratic) settlement curve for sand A

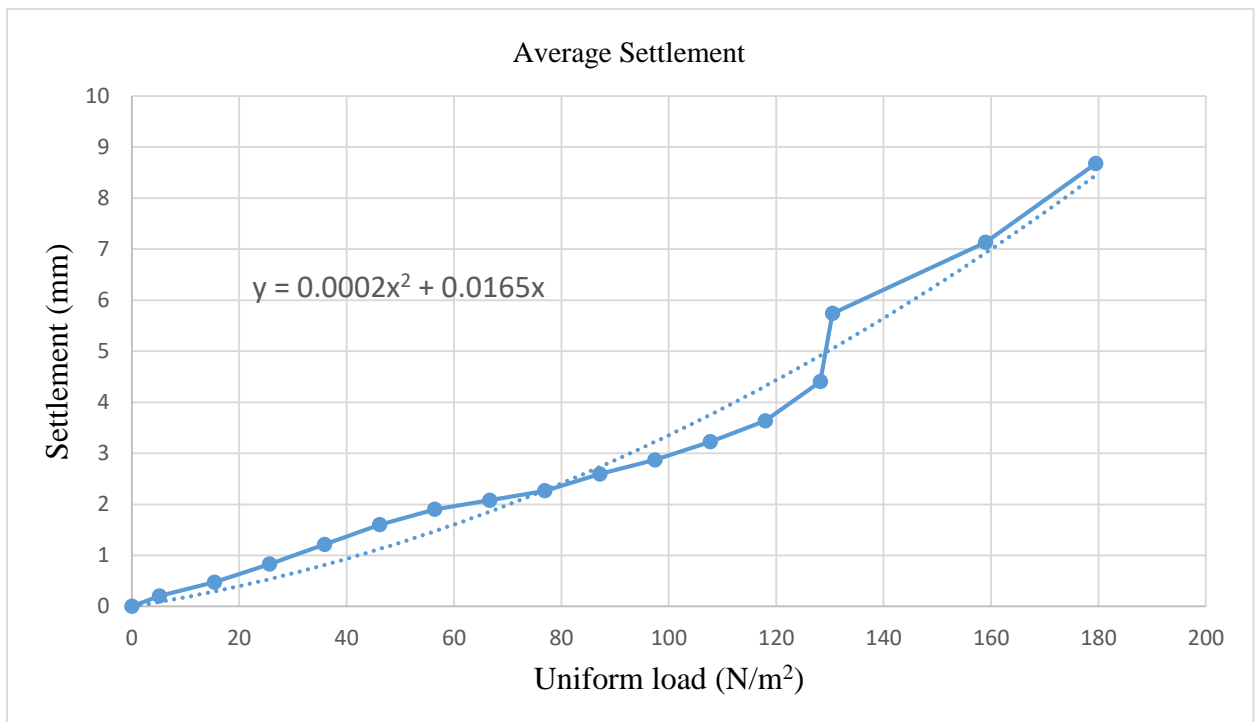


Figure 63 Second order(quadratic) average settlement curve for sand A

Trial no.1 Second order(quadratic) settlement curve for sand A

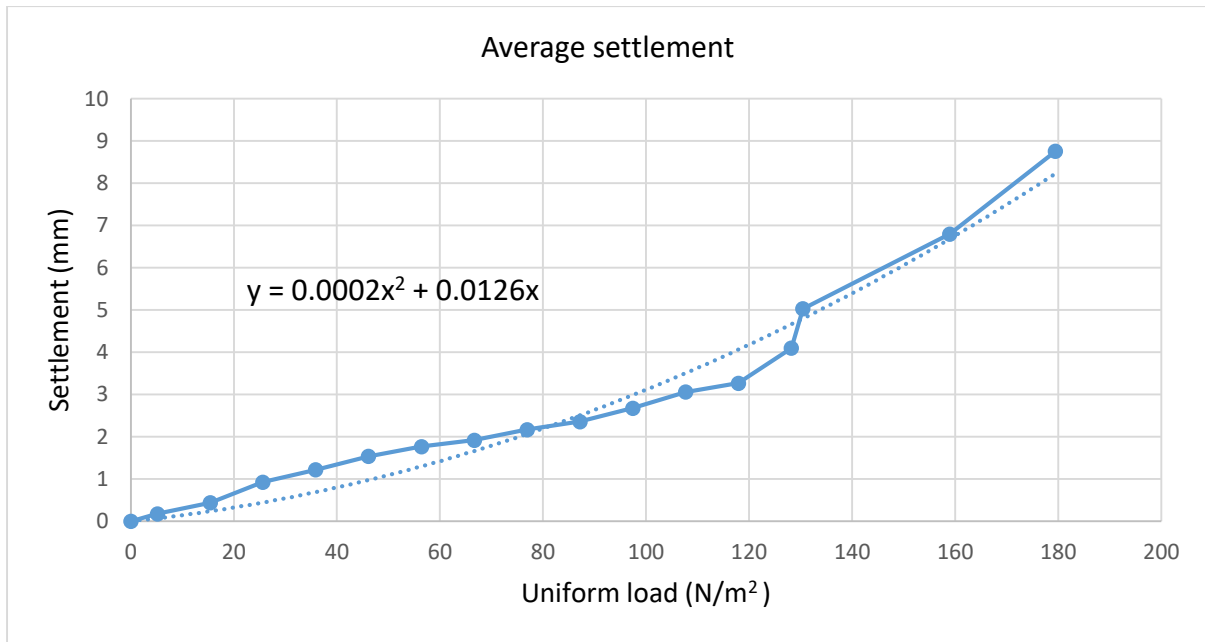


Figure 64 Second order(quadratic) settlement curve for sand A trial no1

Trial no 2 Second order(quadratic) settlement curve for sand A

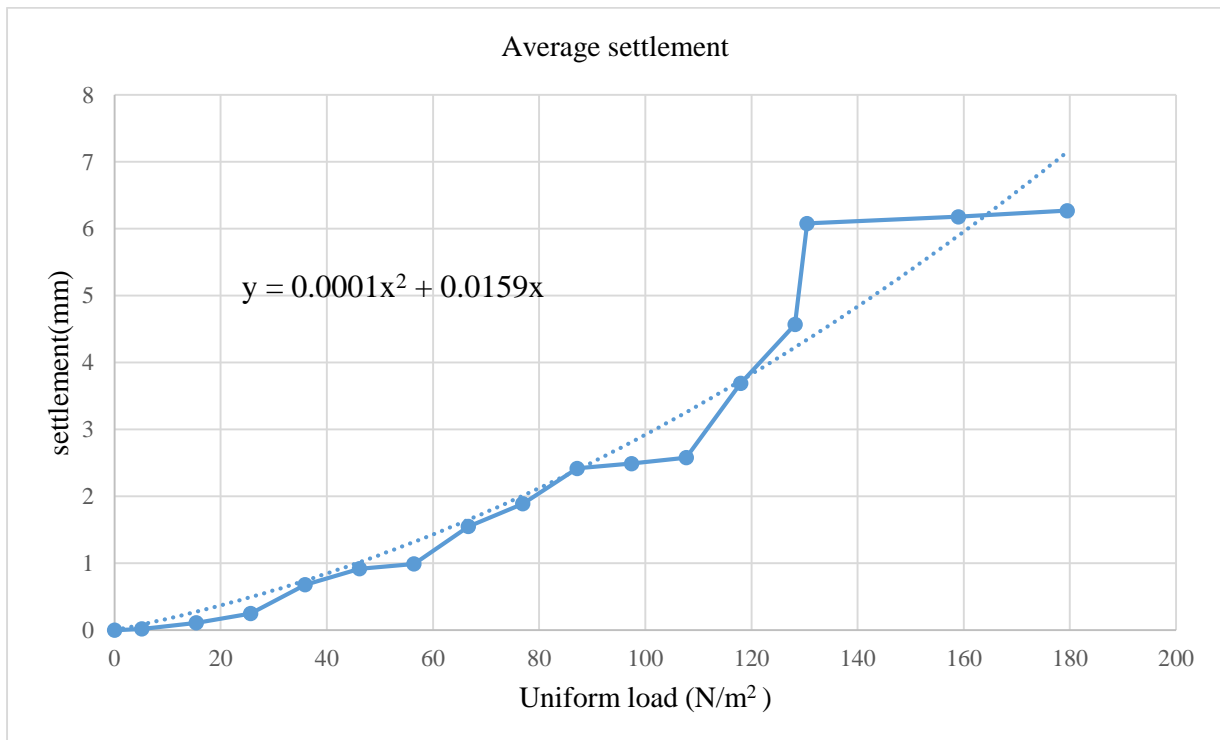


Figure 65 Second order(quadratic) settlement curve for sand A trial no 2

Linear settlement curve for sand B

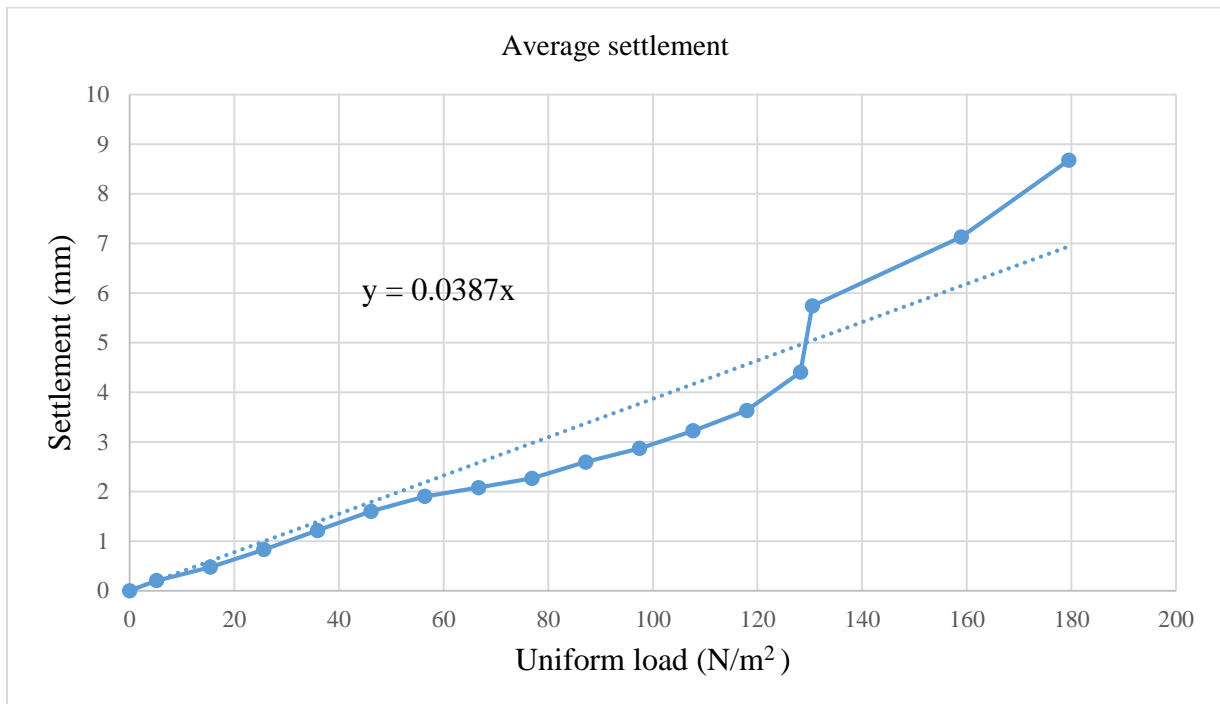


Figure 66 Settlement result for sand B linear variation

Trial 1 for linear settlement curve for sand B

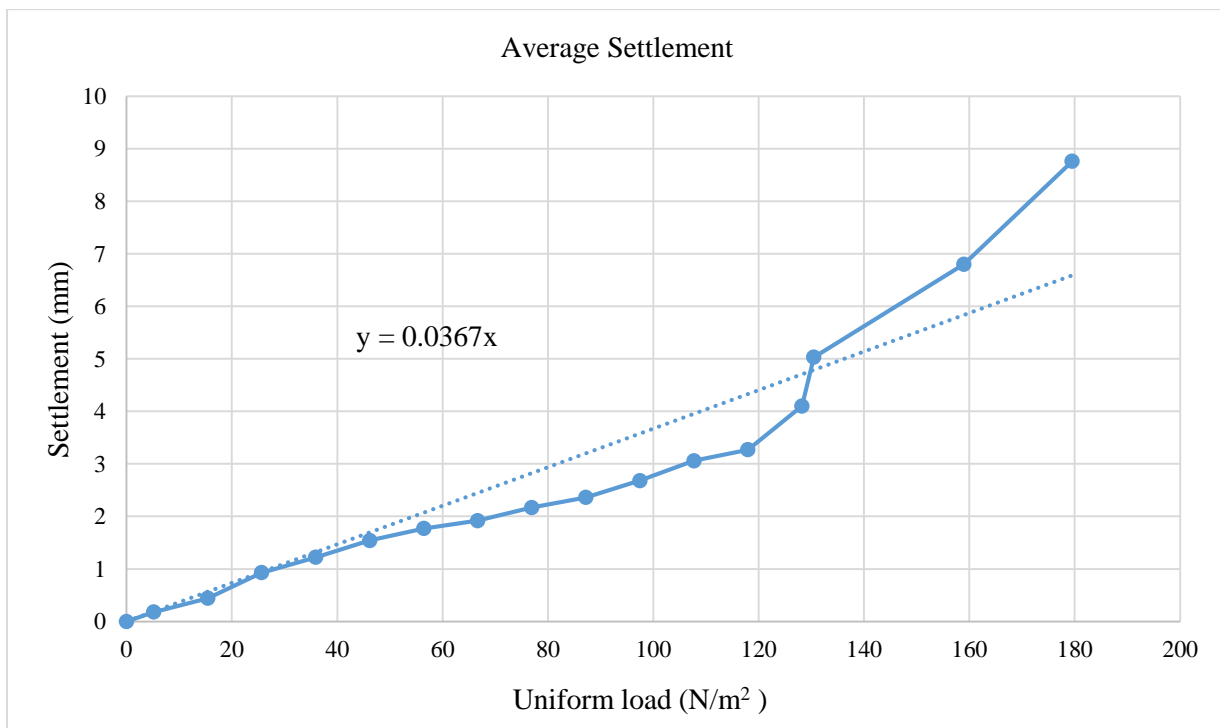


Figure 67 Settlement result for sand B linear variation trial 1

Trial 2 for linear settlement curve for sand B

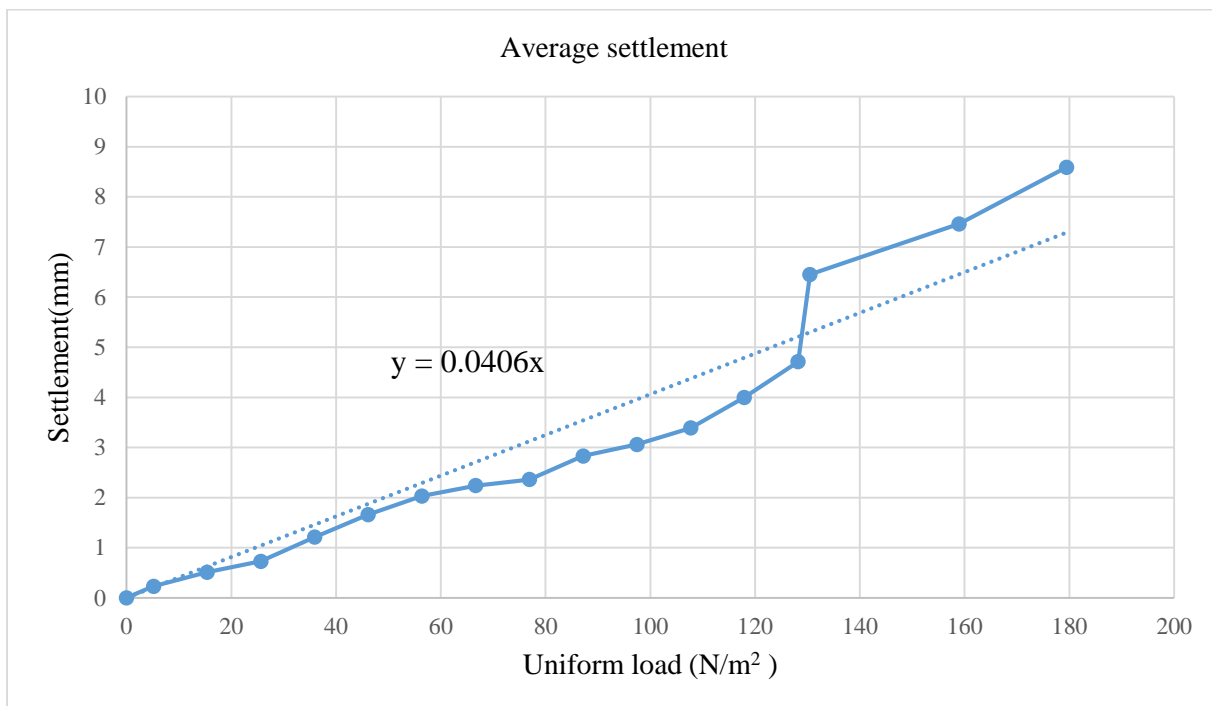


Figure 68 Settlement result for sand B linear variation trial 2

Second order(quadratic) settlement curve for sand B

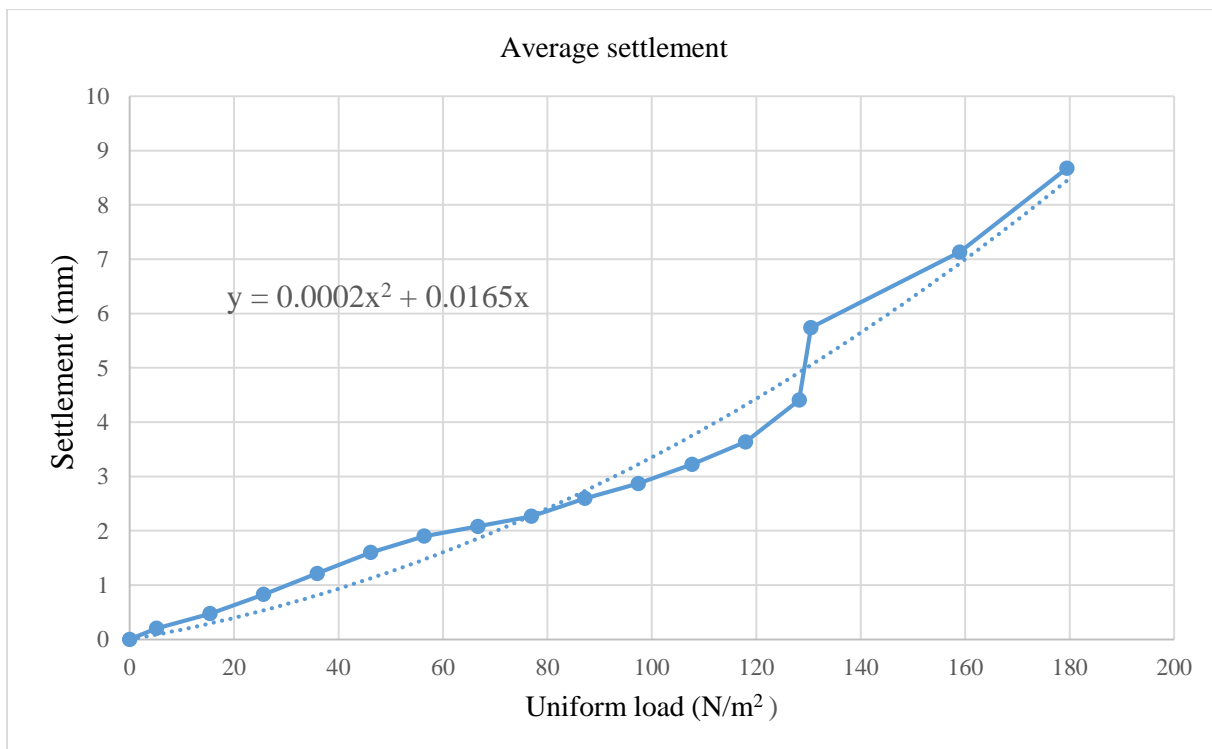


Figure 69 Second order(quadratic) settlement curve for sand B

Trial no.1 Second order(quadratic) settlement curve for sand B

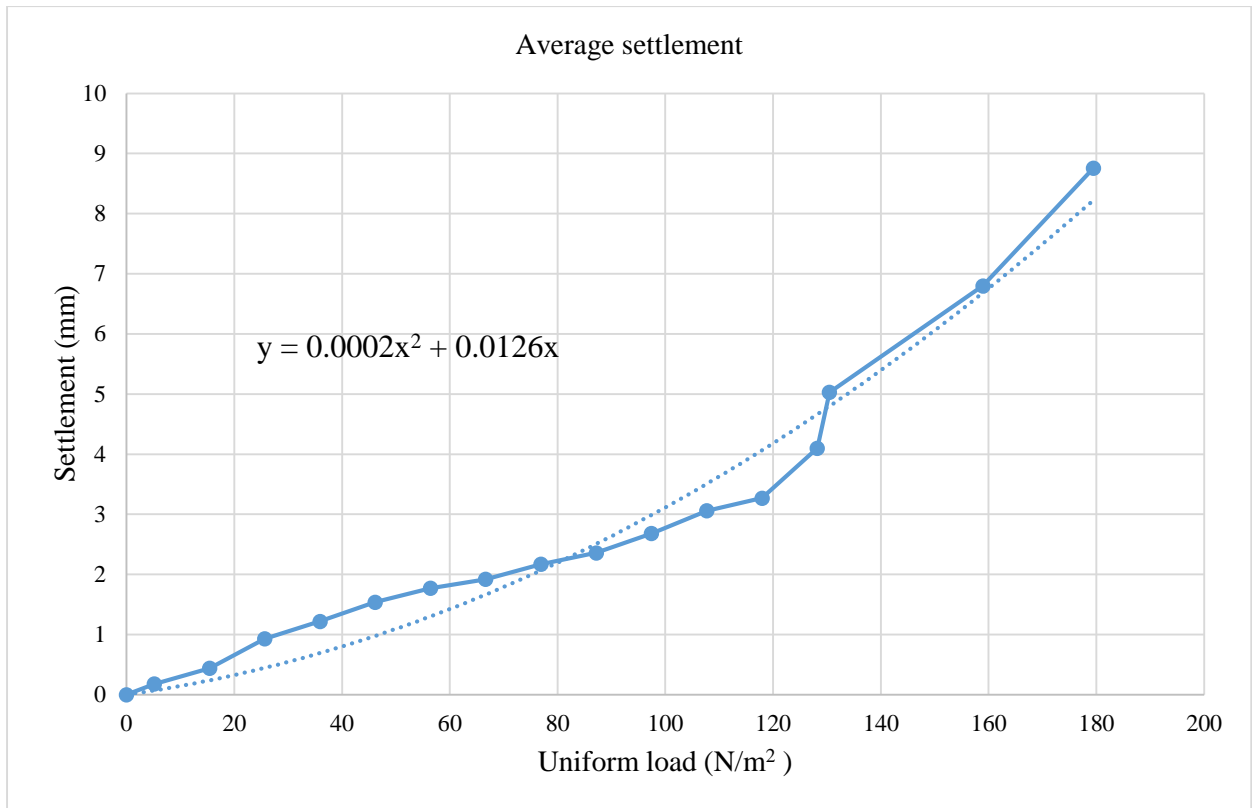


Figure 70 Second order(quadratic) settlement curve for sand B trial 1

Trial no.2 Second order(quadratic) settlement curve for sand B

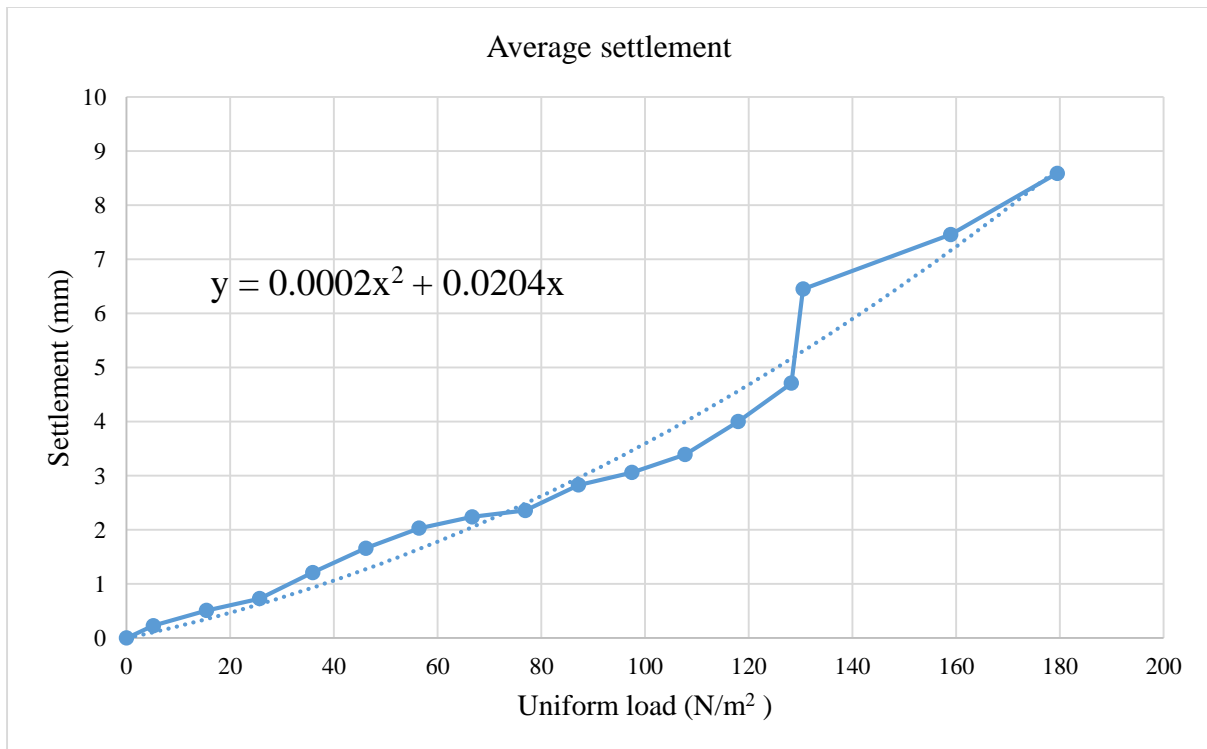


Figure 71 Second order(quadratic) settlement curve for sand B trial 2

Analytical solution for settlement curve for sand A

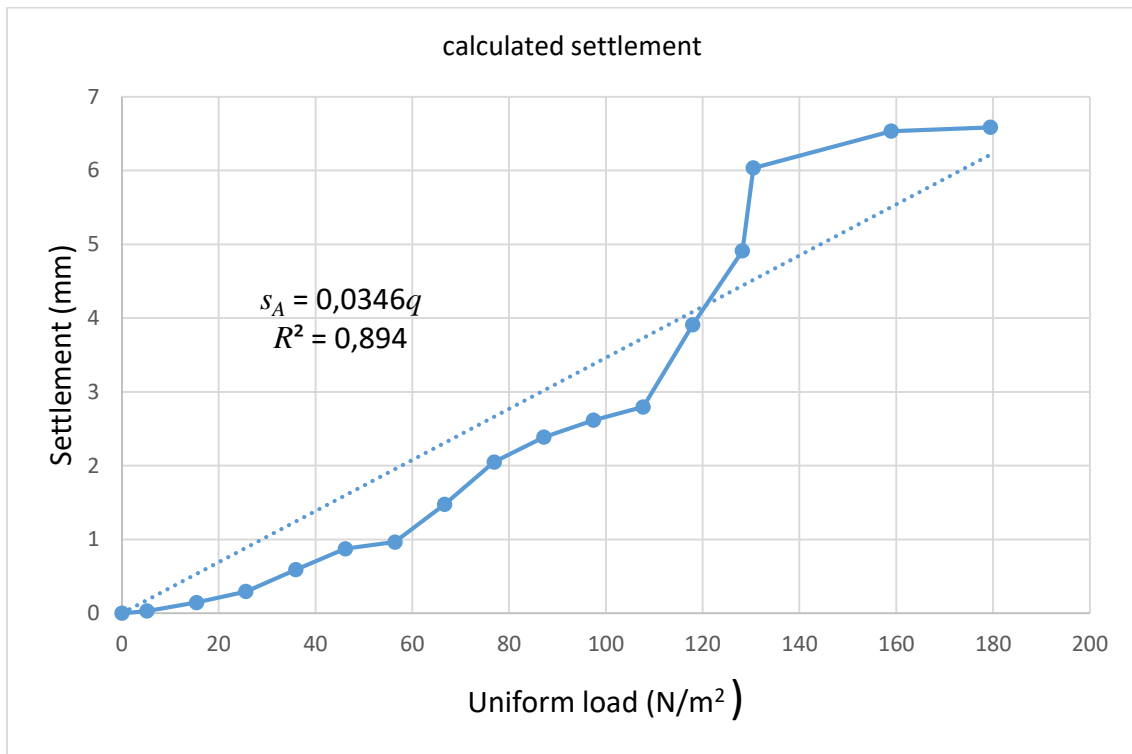


Figure 72 Calculated settlement result for Sand A

Analytical solution for settlement curve for sand B

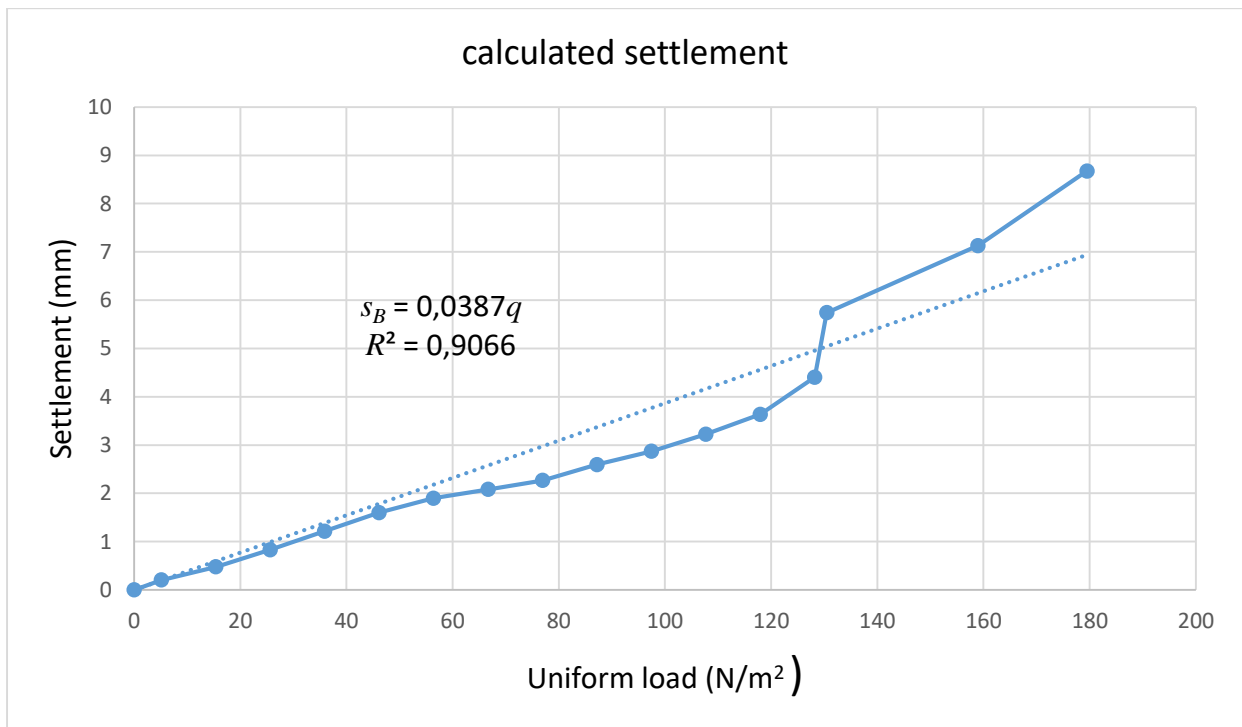


Figure 73 Calculated settlement result for Sand B

The sands were tested using a model footing to study settlement studies in static conditions and loaded until general shear failure is obtained. These studies were done to validate scaling effect and check experimental results to analytical solution by Equ 9. The results obtained during the settlement test on sand A and B are illustrated in Fig. 72 and Fig. 73. The experiments show that can to use obtained empirical equations to calculate the average settlement until uniform load:

$$s_i = a_i q - s_{i0} \quad (5)$$

where: a_i uniform load coefficient, $\frac{m^2}{N} mm$; s_{i0} initial settlement, mm ;

This parameters depends by type of sand, example for sand A are $a_A = 0.0415 \frac{m^2}{M} mm$ and $s_{A0} = 0.7779 mm$

Scaling Effect for Sand A

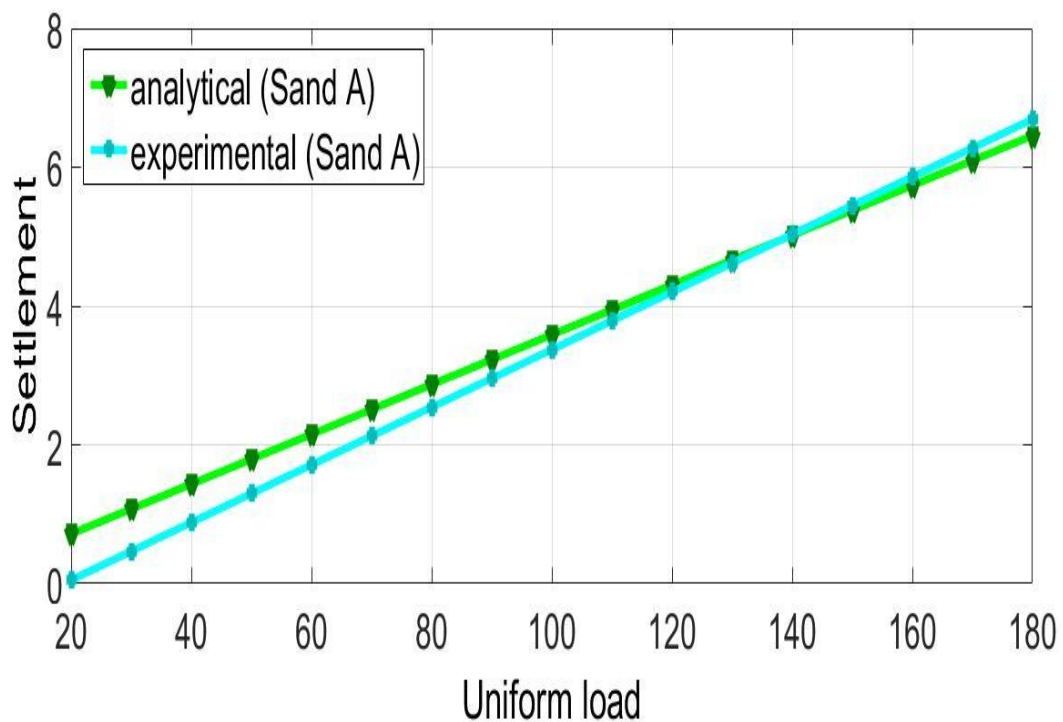


Figure 74 Scaling Effect on Sand A

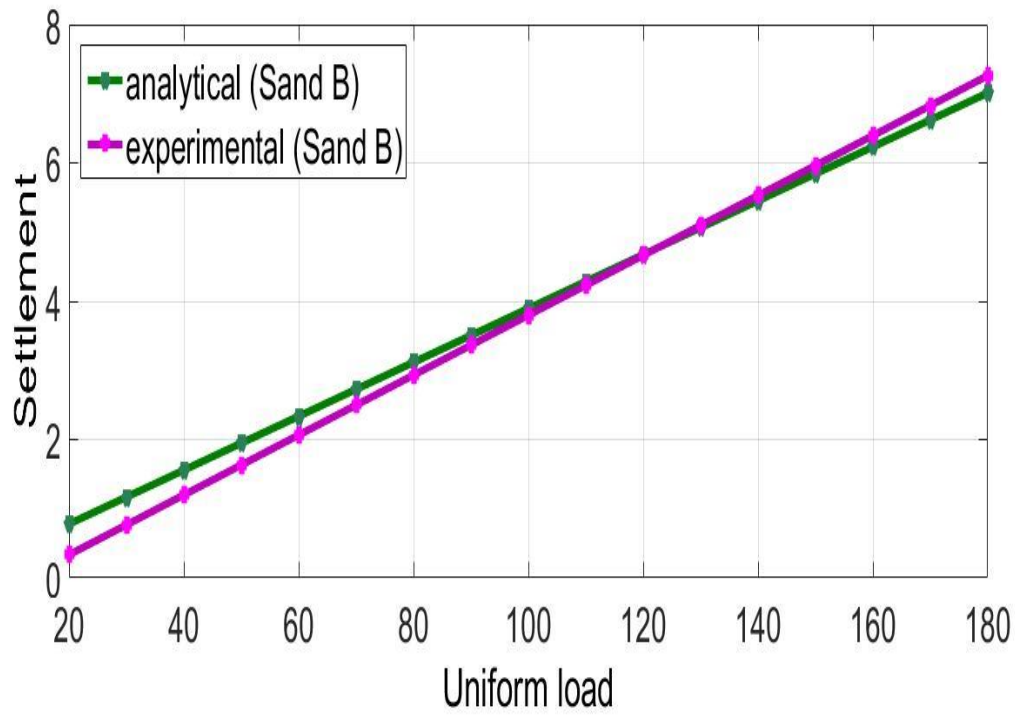


Figure 75 Scaling Effect on Sand B

4. Conclusions and Discussions

4.1. Effect of statical loads on sands

- Statical shear strength of sands are typical values obtained for medium sands and have no significant influence on friction angle
- No cohesion was observed in both sand A or Sand B due to smaller particle sizes
- Cementation or crushing of sand particles is not observed as it is non plastic
- Undrained shear strength is higher for sand A compared to Sand B
- Sands are stable in statical loads and have higher mechanical resistance

4.2. Effect of cyclic loads on sands

- Cyclic loads on sands reduces its shear strength considerably
- Friction angle is affected considerably and decreases with increasing cyclic loads
- Under 50 Hz vibrations the angle of friction decreased by 47% while under low frequency vibrations about (10 Hz) for sand, the angle of friction was equal to 35°.same as statical value
- Saturated samples showed liquefaction effects
- It is essential to design for liquefaction mitigation if such deposits of sands are found on site

4.3. Settlement analysis of model footing

- Settlement studies indicate the general mode of footing failure expected in sands
- Sand A has higher load bearing capacity compared to Sand B
- Sand B tends to have lower settlement compared to Sand A
- Scaling effects have a profound effect on usability of laboratory test values for field applications
- Analytical and experimental values of settlement follow a linear trend and using scaling effect which can be calculated empirical. It is important to take such changes in design for footing on such sand deposits.

4.4. Discussions and scope of further work

The present work has been a new approach to study cyclic loads for medium sands in a lab environment since other methods employ sophisticated methods and instruments to analyze cyclic loads (example resonant column, hollow cylinder torsion test) which are good for seismic site analysis.

The present testing method of using simple shear apparatus was used since it would have no rigid boundary effect on samples and samples would behave like at consolidated state K_0 which is vital for accurate analysis of reasonable accuracy. Since reconstituted samples suffer from change in soil structure and have lesser influence on properties like anisotropy and three dimensional stress state like actual field test like SPT or CPT.

It is important to understand scaling effects in sands as they have an effect on liquefaction potential or the ability to flow under dynamic loads which is very serious issue for seismic design of structures.

Suggestions for further work

- Effect of anisotropy can be studied but the present instrument lacks the ability to determine this important parameter
- Simulation of 3d stress state is also important but further instrumentation is needed like hollow cylinder torsion apparatus to analyze this problem

5. References

- 1) Ambraseys, N. N. (1988). "Engineering seismology." *Earthquake Eng. and Structural Dynamics* 17(1), 1–105.
- 2) Alarcon-Guzman, A., Leonards, G. A. & Chameau, J. L. (1988). Undrained monotonic and cyclic strength of sands. . *J. Geotech. Engng Div. Am. Sot. Cio. Engrs* 114, GTIO, 1089-1109.
- 3) Andrus, R. D. and Youd, T. L. (1987). "Subsurface Investigation of a Liquefaction-Induced Lateral Spread Thousand Springs Valley, Idaho." Misc. paper GL-87-8, U.S. Army Corps of Engineers.
- 4) Andrus, R. D., Stokoe, K. H., II, and Roesset, J. M. (1991). "Liquefaction of gravelly soil at Pence Ranch during the 1983 Borah Peak, Idaho Earthquake." *Soil dynamics and earthquake engineering*, Vol. 5, Computational Mechanics Publications and Elsevier Applied Science, London.
- 5) Arango, I. (1996). "Magnitude scaling factors for soil liquefaction evaluations." *J. Geotechnical Eng., ASCE* 122(11), 929–36, 1996.

- 6) Anderson, D.G. and Stokoe, K.H. (1977) II "Shear modulus: A time dependent material property," Symposium on dynamic soil and rock testing, STP 654, ASTM, Denver, June, pp.66-90,
- 7) ASTM Designation: D 3999-91. Standard Test Methods for the Determination of the Modulus and Damping Properties of Soils using the Cyclic Triaxial Apparatus, Annual Book of ASTM standards, Vol. 04.08.
- 8) ASTM Designation: D 4253-2000. Standard Test Methods for the Maximum Index Density and Unit Weight of Soils Using a Vibratory Table.
- 9) ASTM Designation: D 4254-2000. Standard Test Methods for the Minimum Index Density and Unit Weight of Soils and Calculation of Relative Density
- 10) Bowles J.E. (1986) Engineering properties of soils and their measurement. Mc-Graw Hill Book Co., New York.
- 11) Been, K., Jefferies, M. G. & Hachey, J. (1991). The critical state of sands. *Geotechnique* 41, No. 3, 365-381.
- 12) Bouckovalas, G., Whitman, R. V., & Marr, W. A. (1984). Permanent displacement of sand with cyclic loading. *Journal of Geotechnical Engineering*, 110(11), 1606-1623.
- 13) Boulanger, R. W., and Idriss, I. M. (2012a). "Probabilistic SPT-based liquefaction triggering procedure." *Journal of Geotechnical and Geoenvironmental Engineering*, ASCE, 138(10), 1185-1195.
- 14) Boulanger, R. W., and Idriss, I. M. (2012b). "Evaluation of overburden stress effects on liquefaction resistance at Duncan Dam." *Canadian Geotechnical Journal*, 49, 1052-1058.
- 15) Boulanger, R. W., and Seed, R. B. (1995). "Liquefaction of sand under bi-directional monotonic and cyclic loading." *Journal of Geotechnical Engineering*, ASCE, 121(12), 870-878.
- 16) Boulanger, R. W., Mejia, L. H., and Idriss, I. M. (1997). Liquefaction at Moss Landing during Loma Prieta earthquake, *J. Geotechnical and Geoenvironmental Eng.*, ASCE 123(5), 453-67.
- 17) Boulanger, R. W., Wilson, D. W., and Idriss, I. M. (2012). "Examination and re-evaluation of SPT-based liquefaction triggering case histories." *Journal of Geotechnical and Geoenvironmental Engineering*, ASCE, 138(8), 898-909.

- 18) Boulanger, R. W., Wilson, D. W., and Idriss, I. M. (2013). Closure to "Examination and reevaluation of SPT-based liquefaction triggering case histories." *Journal of Geotechnical and Geoenvironmental Engineering*, ASCE, 138(8), 2000-2001.
- 19) Boulanger, R. W., and Idriss, I. M. (2014). "CPT and SPT based liquefaction triggering procedures." Report No. UCD/CGM-14/01, Center for Geotechnical Modeling, Department of Civil and Environmental Engineering, University of California, Davis, CA, 134 pp.
- 20) Brennan, A.J., Govindaraju, L., Bhattacharya, S. (2007), 'Liquefaction – susceptibility and remediation'. Proceedings of Intl Workshop on Earthquake and Geotechnical Engineering, Ed. S. Bhattacharya National Information Centre of Earthquake Engineering', NICEE, IIT, Kanpur, India.
- 21) Castro, G., & Poulos, S. J. (1977). Factors affecting liquefaction and cyclic mobility. *Journal of Geotechnical and Geoenvironmental Engineering*, 103(6).
- 22) Dash, Suresh R and Govindaraju, L and Bhattacharya, Subhamoy (2009) A case study of damages of the Kandla Port and Customs Office tower supported on a mat--pile foundation in liquefied soils under the 2001 Bhuj earthquake
- 23) Day, R.W. (2001) Soil testing manual: Procedures, classification data and sampling practices. Mc-Graw Hill Book Co., New York.
- 24) Das, B.M. (2008). Soil mechanics laboratory manual. Oxford University press. New York.
- 25) Das, B. M. (1993). Principles of Soil Dynamics. Boston, Massachusetts: PWS Publishers.
- 26) Dahl, K. R. (2011). Evaluation of seismic behavior of intermediate and fine-grained soils. Doctoral thesis, University of California, Davis, CA.
- 27) DeAlba, P., Seed, H. B., and Chan, C. K. (1976). "Sand liquefaction in large scale simple shear tests." *J. Geotechnical Eng. Div., ASCE* 102(GT9), 909–27.
- 28) Dobry, R. and Ladd, R. (1980) "Discussion of soil liquefaction and cyclic mobility evaluation for level ground during earthquakes," by H.B. Seed and "Liquefaction potential: science versus practice," by R.B. Peck, *Journal of Geotechnical Engineering*, ASCE, 106(6), pp. 720-724.
- 29) Dobry, R., Ladd, R.S., Chang, R.M. and Powell, D. 1982 "Prediction of pore water pressure build up and liquefaction of sands during earthquakes by the cyclic strain method," NBS Building Science Series 138, Washington, DC, pp.1-150,

- 30) Dobry, R. (1985) "Liquefaction of soils during earthquakes," Committee on Earthquake Engineering, Commission on Engineering and Technical Systems, National Research Council, National Academy Press, Washington, D.C.,
- 31) Drnevich, V.P. (1972). Undrained cyclic shear of saturated sand. *Journal of Soil Mechanics and Foundations Division, ASCE*, 98, SM8, pp. 807-25.
- 32) Drnevich, V.P. and Richart, F.E. Jr. (1970) "Dynamic pre-straining of dry sand," *Journal of Soil Mechanics and Foundations Division, ASCE*, Vol. 98, No. SM6, June, pp. 603-624.
- 33) Eurocode 7 – tests on soils
- 34) EERI archives University of California Berkeley
- 35) Govindaraju L, Sitharam T.G (2007) Effect of loading frequency on cyclic behaviour of soils 4th International Conference on Earthquake Geotechnical Engineering
- 36) Hardin, B.O. "The nature of damping in sands," *Journal of Soil Mechanics and Foundations Division, ASCE*, Vol. 91, No. SM1, January, pp. 63-97, 1965.
- 37) Hardin, B.O. and Drnevich, V.P. (1972) "Shear Modulus and Damping in soils: Measurement and Parameter Effects," *Journal of Soil Mechanics and Foundations Division, ASCE*, Vol. 96, No. SM2, March, pp. 453-469.
- 38) Hall, J.R. and Richart, F.E. (1963). Dissipation of elastic wave energy in granular soils. *Journal of Soil Mechanics and Foundations Division, ASCE*, 89, SM6, pp. 27-56.
- 39) Ishihara, K. (1971). On the longitudinal wave velocity and Poisson's ratio in saturated soils. *Proceedings of the 4th Asian Regional Conference on Soil Mechanics and Foundation Engineering, Bangkok*, Vol. 1, pp. 197-201.
- 40) Ishihara, K. and Yamazaki, F. (1980). Cyclic simple shear tests on saturated sand in multi- directional loading. *Soils and Foundations*, 20 (1), pp. 45-59.
- 41) Ishihara, K. (1983). Soil response in cyclic loading induced by earthquakes, traffic and waves. *Proceedings of the 7th Asian Regional Conference on Soil Mechanics and Foundation Engineering, Haifa, Israel*, Vol. 2, pp. 42-66.
- 42) Ishihara, K. and Towhata, I. (1983). Sand response to cyclic rotation of principal stress directions as induced by wave loads. *Soils and Foundations*, 23(4), pp. 11-26.
- 43) Ishihara, K. and Yamazaki, A. (1984). Analysis of wave-induced liquefaction in seabed deposits of sand. *Soils and Foundation* 24 (3), pp. 85-100.
- 44) Ishihara, K (1993). Liquefaction and flow failure during earthquakes. *Géotechnique*, 43: 351-415.

- 45) Ishihara, K (1996). *Soil Behaviour in Earthquake Geotechnics*, Oxford University Press Inc., New York. 340 pp
- 46) Ishihara, K., Tatsuoka, F., and Yasuda, S. (1975). Undrained deformation and liquefaction of sand under cyclic stresses. *Soils and Foundations*,15: 29-44.
- 47) Iwasaki, T., Tatsuoka, F., Tokida, K., and Yasuda, S. (1978). A practical method for assessing soil liquefaction potential based on case studies in various sites in Japan. *Proceedings of the 2nd International Conference on Microzonation for Safer Construction-Research and Application*. Vol. 2, pp. 885-96.
- 48) Kandasami R.K., Murthy T.G. (2015). “Experimental studies on the influence of intermediate principal stress and inclination on the mechanical behaviour of angular sands”. *Granular Matter*; 17(2): 217-230
- 49) Kokusho, T. (1980). Cyclic triaxial test of dynamic soil properties for wide strain range. *Soils and Foundations*, 20(2), pp, 45-60.
- 50) Kokusho, T. (1987). In situ dynamic soil properties and their evaluation. *Proceedings of the 8th Asian Regional Conference on Soil Mechanics and Foundation Engineering*, Kyoto, Vol. 2, pp. 215435
- 51) Kuribayashi, E., Iwasaki, T., Tatsuoka, F., and Horiuchi, S. (1974). Dynamic deformation characteristics of soils-measurements by the resonant column test device. *Report of the Public Works Research Institute, Japan*, No. 912 (in Japanese).
- 52) Kramer, S.L. (1996), *Geotechnical earthquake engineering*. Prentice Hall, New Jersey
- 53) Lin, J. S., Whitman, R. V., & Vanmarcke, E. H. (1983). Equivalent stationary motion for liquefaction study. *Journal of Geotechnical Engineering*, 109(8), 1117-1121.
- 54) Madsen, O.S. (1978). Wave-induced pore pressure and effective stresses in a porous bed. *Geotechnique*, 28(4), pp. 377-93.
- 55) National Research Council. 1985. *Liquefaction of soils during earthquakes*. National Research Council, Report of the Committee on Earthquake Engineering. National Academy Press, Washington, D.C.
- 56) Parthiban S, Kandasami R.K. (2016). “Latest advancements in Geotechnical testing methodologies - Laboratory and In-situ” *Advanced construction 2016: proceedings of the 5th international conference*, 6 October, 2016, Kaunas, Lithuania, p. 77-85, ISSN 2029-1213
- 57) Pyke, R.M., Chan, C.K., and Seed, H.B. (1974) “Settlement and liquefaction of sands under multidirectional shaking,” Report No. EERC 74-2, Earthquake Engineering Research Center, University of California, Berkeley.

- 58) Richart, F.E., Hall, J.R., and Woods, R.D. (1970). *Vibration of soils and foundations*. Prentice Hall.
- 59) Richards, R., Jr., D. G. Elms, and M. Budhu. (1993). Seismic bearing capacity and settlement of foundations. *J. Geotech. Eng.*,119(4), 622.
- 60) Saada, A.S. 1988. Hollow cylinder torsional devices: their advantages and limitations. In *Symposium on Advanced Triaxial Testing of Soil and Rock*. Edited by R.T. Donaghe, R.C. Chaney, and Marshall L. Silver. American Society for Testing and Materials, Special Technical Publication 977, pp. 766 -795.
- 61) Saada, A.S., and Ou, C.-D. 1973. Strain -stress relations and failure of anisotropic clays. *Journal of the Soil Mechanics and Foundation Division, ASCE*,99: 1091–1111.
- 62) Sayao, A.S.F., and Vaid, Y.P. 1989. Deformation due to principal stress rotation. In *Proceedings of 12th International Conference on Soil Mechanics and Foundation Engineering, Rio de Janeiro, Aug.13-18*. Edited by Committee of 12th ICSMFE. Balkema, Rotterdam, Vol. 1, pp. 107 -110
- 63) Shannon, W.L., Yamane, G., and Dietrich, R.J. (1959). Dynamic triaxial tests on sand. *Proceedings of the 1st Pan-American Conference on Soil Mechanics and Foundation Engineering, Mexico City, Vol. 1*, pp. 473-86.
- 64) Seed, H.B. 1979 “Soil liquefaction and cyclic mobility evaluation for level ground during earthquakes,” *Journal of Geotechnical Engineering Division, ASCE*, Vol. 105 No. GT2, pp. 201-252.
- 65) Seed, H.B. and Idriss, I.M. (1970) “Soil moduli and damping factors for dynamic response analysis,” EERC Report No. 70-10, Earthquake Engineering Research Center, University of California, Berkeley, December,
- 66) Seed, H.B. and Idriss, I.M. (1971) “Simplified procedure for evaluating soil liquefaction potential,” *Journal of Soil Mechanics and Foundations Division, ASCE*, Vol. 97, No. SM9, pp. 1249-1274.
- 67) Silver, M. L., & Seed, H. B. (1971). Volume changes in sands during cyclic loading. *Journal of Soil Mechanics & Foundations Div.*
- 68) Silver, M. L., & Seed, H. B. (1971). Deformation characteristics of sands under cyclic loading. *Journal of Soil Mechanics & Foundations Div.*
- 69) Skempton, A. W. (1986). Standard penetration test procedures and the effects in sands of overburden pressure, relative density, particle size, ageing and over consolidation. *Geotechnique*, 36(3), 425-447.

- 70) S. Singh, R. K. Kandasami, T. G. Murthy, (2017) *Mechanics and Modeling of Cohesive Frictional Granular Materials*, Chapter in Springer Series in Geomechanics and Geoengineering, January in book: *Advances in Laboratory Testing and Modelling of Soils and Shales (ATMSS)*, pp.493-500.
- 71) Talaganov, K.V. (1996) "Stress-strain transformations and liquefaction of sands," *Soil Dynamics and Earthquake Engineering*, No.15, pp. 411-418.
- 72) Tatsuoka, F. and Shibuya, S. (1991). Deformation characteristics of soils and rocks from field and laboratory tests. *Proceedings of the 9th Asian Regional Conference on Soil Mechanics and Foundation Engineering*, Bangkok, Vol. 2, pp. 101-77.
- 73) Tatsuoka, F., Iwasaki, T., & Takagi, Y. (1978). Hysteretic damping of sands under cyclic loading and its relation to shear modulus. *Soils and Foundations*, 18(2), 25-40.
- 74) Towhata, I. and Ishihara, K. (1985). Undrained strength of sand undergoing cyclic rotation of principal stress axes. *Soils and Foundations*, 25(2), pp. 135-47.
- 75) Timoshenko & Goodier 1982 *Theory of elasticity* TMH New York
- 76) Venkataramaiah (2006) *Textbook of geotechnical Engineering*, New age international (p) limited
- 77) Vaid, Y.P., and Chern, J.C. (1985). Cyclic and monotonic undrained response of saturated sands. In *Advances in the Art of Testing Soils under Cyclic Conditions*, ASCE Convention, Detroit, Oct.24. Edited by V. Khosla. American Society of Civil Engineers, New York, pp. 120 -147.
- 78) Vaid, Y.P., and Sivathayalan, S. 1996. Static and cyclic liquefaction potential of Fraser Delta sand in simple shear and triaxial tests. *Canadian Geotechnical Journal*, 33: 281-289.
- 79) Vaid, Y.P., and Thomas, J (1995). Liquefaction and post liquefaction behaviour of sand. *Journal of Geotechnical Engineering*, ASCE 121: 163-173
- 80) Vaid, Y.P., Uthayakumar M (1997). Static liquefaction of sands under multiaxial loading. *Canadian Geotechnical Journal*, 35: 273-283.
- 81) Viggiani, G. (1991). Dynamic measurements of small strain stiffness of fine grained soils in the triaxial apparatus. *Experimental Characterization and Modelling of Soils and Soft Rocks*, *Proceedings of the Workshop in Napoli*, pp. 75-97.
- 82) Wang, J.N. and Kavazanjian, E. (1989) "Pore pressure development during non-uniform cyclic loading," *Soils and Foundations*, Vol. 29, No. 2, pp. 1-14.
- 83) Wong, R.T., Seed, H.B. and Chan, C.K(1975) "Cyclic loading liquefaction of gravelly soils," *Journal of Geotechnical Engineering*, ASCE, Vol. 101, No. GT6, pp. 571-583.

- 84) Yamamoto, O.S. (1978). Seabed instability from waves. Proceedings of the 10th Annual Offshore Technology Conference, Houston, Texas, Vol. 1, pp. 1819-24.
- 85) Youd, T.L(1970). Densification and shear of sand during vibration. Journal of the Soil Mechanics and Foundation Division, Vol. 96, No. SM 3, May 1970 pp 863-880
- 86) Youd, T.L(1972). Compaction of sand by repeated shear straining. Journal of the Soil Mechanics and Foundation Division, Vol. 98, 1972, pp 709-725
- 87) Youd, T.L(1977). Packing changes and liquefaction susceptibility. Journal of the Geotechnical Engineering Division, Proceedings of the American Society of Civil Engineers, Vol. 103, No. GT8, August 1977, pp 918-922